



RESEARCH ARTICLE

Chromium Induced Alterations in Different Individual Microalga and their Consortia

Adinath, Akhlaqur Rahman, Shailendra Singh, Kritika Dixit and Shanthy Sundaram*

Centre of Biotechnology, University of Allahabad, Allahabad-211002, India

Received: 21 Jul 2015

Revised: 24 Aug 2015

Accepted: 28 Sep 2015

***Address for correspondence.**

Shanthy Sundaram
Centre of Biotechnology,
University of Allahabad,
Allahabad-211002, India



This is an Open Access Journal / article distributed under the terms of the **Creative Commons Attribution License (CC BY-NC-ND 3.0)** which permits unrestricted use, distribution, and reproduction in any medium, provided the original work is properly cited. All rights reserved.

ABSTRACT

Microalgae are well known photosynthetic autotrophs for environmental remediation and simultaneous production of value-added compounds enriched biomass. Major source of hexavalent Cr is water drainage from industries and consequently its use in plant irrigation or its direct use as drinking water, it leads the troubles associated with biomagnification. Therefore, inadequate disposal of Cr in the environment is related to several health issues and diseases. In this present work we have focused on monocultures as well as microalgae community of photosynthetic organisms community consisting *Chlorella* sp., *Scenedesmus dimorphus* and *Oscillatoria* sp., *Lyngbya* sp. was employed to see their potential individually as well as in community towards Cr adsorption and biomass production.

However, with increasing the levels of Cr toxicity, the niche partitioning and growth rates were altered from the natural community, it led to the early stationary phase of all the cells of *S. dimorphus* at the highest concentration of Cr. In contrast, *Chlorella* and *Lyngbya* were found to have good tolerance to Cr amongst all the organisms. The photosynthetic pigments, carbohydrate content, protein content were influenced by the increasing Cr concentration. To combat this stress, proline was synthesized with increasing Cr.

Keyword: Microalgae, *Chlorella* and *Lyngbya*, carbohydrate, photosynthetic.

INTRODUCTION

A variety of anthropogenic activities such as high rates of urbanization, the excess use of heavy metals based products in routine life, and weathering of rocks has directly affected the soil fertility and generated a number of



**Shanthy Sundaram et al.**

issues related to biomagnification at higher tropic levels in different ecosystems (Cardinale. 2011). Excess use of nitrates and phosphates in agriculture systems are direct factors that cause eutrophication of freshwater systems and prevailing harmful algal blooms which cause loss of original biodiversity (Stevenson. 2014). Microalgae are well known photosynthetic autotrophs for environmental remediation and simultaneous production of value-added compounds enriched biomass (Behera et al. 2015). These important features vary from one to another taxon in a community and directly affect the structure and functions of residing members. Individually, these photosynthetic microbes may have better or worse performance; however, in a community their functional attributes are highly altered due to the presence or absence of other individuals, or biotic and abiotic perturbations in community (Cardinale 2011).

Extreme heavy metals and nutrients in water systems are prime cause of water pollution at global level; in contrast, restoring the water parameters is a chief objective of most of the environmental policy of growing research councils (Chakraborty et al. 2011). In past scenario, a lot of researches have shown that ecosystem with larger number of species usually have more efficient water remediation capability than an ecosystem with fewer species (Loreau. 2001). Therefore, microalgae biodiversity plays significant role in managing the water quality.

The inherent mechanism of heavy metal absorption and nutrient uptake by these microalgae in a polluted lake or water system is unknown. Several efforts are underway to understand the role of these photosynthetic organisms in heavy metal removal. Several specific biological mechanisms have been studied by which particular microalgae uptake heavy metal. However, the researches focused towards the synthesis of metallothioneins peptides or phytochelatins in microalgae absorption and adsorption processes (Perales-Vela et al. 2006, Chekroun and Baghour. 2013). Chromium generates different types of reactive oxygen species which damages the DNA and proteins (Jaishankar et al. 2014).

Chromium (Cr) in its hexavalent form is highly toxic, it naturally occurs in soil and rocks, however due to biomagnification; its level has been increasing within plant and animal systems continuously and causing serious ailments. Although, they have their own defense system, instead this several disorders have been reported in humans and other animals (Tchounwou et al. 2012). Major source of hexavalent Cr is water drainage from industries and consequently its use in plant irrigation or its direct use as drinking water, it leads the troubles associated with biomagnification. Therefore, inadequate disposal of Cr in the environment is related to several health issues and diseases.

The microalgae have the potential to purify the water and enhance the oxygen concentrations in environment. Therefore, different groups are suggesting that their biodiversity conservation might be useful management tool in reducing the concentration of heavy metals in different water reservoirs (Pereira et al. 2013, Cervantes et al. 2001). Production of the novel bioactive compounds and lipid enriched biomass by these organisms, calls for their dual purpose including, remediation of heavy metal (Dwivedi et al. 2010, Singhvi and Chhabra. 2013).

Chlorella and *Scenedesmus* are green algal strains of Chlorophyceae, being engaged in heavy metal adsorption and water purification at several water tanks globally. Similarly, *Oscillatoria* and *Lyngbya*, the non-heterocystous species of phylum Cyanophyta are well known for their nitrogen fixing potential, heavy metal adsorption as well as high quality biomass yields. Collectively, these green algae and cyanobacteria could be engaged for dual benefits; in water detoxification and biomass production. *Chlorella* has good potential towards different heavy metals adsorption, especially Cr. Lot of efforts have been made to cleanse the water by adsorption of Cr through employing different strains of *Chlorella* and *Scenedesmus*. In the same way, different cyanobacteria, including *Oscillatoria* and *Lyngbya* were also used to detoxify the water and simultaneous production of valuable biomass. Sometimes, combinatorial activities of these organisms either in fresh or in contaminated water may lead to enhanced rates of CO₂ mitigation, heavy metal adsorption and biomass production (Subashchandra Bose et al. 2011).



**Shanthy Sundaram et al.**

Considering the Cr induced issues in irrigation as well as in drinking water, and increasing demands for sustainable biomass production, a study was proposed in which effects of Cr toxicity was enumerated at four different concentrations to see the changes in structure and function of artificially synthesized microalgae community having the members of Chlorophyceae (*Chlorella* and *Scenedesmus*) and Cyanophyceae (*Oscillatoria* and *Lyngbya*).

In this present work we have focused on monocultures as well as microalgae community of these photosynthetic organisms was employed to see their potential individually as well as in community towards Cr adsorption and biomass production. Another objective of this study was to see that how the presence of one organism affects the functioning of others in community.

MATERIALS AND METHODS

Strains

The members of Chlorophyceae and Cyanophyceae; *Chlorella* sp., *Scenedesmus dimorphus* and *Oscillatoria* sp., *Lyngbya* sp were selected for study. These cultures were available at Phycology laboratory, Centre of Biotechnology, University of Allahabad, India. The auxenic cultures were maintained on BG11+ agar media (pH 7.8) supplemented with 10 mM sodium thiosulphate.

Culture conditions:

Microalgae cultures were incubated at 27±1°C and daylight fluorescent lamps was used for providing illumination with an irradiance of 92.5 $\mu\text{mole photons m}^{-2} \text{S}^{-1}$ under the 14:10 light-dark diurnal cycle. Furthermore, at start of experiments and for various physico-chemical studies equal number of microalgae cells of members of both Chlorophyceae, Cyanophyceae and their consortia (optimized through corresponding O.D. and cell counts) were inoculated from the late log phase; in equal volume of fermentation broth (with or without chromium). While equal volume (100 mL) was considered for analytical methods.

Experimental designs:

The experiment was performed in triplicates, a completely randomized design (CRD) was used to elucidate the effects of hexavalent chromium on structure and function of microalgae community consisting *Chlorella* sp., *Scenedesmus dimorphus* and *Oscillatoria* sp., *Lyngbya* sp. Hexavalent chromium stock (2830 ppm) was prepared by dissolving its 0.283 g in 100 mL distilled water. Consequently, the stock was used to make further dilutions of 0.5ppm, 1.0 ppm, 3.0ppm and 5.0 ppm. Before start of experiment, inoculums were grown up to late log phase. Equal number of cells or filaments of green algae and cyanobacteria were mixed to get the microalgae consortia. Based on our previous standardizations (O.D. versus. cell counts), we mixed the cells or filaments. In each different treatment, equal number of monoculture or consortia was inoculated. Thus initially each flask has 1×10^7 cells mL^{-1} of fermentation broth (BG11+ media supplemented with or without different doses of hexavalent chromium). The flasks without chromium treatments were considered as experimental controls. To nullify the experimental error, optical density of BG11+ supplemented with chromium was measured at O.D_{730} in BG11+media, same considerations were made throughout the experiments.

Group 1: Experimental control (BG11+ Media) + (microalgae cells)

Group 1: Experimental control

1. (BG11+ Media) + (*Scenedesmus dimorphus*) + (0.5 ppm Cr^{VI})
2. (BG11+ Media) + (*Chlorella* sp.) + (0.5 ppm Cr^{VI})





Shanthy Sundaram et al.

3. (BG11+ Media) + (*Oscillatoria* sp.) + (0.5 ppm Cr^{VI})
4. (BG11+ Media) + (*Lyngbya* sp.) + (0.5 ppm Cr^{VI})

Group 3: Treatments (1.0 ppm chromium)

1. (BG11+ Media) + (*Scenedesmus dimorphus*) + (1.0 ppm Cr^{VI})
2. (BG11+ Media) + (*Chlorella* sp.) + (1.0 ppm Cr^{VI})
3. (BG11+ Media) + (*Oscillatoria* sp.) + (1.0 ppm Cr^{VI})
4. (BG11+ Media) + (*Lyngbya* sp.) + (1.0 ppm Cr^{VI})

Group 4: Treatments (3.0 ppm chromium)

1. (BG11+ Media) + (*Scenedesmus dimorphus*) + (3.0 ppm Cr^{VI})
2. (BG11+ Media) + (*Chlorella* sp.) + (3.0 ppm Cr^{VI})
3. (BG11+ Media) + (*Oscillatoria* sp.) + (3.0 ppm Cr^{VI})
4. (BG11+ Media) + (*Lyngbya* sp.) + (3.0 ppm Cr^{VI})

Group 4: Treatments (5.0 ppm chromium)

1. (BG11+ Media) + (*Scenedesmus dimorphus*) + (5.0 ppm Cr^{VI})
2. (BG11+ Media) + (*Chlorella* sp.) + (5.0 ppm Cr^{VI})
3. (BG11+ Media) + (*Oscillatoria* sp.) + (5.0 ppm Cr^{VI})
4. (BG11+ Media) + (*Lyngbya* sp.) + (5.0 ppm Cr^{VI})

Microscopy

Microalgae cultures were collected from late logarithmic phase, washed twice with phosphate buffer (pH, 7.8), rinsed with sterile water and enriched in fresh sterile BG11+ media. 20 µL of each culture was placed on clean glass slide, covered with slips and seen below 63X objective. The micrographs were recorded at 20 µm bar scale. The compound light microscopy was performed using Olympus microscope. (Company name and model no). Different micrographs were compared, and used to see the changes in community structure and niche partitioning of each monoculture in artificial habitat.

Analytical methods

Chlorophyll (Mackinney G., 1941)

The 1 mL cyanobacterial cell suspension from initial stationary phase was harvested by centrifugation at 10000 rpm for 10 minutes. Supernatant was discarded and transferred the pellet to a clean and dried test tube; added 1 mL of 95 % methanol and 1% CaCO₃ to prevent the degradation of chlorophyll-a, covered the whole tube with aluminium foil. Cells were placed in -20°C for 2 hours, and provided 37°C water bath treatments (similarly repeated freeze-thaw method used until pellet become colourless). Supernatant was used to measure the absorbance at 665 nm using 95% methanol as blank. Concentration of chl-a was calculated via using the following formula.

$$Chl-a (\mu\text{g mL}^{-1}) = (OD_{665} \times 13.9)$$

$$Chl-b (\mu\text{g mL}^{-1}) = (OD_{663} \times 13.9)$$



**Shanthy Sundaram et al.****Carotenoid (Jensen, 1978)**

A known volume (1 mL) of homogenized microalgal suspension was centrifuged (4000g, 10 min) and supernatant was discarded, washed the pellet 2-3 times with distilled water to remove traces of adhering salts. Took the OD at 450 nm using 85% acetone as blank and calculated the total amount of carotenoids as follows.

$$\text{Carotenoids (mg/mL)} = \frac{D \times V \times f \times 10}{2500}$$

Where, 'D' is the absorbance at 450nm, 'V' is volume of the extract, and 'f' is the dilution factor

It is assumed that these pigments have an average extinction coefficient of 2500.

Phycobiliprotein was estimated according to Siegelman and Kygia, 19

And the concentration of phycocyanin was determined spectrophotometrically at 620nm using the 0.05m phosphate buffer as blank.

Carbohydrate estimation (Loweus., 1951)

Total carbohydrate in community and monoalgal biomass was determined according to Loweus., 1952. Glucose was used as standard curve.

Protein estimation

Protein content was estimated according to Lowry et al., 1951

Protein content was evaluated from the concentration of BSA solution known from standard curve.

Proline estimation

Proline was estimated using the standard protocol of Bates et al. (1973). Proline was quantified spectrophotometrically at 520 nm from organic phase.

Antioxidant activity measurements:**MDA**

MDA was estimated by the method of Heath and Packer, 1968. The absorbance of the supernatant was recorded at 532 nm and corrected by subtracting the absorbance at 600 nm, 0.5% TBA in 20% TCA was used as the blank MDA contents was determined using the coefficient of 15 mM cm⁻¹.

SOD

SOD was estimated by the method of Dhindsa et al., 1981.

The enzyme assay for SOD activity was assayed by monitoring the inhibition of photochemical reduction of nitro blue tetrazolium chloride (NBT), using a reaction mixture consisting of 1 M Na₂CO₃, 200 mM methionine, 2.25mMNBT, 3mMEDTA, 60 μM Riboflavin and 0.1M phosphate buffer (pH 7.8). Absorbance was read at 560 nm.

Statistics

Various experimental data were analyzed by either one way or two way ANOVA as where needed by using the Graph Pad Prism 5.0 or Sigma Plot 12.0 statistical tools. The significant differences in various treatments were considered on the basis of Fisher ratios (F value) and probability (p≤0.05) at 95% confidence levels.



**Shanthy Sundaram et al.**

RESULTS AND DISCUSSIONS

The microalgae community growth and biomass production. In order to find out the tolerance levels of these cyanobacteria, green algae and their community against hexavalent Cr, their growth environment was treated with four concentrations of Cr in different experimental flasks up to 16 days. Continuous monitoring of growth showed varying growth behavior in natural and Cr treated communities.

The microscopic observations clarified the severe changes in the structure of various Cr treated communities and monocultures. In the natural community, niche partition of habitat plays important role in acclimatization of different microalgae. The filamentous organisms usually confined to sub-surface portion, *Lyngbya* was floating on surface while *Oscillatoria* was trapped below the filaments of *Lyngbya*. In contrast, unicells of *Chlorella* and coenobia of *S. dimorphus* clumped near the bottom. However, with increasing the levels of Cr toxicity, the niche partitioning and growth rates were altered from the natural community, it led to the early stationary phase of all the cells of *S. dimorphus* at the highest concentration of Cr. In contrast, *Chlorella* and *Lyngbya* were found to have good tolerance to Cr amongst all the organisms. Continuous growth monitoring from zeroth to 16th day showed interesting changes in the doubling patterns of these microbes. Their growth rates were significantly affected at the different doses of Cr. The growth behavior of these four organisms at 0.5 ppm Cr was not affected significantly ($p \geq 0.05$) (Fig.1). Furthermore, with increasing the doses of Cr from 1 ppm to 5 ppm showed decline in the growth of *Oscillatoria* sp., *S. dimorphus*. And *Lyngbya* sp. showed good response upto 5.0 ppm. On other hand, growth of consortia was affected after Cr dose of 1ppm and higher.

The biomass yields after 20 days of various microalgae individually and in consortia showed approximately 6gms/Litre dried biomass yield and control and 0.5 ppm Cr treated followed by *Chlorella* sp. The other individual microalgae comparatively showed lower biomass yield of 3gm/Litre or less.

Fig 2 shows the structure of these photosynthetic organisms was altered with increasing the doses of Cr. However, at the lowest dose of 0.5 ppm, slight swelled cells were seen under compound microscope. It might be reason behind their enhanced metabolic attributes and enhanced yields of biochemicals like carotenoids, carbohydrates and others. Furthermore, increasing the doses of Cr above 0.5 ppm, affected the morphology and biomass production of these organisms significantly. The LD₅₀ of Cr for the individual microalgae and consortia was determined for further analytical and biochemical assays. Except for *Lyngbya* sp. which showed a LD₅₀ of 3 ppm Cr all other individual and consortia showed an LD₅₀ between 0.5 ppm to 1 ppm Cr.

Changes in photosynthetic pigments in monocultures and consortia

The chl a content of the control and Cr treated microalgae and the consortia on the 12th day showed a very typical pattern. The consortia, *Scenedesmus dimorphus* and *Chlorella* all showed high level of inhibition of chl a in Cr treated samples in comparison to the control. With increasing concentrations of Cr, chl-a content decreased simultaneously (Fig.3a). *Lyngbya* spp. and *Oscillatoria* spp. showed less inhibition of chl a in Cr treated cells as compared to control.

Fig.3b shows that *Chlorella* spp and *Scenedesmus dimorphus* control showed higher carotenoid content compared to Cr treated cells. Both *Lyngbya* and the consortia showed no difference between the Cr treated and control. The content of phycocyanin in the Cr treated consortia was higher than untreated control (Fig 3c). *Chlorella* spp., *Oscillatoria* spp., *Scenedesmus dimorphus* showed no effect. With increase in concentrations of Cr from 1.0 to 5.0 ppm, carbohydrate yield was reduced in some micro algae (Fig 4). However at 0.5 ppm Cr no significant changes were observed. Thus, Cr affected not only the biomass productivity but also its carbohydrate yield in presence of Cr. Maximum carbohydrate content of 703 μ g was observed in control community while in communities treated with 0.5, 1.0, 3.0 and 5.0 ppm carbohydrate content was 692, 200, 118 and 76 μ g respectively. These results suggested that





Shanthy Sundaram et al.

increasing doses of Cr negatively affected the carbon fixation rates and overall carbohydrate productivity. Two way ANOVA and Bonferroni posttests rejected the Null hypothesis about the consistency of carbohydrate production in control and treatments. Treated consortia had decreased carbohydrate contents ($p \leq 0.001$).

On other hand, total carbohydrate content in monocultures of *Chlorella*, *Lyngbya*, *S. dimorphus* and *Oscillatoria* were 587, 442, 377 and 252 $\mu\text{g mL}^{-1}$ whilst with treatment of 1.0 ppm Cr content was decreased in all the organisms. The carbohydrate yields of monocultures clearly showed that *Chlorella* biomass is more enriched with carbohydrates than other strains. Therefore, carbon storage was highest in *Chlorella* whilst least in *Oscillatoria*. Two way ANOVA and Bonferroni posttests showed the statistically different carbohydrate contents in different monocultures ($p\text{-value} \leq 0.01$, $F=35.39$). The protein content (Fig 5a) indicates that *Chlorella* (1 ppm) showed no effect of (Cr^{+6}) stress. As compared to control at Hexavalent chromium treated cells showed lesser protein concentration. The decrease in protein content may also be due to increased level of ROS (leitaio et al. 2003) or increased protease activity. It is related growth and decreased carbon and nitrogen assimilation under stress (Babu et al. 2001)

The proline content (Fig. 5b) increased under Hexavalent chromium stress conditions in comparison to control. It was maximum in presence of 5ppm chromium in *Lyngbya* then started decreasing gradually. The actual reason behind the accumulation of proline (presumably by way of synthesis from glutamic acid) is yet to be known, in plants or plant parts exposed to stress, it could probably be due to a decrease in the study of electron transport system (Venekemp, 1989).

In present study percent inhibition of SOD was more or less the same in control and treated micro algae (Fig. 6a). MDA content increased with increasing 5ppm in *Chlorella* only. (Fig. 6b) suggesting formation of free radicals. The generation of the hydrocarbon gas, ethane, the production of malonaldehyde and changes in electrolytic conductivity has frequently been used as sensitive marker for heavy metal action in plants. (Kunert et al. 1985, Peleg et al. 2001). Compounds such as paraquat (also known as methyl viologen) induce light dependent oxidative damage in plants (Dodge, 1971). The PSI Mediated reduction of the paraquat di cation results in the formation of a mono-cation radical which then reacts with molecular oxygen to produce O_2 with the subsequent production of other toxic species, such as H_2O_2 and OH (Elstner et al. 1988). These compounds cause several toxicological problems and results in peroxidation of membrane lipids and general cellular oxidation and an increase in Proline.

ACKNOWLEDGEMENTS

Adinath is thankful to UGC New Delhi, India for providing him UGC-D.Phil research fellowship.

REFERENCES

1. Cardinale B J. (2011) Biodiversity improves water quality through niche partitioning. *Nature*. 472: 86-89.
2. Stevenson J. (2014) Ecological assessments with algae: a review and synthesis. *J. Phycol.* 50, 437–461 (2014)
3. Behera S, Singh R, Arora R, Sharma N K, Shukla M, Kumar S. (2015) Scope of algae as third generation biofuels. *Front. Bieng. Biotechnol.* 2: 1-13
4. Chakraborty N, Banerjee A, Pal R. (2011) Biomonitoring of lead, cadmium and chromium in environmental water from Kolkata, North and South 24-Parganas using algae as bioreagent. *J. Algal Biomass Utln.* 2 (3): 27– 41
5. Loreau M, Naeem S, Inchausti P, Bengtsson J, Grime J P, Hector A, Hooper D U, Huston M A, Raffaelli D, Schmid B, Tilman D, Wardle D A (2001). *Science* 294:804–808
6. Perales-Vela H V, Pen a Castro J N M, Canizares-Villanueva R O. (2006) Heavy metal detoxification in eukaryotic microalgae. *Chemosphere* 64:1-10.
7. Chekroun K B, Baghour M. (2013) The role of algae in phytoremediation of heavy metals: A review. *J. Mater. Environ. Sci.* 4 (6):873-880.





Shanthy Sundaram et al.

8. Jaishankar M, Tseten T, Anbalagan N, Mathew B B, Beeregowda K N. (2014) Toxicity, mechanism and health effects of some heavy metals. *Interdiscip Toxicol.* 7(2): 60–72.
9. Tchounwou P B, Yedjou C G, Patlolla A K, Sutton D J. (2012) Heavy Metals Toxicity and the Environment. *EXS.* 101: 133–164. doi:10.1007/978-3-7643-8340-4_6.
10. Pereira M, Bartolomé MC, Sánchez-Fortún S. (2013) Bioadsorption and bioaccumulation of chromium trivalent in Cr (III)-tolerant microalgae: a mechanisms for chromium resistance. *Chemosphere.* 93(6):1057-63.
11. Cervantes C, Campos-García J, Devars S, Gutiérrez-Corona F, Loza-Tavera H, Torres-Guzmán J C, Moreno-Sánchez R. (2001) Interactions of chromium with microorganisms and plants. *FEMS Microbiol. Rev.* 25:335-347
12. Dwivedi S, Srivastava S, Mishra S, Kumar A, Tripathi RD, Rai UN, Dave R, Tripathi P, Chakrabarty D, Trivedi PK. (2010) Characterization of native microalgal strains for their chromium bioaccumulation potential: phytoplankton response in polluted habitats. *J Hazard Mater.* 173 (1-3):95-101.
13. Singhvi P, Chhabra M (2013) Simultaneous Chromium Removal and Power Generation Using Algal Biomass in a Dual Chambered Salt Bridge Microbial Fuel Cell. *J Bioremed Biodeg* 4:190. doi: 10.4172/2155-6199.1000190.
14. Subashchandrabose S R, Ramakrishnan B, Megharaj M, Venkateswarlu K, Naidu R. (2011) Consortia of cyanobacteria/microalgae and bacteria: Biotechnological potential. *Biotechnology Advances* 29:896–907.
15. Philipose M. T. (1967) *Chlorococcales, monographs on algae*, Indian Council of Agricultural Research
16. Mackinney G. (1941) Absorption of light by chlorophyll solutions. *J. Biol. Chem.* 140:315-322.
17. Jensen A. (1978) Chlorophylls and carotenoids. *Handbook of physiological methods: physiological and biochemical methods.* Cambridge Univ Press Cambridge 59-70.
18. Loewus FA. (1952) Improvement in the anthrone method for determination of carbohydrates. *Anal. Chem.* 24: 219-223.
19. Maxwell K, Johnson GN. (2000) Chlorophyll fluorescence--a practical guide. *J Exp Bot.* 51(345):659-68.

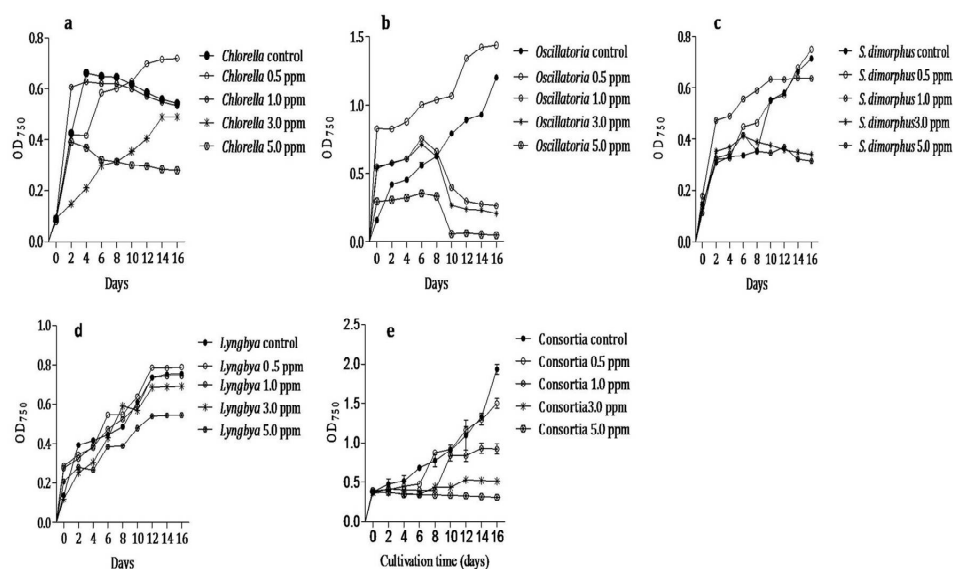


Fig.1 Growth curves of various microalgae under the effects of chromium(a) *Chlorella* (b) *Oscillatoria* (c) *S. dimorphus* (d) *Lyngbya* (e) Consortia of *Chlorella*, *Oscillatoria*, *S. dimorphus* and *Lyngbya*.





Shanthy Sundaram et al.

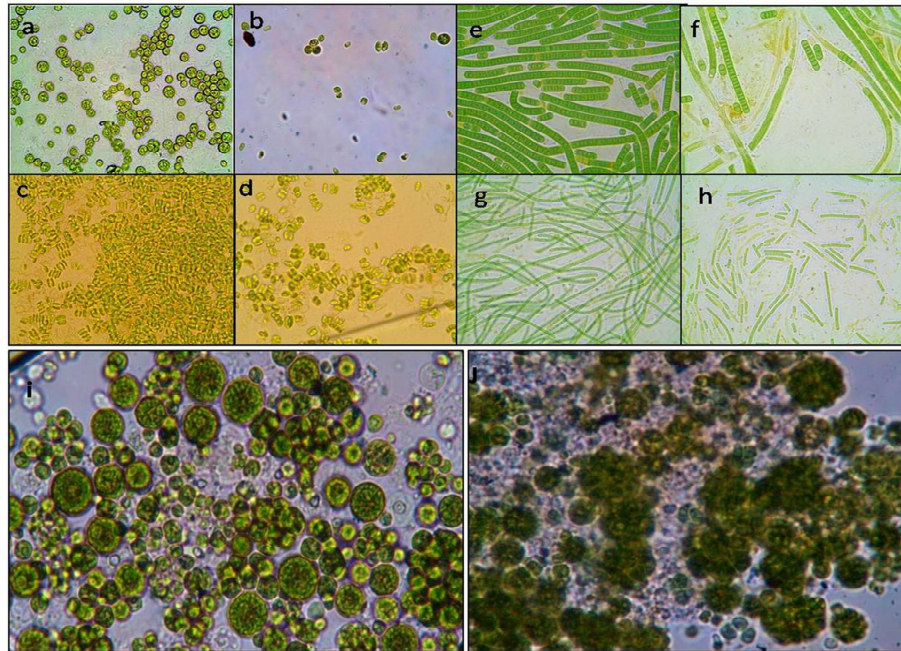


Fig.2 Micrographs of various microalgae showing the effects of 5.0 ppm chromium on their morphology (a) *Chlorella* (b) *Chlorella* 5.0 ppm Cr (c) *S. dimorphus* (d) *S. dimorphus* treated with 5.0 ppm Cr (e) *Oscillatoria* (f) *Oscillatoria* treated with 5.0 ppm Cr (g) *Lyngbya* (h) *Lyngbya* treated with 5.0 ppm Cr (i) Consortia (j) Consortia treated with 5.0 ppm Cr





Shanthy Sundaram et al.

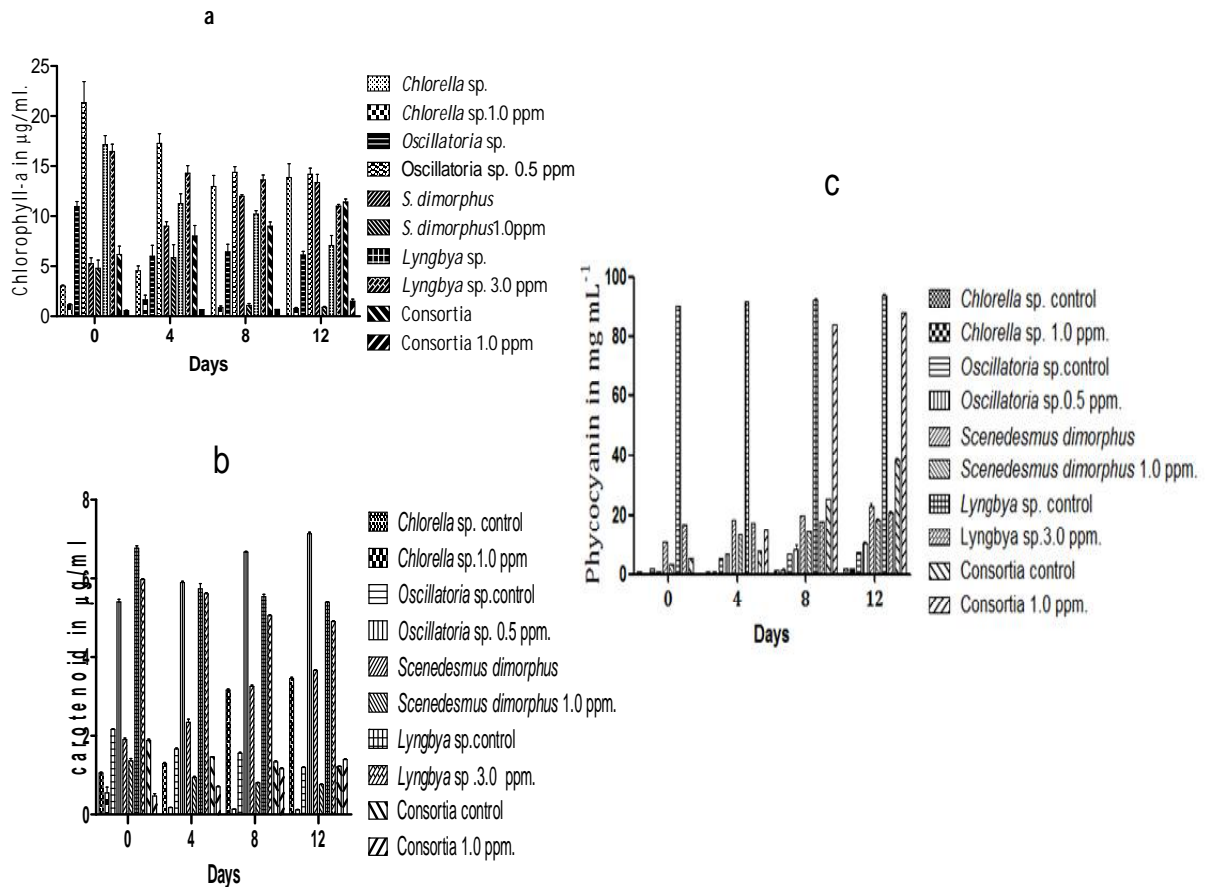


Fig.3 Pigment analysis of various microalgae under the effects of chromium(a) Chlorophyll-a (b) Carotenoid (c) Phycocyanin





Shanthy Sundaram et al.

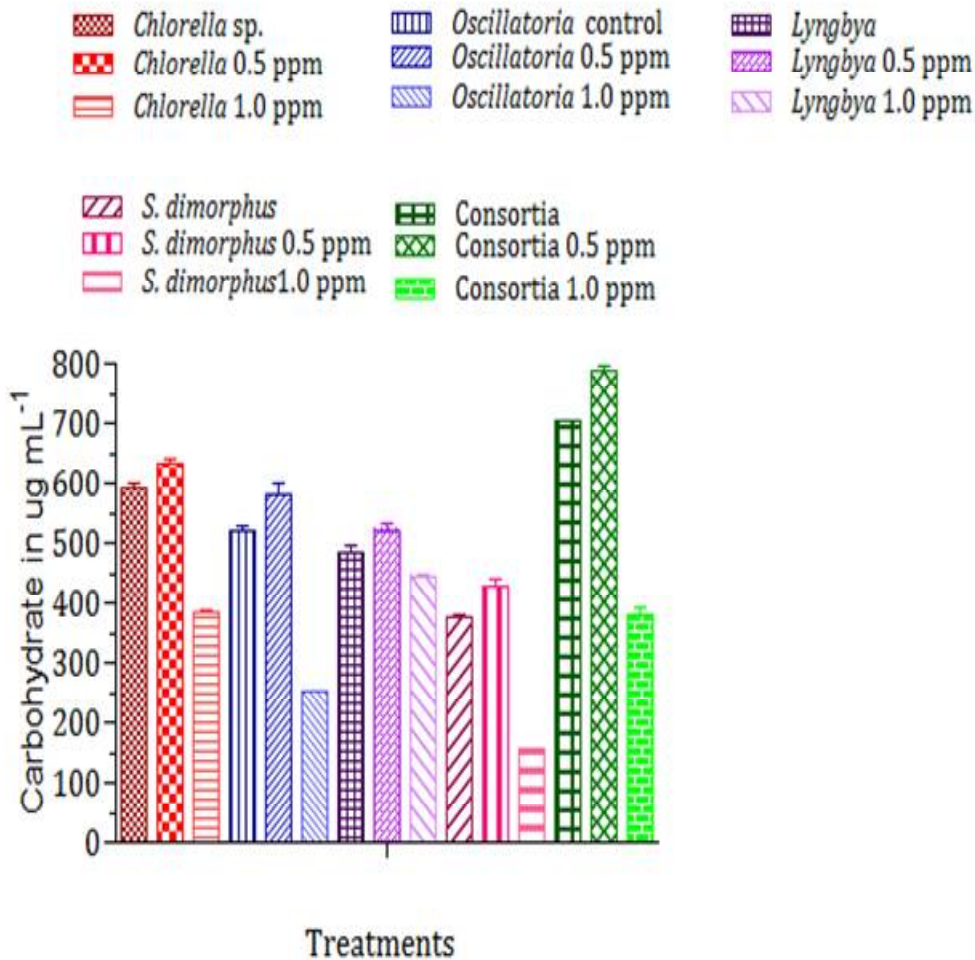


Fig. 4 Carbohydrate yields at the day of harvesting by different microalgae monocultures, their consortia with two different doses; 0.5 ppm and 1.0 ppm of chromium.





Shanthy Sundaram et al.

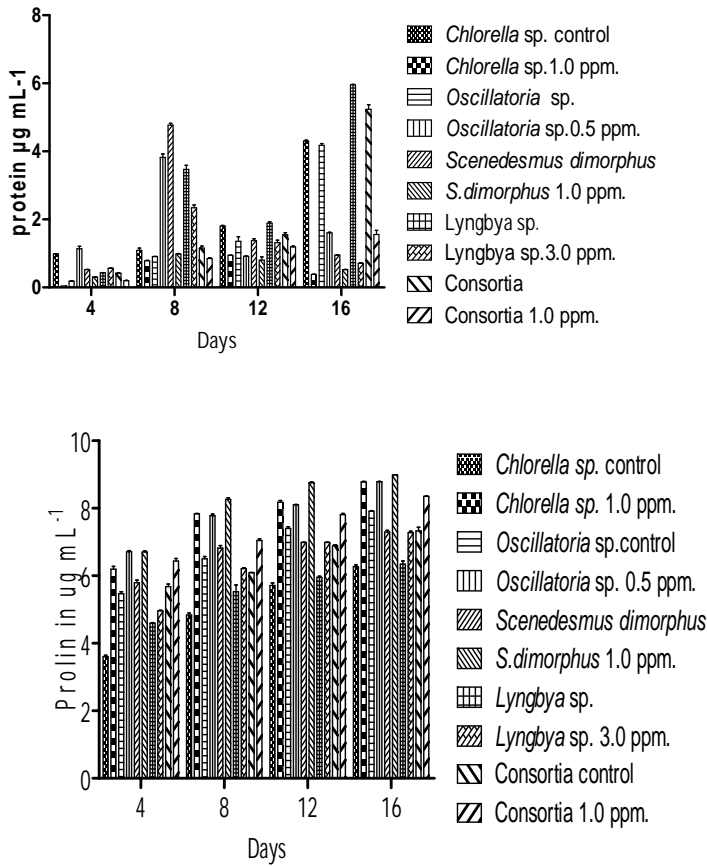


Fig. 5 Protein and Proline yields at various microalgae





Shanthy Sundaram et al.

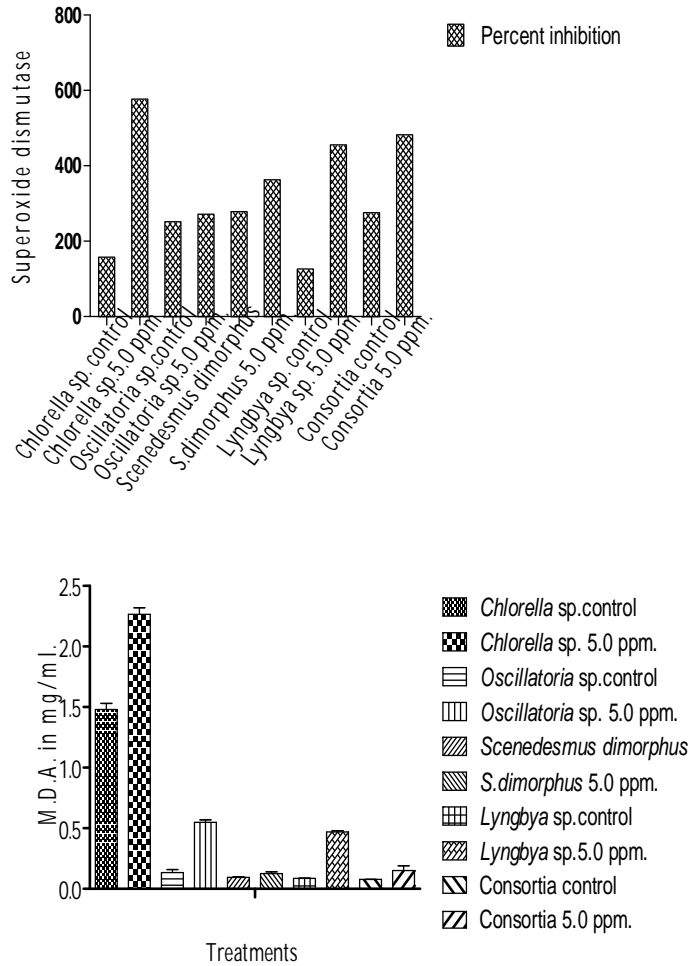


Fig. 6a, 6b showing the percent inhibition of SOD and the MDA activity in g/ml.





Properties of Sequences Generated by Summing the Digits of Cubed Positive Integers

H. I.Okagbue^{1*}, M.O.Adamu², S.A.Bishop¹ and A.A.Opanuga¹

¹Department of Mathematical Sciences, Covenant University, Canaanland, Ota, Nigeria

²Department of Mathematics, University of Lagos, Akoka, Lagos, Nigeria.

Received: 20 Jul 2015

Revised: 29 Aug 2015

Accepted: 28 Sep 2015

*Address for correspondence.

H. I.Okagbue

Department of Mathematics,

Covenant University,

Canaanland, Ota, Nigeria.

Email: hilary.okagbue@covenantuniversity.edu.ng



This is an Open Access Journal / article distributed under the terms of the **Creative Commons Attribution License** (CC BY-NC-ND 3.0) which permits unrestricted use, distribution, and reproduction in any medium, provided the original work is properly cited. All rights reserved.

ABSTRACT

Having established some properties of sequences generated by summing the digits of squared positive integers (Okagbue et al, 2015), we go a step further to explore the properties and characteristics of sequences generated by summing the digits of cubed positive integers. The results are different from summing the digits of squared positive integers. Two distinct sequences were obtained: one generated by summing the digits of cubed positive integers and the other sequence as the complement of the first but the domain remains the positive integers. The properties of these two sequences are discussed. The properties include their decompositions, subsequences, algebraic, additive, multiplicative, divisibility, uniqueness and ratios.

Keywords: Sequence, cube, digits, subsequence, positive integers.

INTRODUCTION

Mathematically, a cube of a number is its third power or when the number is raised to power of positive 3. It can also be defined as when a number is multiplied by its square. The positive perfect cube formed a sequence which can be found in A000578 –OEIS. $1, 8, 27, 64, 125, 216, 343, 512, 729, 1000, \dots$ (A)

Hardy and Wright (1980) book on number theory contained some details on cube integers or numbers. Sum of digits of some sequence of integers have appeared in scientific literature such as Cilleruelo et al, (2013) and Allouche and Shallit (2000). Some cubes are also squares; examples are $64, 729, 4096, \dots$ (B)





Okagbue et al.

Some relationships between sums of consecutive cubed integers and squared integers were given by Pletser (2015). See Madachy (1979) for relationship between sum of digits of numbers and Narcissistic numbers. Broughan (2003) showed that every integer has a smallest multiple which is a sum of two cubes. Luca (2006) looked at various arithmetic properties of positive integers with fixed digit sum.

RESEARCH MOTIVATION AND OBJECTIVES

The research is to give another direction to the earlier research by Lietzmann (1948). In his book, he discovered that a cube number is the third power of its digit sum and a number is the sum of the third power of its digits. Both Lietzmann and Hardy (1993) researched on the sums of the cubes of digits while this research is the sum of the digits of cube of positive integers. This research is to show that the sum of the digits of cube positive integers generate sequence. The sequence and its properties are subject of interest in this research. Okagbue et al (2015) have written on the properties of sequences generated by summing the digits of square positive integers.

METHODOLOGY

The first 16,000 positive integers or natural numbers were cubed and their respective individual digits were summed to obtain a sequence with varying frequencies. The sequence is:
 1,8,9,10,17,18,19,26,27,28,35,36,37,44,45,46,53,54,55,62,63,64,71,72,... (C)

However, when a positive number is cubed and the digits summed, the following numbers cannot be obtained which also formed a sequence. The sequence is:
 2,3,4,5,6,7,11,12,13,14,15,16,20,21,22,23,24,25,29,30,31,32,33,34,... (D)

RESULTS AND DISCUSSION

PROPERTIES OF SEQUENCES (C) AND (D) 1. Decomposition of sequence C

Apart from the first term of sequence C, the other terms appear in the form

8	9	10	
17	18	19	
26	27	28	
35	36	37	and so on.

All the three columns formed some unique sequences.
 8,17,26,35,44,53,62,71,80,89,98,... (E)
 9,18,27,36,45,54,63,72,81,90,99 (F)
 10,19,28,37,46,55,64,73,82,91,100,... (G)

All the three sequences have 9 as their common difference; Sequence F is the multiples of 9.

Decomposition of sequence D

The terms of sequence D appears in the form;

2	3	4	5	6	7
11	12	13	14	15	16
20	21	22	23	24	25
29	30	31	32	33	34 and so on.

The six columns formed unique sequences.





Okagbue et al.

2, 11, 20, 29, 38, 47, 56, 65, 74, 83, 92, ...	(H)
3, 12, 21, 30, 39, 48, 57, 66, 75, 84, 93, ...	(I)
4, 13, 22, 31, 40, 49, 58, 67, 76, 85, 94, ...	(J)
5, 14, 23, 32, 41, 50, 59, 68, 77, 86, 95, ...	(K)
6, 15, 24, 33, 42, 51, 60, 69, 78, 87, 96, ...	(L)
7, 16, 25, 34, 43, 52, 61, 70, 79, 88, 97, ...	(M)

All the six sequences have 9 as their common difference; Sequence I and L are multiples of 3.

Algebraic properties of sequences (C) and (D)

- (a). $(C) \cap (D) = \phi$
- (b). $(C) \cup (D) = \mathbb{N} - \mathbb{Z}^+$
- $(C) \cup (D) \cup 0 \cup (C) \cup (D) = \mathbb{Z}$

Subsequences of sequence (C)

Each of the elements of sequence C also form a unique sequence. For an illustration, the first 100 positive integers can be grouped based on the numbers in sequence C. This is represented in in **figure 1**. It is also like a histogram. The values are clustered in the center. .

Additive properties of sequence C

Addition of two numbers of sequence C will not necessarily yield a number in the sequence. This is illustrated in **table 1**

Additive properties of sequence D

Addition of two numbers of sequence D will not necessarily yield a number in the sequence. This is illustrated in **table 2**.

Addition of elements of both sequences C and D

Addition of one element of sequence C and another element of sequence D will most likely yield an element of sequence D as illustrated in **table 3**.

Absolute value of the differences of any two elements of sequence C

Finding the difference of any two elements of sequence C and then obtain the corresponding absolute value will not necessarily yield an element of sequence C. This is illustrated in **table 4**.

Absolute value of the differences of any two elements of sequence D

Finding the difference of any two elements of sequence D and then obtain the corresponding absolute value will not necessarily yield an element of sequence D. This is illustrated in **table 5**.

Absolute value of the difference of elements of both sequences C and D





Okagbue et al.

Find the difference of any one element of sequence C and another from sequence D and then obtain the corresponding absolute value will not necessarily yield an irregular pattern of numbers as illustrated in **table 6**. This is evidence that the sequences have no element common to them.

Multiplicative properties of sequence C

Multiplication of two numbers of sequence C yields a number in the sequence. This is illustrated in **table 7**.

Multiplicative properties of sequence D

Multiplication of two numbers of sequence D will not necessarily yield a number in the sequence. This is illustrated in **table 8**.

Multiplication of elements of both sequences C and D

Multiply of one element of sequence C and another element of sequence D will most likely yield an element of sequence D as illustrated in **table 9**. Elements of sequence C can be obtained only when the multiples of 9 in the sequence are multiply with the any element of sequence D.

Divisibility properties

1. All multiples of 9 are contained in sequence C.
2. Squares of the multiples of 3 are also contained in sequence C. The sequence is:
1,9,36,81,144,225,324,441,576,... (N)
3. All two consecutive elements of sequence C are coprime.
4. No clear multiples of numbers can be obtained from sequence D.

The observed uniqueness of sequences C and D

Any form of general additions to or subtractions from all the elements of both sequences yield different sequences.

The line graph of sequences C and D

A line graph was used to graphically display the behavior of both sequences. The first 25 terms of both sequences were used and can be seen in **figure 2**. Both sequences increase steadily in a step-like way as the number of terms increases. The behaviors are similar but sequences C have higher values than sequence D

The ratio of sequence C

A new sequence can be obtained from the ratio of the two consecutive terms of sequence

$$C. \frac{3}{1}, \frac{9}{8}, \frac{10}{9}, \frac{17}{10}, \frac{18}{17}, \frac{19}{18}, \frac{26}{19}, \frac{27}{26}, \dots \tag{O}$$

The behavior of the sequence can be seen in **figure 3**. The sequence obtained from the ratio of sequence C converges to almost one. The closed form solution of the ratio can be written as:

$$\varphi = \frac{4}{5} \left[\frac{1+\sqrt{5}}{2} \right] \approx 1.298387$$

To see a clearer view of the graph, 8 which is first term of the sequence is removed and the corresponding line graph can be seen in **figure 4**. The first term is an extreme value. It can be seen that it is a decreasing as the number of terms increases. The ratio converges to 1.





Okagbue et al.

The ratio of sequence D

A new sequence can be obtained from the ratio of the two consecutive terms of sequence C

$$\frac{3}{2}, \frac{4}{3}, \frac{5}{4}, \frac{6}{5}, \frac{7}{6}, \frac{11}{7}, \frac{12}{11}, \frac{13}{11}, \dots \tag{P}$$

The behavior of the sequence can be seen in **figure 5**. The sequence obtained from the ratio of sequence D converges to almost one. The closed form solution of the ratio can be written as:

$$\varphi = \left[\frac{7}{10} \right]^n (1 + \sqrt{5}) \approx 1.10936$$

The subsequences obtained from the various factors or multiples of sequences C and D

Some subsequences are obtained by the various factors or multiples of both sequences such as 2n, 3n, 4n... For all cases in this section, the first sequence is for C and the second is for sequence D.

Multiples of two

A subsequence is obtained for both sequences. That is the 2nd, 4th, 6th...terms of both sequences

$$8, 10, 18, 26, 28, 36, 44, 46, 54, 62, 64, 72, 80, 82, 90, \dots \tag{Q1}$$

$$3, 5, 7, 12, 14, 16, 21, 23, 25, 30, 32, 34, 39, 41, 43, \dots \tag{Q2}$$

Multiples of three

A subsequence is obtained for both sequences. That is the 3rd, 6th, 9th,terms of both sequences

$$9, 18, 27, 36, 45, 54, 63, 72, 81, 90, 99, \dots \tag{Q3}$$

$$4, 7, 13, 16, 22, 25, 31, 34, 40, 43, 49, \dots \tag{Q4}$$

Multiples of four

A subsequence is obtained for both sequences. That is the 4th, 8th, 12th...terms of both sequences

$$10, 26, 36, 46, 62, 72, 82, 98, 108, 118, \dots \tag{Q5}$$

$$5, 12, 16, 23, 30, 34, 41, 48, 52, 59, 66, \dots \tag{Q6}$$

Multiples of five

A subsequence is obtained for both sequences. That is the 5th, 10th, 15th...terms of both sequences

$$17, 28, 45, 62, 73, 90, 107, 118, 135, 152, \dots \tag{Q7}$$

$$6, 14, 22, 30, 38, 43, 51, 59, 67, 75, 83, 84, \dots \tag{Q8}$$

Prime multiples

A subsequence is obtained for both sequences. That is the 2nd, 3rd, 5th...terms of both sequences.

$$8, 9, 17, 19, 35, 37, 53, 55, 71, 89, 91, 109, \dots \tag{Q9}$$

$$3, 4, 6, 11, 15, 20, 24, 29, 33, 42, 47, 56, \dots \tag{Q10}$$

The sequence C / D

A new sequence can be obtained from the ratio of sequence C to sequence D.





Okagbue et al.

$$\frac{1}{2}, \frac{0}{3}, \frac{9}{4}, \frac{10}{5}, \frac{17}{6}, \frac{10}{7}, \frac{17}{11}, \frac{20}{12}, \dots \tag{R}$$

The sequence converges to 2 and the line graph is shown in **figure 6**. The closed form solution of the sequence C/D can be written as:

$$\varphi = \frac{639}{500} \left[\frac{1+\sqrt{5}}{2} \right] \approx 2.068329$$

The sequence D / C

A new sequence can be obtained from the ratio of sequence D to sequence C.

$$\frac{2}{1}, \frac{3}{8}, \frac{4}{9}, \frac{5}{10}, \frac{6}{17}, \frac{7}{18}, \frac{11}{19}, \frac{12}{26}, \dots \tag{S}$$

The sequence converges to 0.5 and the line graph is shown in **figure 6**. The closed form solution of the sequence D/C can be written as:

$$\varphi = \frac{81}{250} \left[\frac{1+\sqrt{5}}{2} \right] \approx 0.524275$$

The sequence Q1/Q2A

sequence can be generated from the ratio of sequence Q1 to Q2, since both are subsequences formed from the multiples of two of the sequences C and D respectively.

$$\frac{8}{3}, \frac{10}{5}, \frac{18}{7}, \frac{26}{12}, \frac{18}{14}, \frac{36}{16}, \frac{44}{21}, \frac{46}{23}, \frac{54}{25}, \dots \tag{T}$$

The sequence converges to 2 and the line graph is shown in **figure 8**. The closed form solution of the sequence Q1/Q2 can be written as:

$$\varphi = \frac{328}{230} \left[\frac{1+\sqrt{5}}{2} \right] \approx 2.091256$$

These results are similar to the results of the sequence C/D, an indication that subsequences exhibit similar characteristics with their parent sequences.

The sequence Q2/Q1

A sequence can be generated from the ratio of sequence Q2 to Q1, since both are subsequences formed from the multiples of two of the sequences D and C respectively.

$$\frac{3}{8}, \frac{5}{10}, \frac{7}{18}, \frac{12}{26}, \frac{14}{23}, \frac{10}{36}, \frac{21}{44}, \frac{23}{46}, \frac{20}{54}, \dots \tag{U}$$

The sequence converges to 0.5 and the line graph is shown in **figure 8**.

The closed form solution of the sequence Q2/Q1 can be written as:

$$\varphi = \frac{3}{115} \left[\frac{1+\sqrt{5}}{2} \right] \approx 0.480417$$

These results are similar to the results of the sequence C/D, an indication that subsequences exhibit similar characteristics with their parent sequences but with slight variability as seen from this research.

CONCLUSION

The various observed properties of sequences generated by summing the digits of cube positive integers have been considered. More research is needed to discover more properties of the sequences. Also the subsequences exhibit similar characteristics with their parent sequences.





Okagbue et al.

REFERENCES

- 1.H. I. Okagbue, M. O. Adamu, S. A. Iyase, and A. A. Opanuga(2015) Sequence of integers generated by summing the digits of their squares. *Indian Journal of Science and Technology*, 8(15), 69912.
2. G. H. Hardy and E. M. Wright (1980) An introduction to the Theory of Numbers (5thed) Oxford, Oxford University Press. ISBN: 978-0-19-853171-5.
3. Javier Cilleruelo, Florian Luca, JuanjoRuè& Ana Zumalacarregui(2013) On the sum of digits of some Sequences of integers. *Central European Journal of Mathematics*.11(1), 188-195.
4. J. P. Allouche& J. O. Shallit (2000) Sums of digits, overlaps and palindromes. *Discrete Mathematics and Theoretical Computer Science*.4(1), 1-10.
5. V. Pletser (2015) General solutions of sums of consecutive cubed integers equal to squared integers. *Journal of Number Theory*, 156, 394-413.
6. J. S. Madachy (1979) "Narcissistic Numbers" *Madachy's Mathematical Recreations*. Dover, New York, 163-173.
7. Kelvin A. Broughan (2003) Characterizing the Sum of Two Cubes. *Journal of Integer Sequences*, 6, Article 03.4.6.
8. Florian Luca (2006) Arithmetic properties of positive integers with fixed digit sum. *Rev. Mat. Iberoamericana*, 22(2), 369-412.
9. Walter Lietzmann (1948) *Sonderlingeim Reich der Zahlen*, Bonn.
10. G. H. Hardy (1993) *A Mathematician's Apology*. Cambridge University Press, New York p 105.

1	1 10 100
8	2 5 8 11 20 50 80
9	3 6 30 60
10	4 7 40 70
17	14 17 23 47 68 74
18	9 12 15 18 21 24 45 48 51 63 81 90
19	13 16 22 25 28 34 37 52 58 64 67 85
26	26 29 32 35 38 41 44 56 59 62 65 71 77 86 98
27	27 33 36 39 42 54 57 69 72 75 78 84 87 93
28	19 31 43 46 49 55 61 73 79 82 88 91 94 97
35	53 83 89 95
36	66 96 99
37	76
44	92
45	

Figure 1 The subsequences of C for the first 100 positive integers.





Okagbue et al.

Table 1 Addition of numbers of sequence C

$a + b$	1	8	9	10	17	18	19	26	...
1	2	9	10	11	18	19	20	27	...
8	9	16	17	18	25	26	27	34	...
9	10	17	18	19	26	27	28	35	...
10	11	18	19	20	27	28	29	36	...
17	18	25	26	27	34	35	36	43	...
18	19	26	27	28	35	36	37	44	...
19	20	27	28	29	36	37	38	45	...
.

Table 2. Addition of numbers of sequence D.

$a + b$	2	3	4	5	6	7	11	12	...
2	4	5	6	7	8	9	13	14	...
3	5	6	7	8	9	10	14	15	...
4	6	7	8	9	10	11	15	16	...
5	7	8	9	10	11	12	16	17	...
6	8	9	10	11	12	13	17	18	...
7	9	10	11	12	13	14	18	19	...
11	13	14	15	16	17	18	22	23	...
.

Table 3. Addition of numbers of both sequence C and D.

$a + b$	2	3	4	5	6	7	11	12	...
1	3	4	5	6	7	8	12	13	...
8	10	11	12	13	14	15	19	20	...
9	11	12	13	14	15	16	20	21	...
10	12	13	14	15	16	17	21	22	...
17	19	20	21	22	23	24	28	29	...
18	20	21	22	23	24	25	29	30	...
19	21	22	23	24	25	26	30	31	...
.

Table 4. Absolute value of the differences of any two elements of sequence C

$ a - b $	1	8	9	10	17	18	19	26	...
1	0	7	8	9	16	17	18	25	...
8	7	0	1	2	9	10	11	18	...
9	8	1	0	1	8	9	10	17	...
10	9	2	1	0	7	8	9	16	...
17	16	9	8	7	0	1	2	9	...
18	17	10	9	8	1	0	1	8	...
19	18	11	10	9	2	1	0	7	...
.





Okagbue et al.

Table 5 Absolute value of the differences of any two elements of sequence D

$ a - b $	2	3	4	5	6	7	11	12	...
2	0	1	2	3	4	5	9	10	...
3	1	0	1	2	3	4	8	9	...
4	2	1	0	1	2	3	7	8	...
5	3	2	1	0	1	2	6	7	...
6	4	3	2	1	0	1	5	6	...
7	5	4	3	2	1	0	4	5	...
11	9	8	7	6	5	4	0	1	...
.

Table 6 Absolute value of the difference of elements of both sequences C and D

$ a - b $	2	3	4	5	6	7	11	12	...
1	1	2	3	4	5	6	10	11	...
8	6	5	4	3	2	1	3	4	...
9	7	6	5	4	3	2	2	3	...
10	8	7	6	5	4	3	1	2	...
17	15	14	13	12	11	10	6	5	...
18	16	15	14	13	12	11	7	6	...
19	17	16	15	14	13	12	8	7	...
.

Table 7 Multiplication of any 2 numbers of sequence C

$a \times b$	1	8	9	10	17	...
1	1	8	9	10	17	...
8	8	64	72	80	136	...
9	9	72	81	90	153	...
10	10	80	90	100	170	...
17	17	136	153	170	289	...
18	18	144	162	180	306	...
.

Table 8 Multiplication of any 2 numbers of sequence D

$a \times b$	2	3	4	5	6	7	11	12	...
2	4	6	8	10	12	14	22	24	...
3	6	9	12	15	18	21	33	36	...
4	8	12	16	20	24	28	44	48	...
5	10	15	20	25	30	35	55	60	...
6	12	18	24	30	36	42	66	72	...
7	14	21	28	35	42	49	77	84	...
11	22	33	44	55	66	77	121	132	...
.





Okagbue et al.

Table 9 Multiplication of elements of both sequences C and D

$a \times b$	2	3	4	5	6	7	11	12	...
1	2	3	4	5	6	7	11	12	...
8	16	24	32	40	48	56	88	96	...
9	18	27	36	45	54	63	99	108	...
10	20	30	40	50	60	70	110	120	...
17	34	51	68	85	85	119	187	204	...
18	36	54	72	90	90	126	198	216	...
.

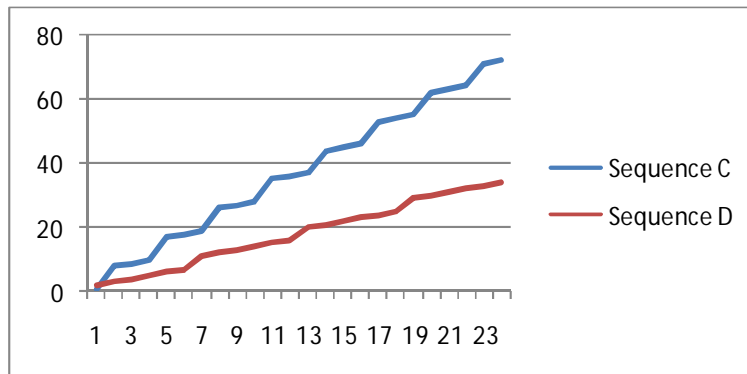


Figure 2 The line graph of sequences C and D.

x axis = the number of terms y axis = the values of the terms in both sequences

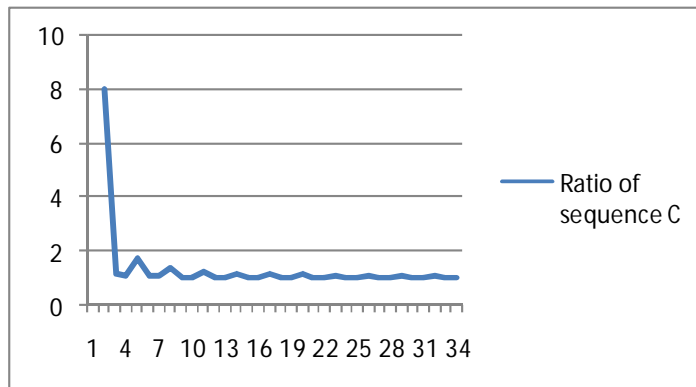


Figure 3 The ratio of sequence C

x axis = terms of the sequence y axis = ratio of 2 consecutive numbers of sequence C





Okagbue et al.

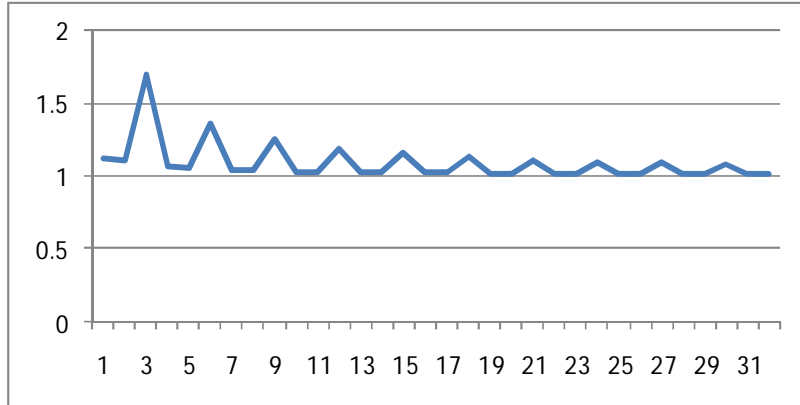


Figure 4 The ratio of sequence C with the first term removed
 x axis = terms of the sequence y axis = ratio of 2 consecutive numbers of sequence C

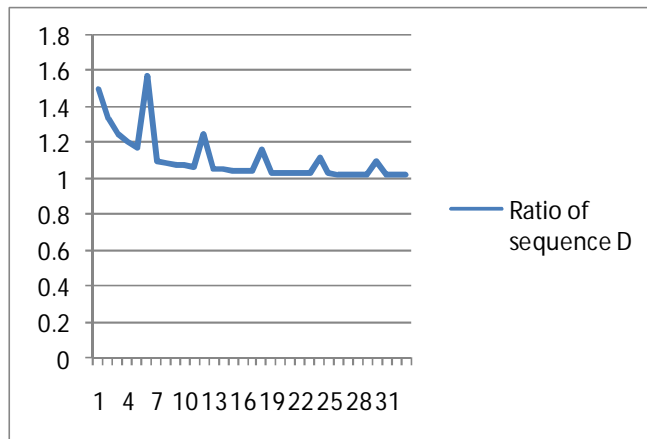


Figure 5 The ratio of sequence D
 x axis = terms of the sequence y axis = ratio of 2 consecutive numbers of sequence D

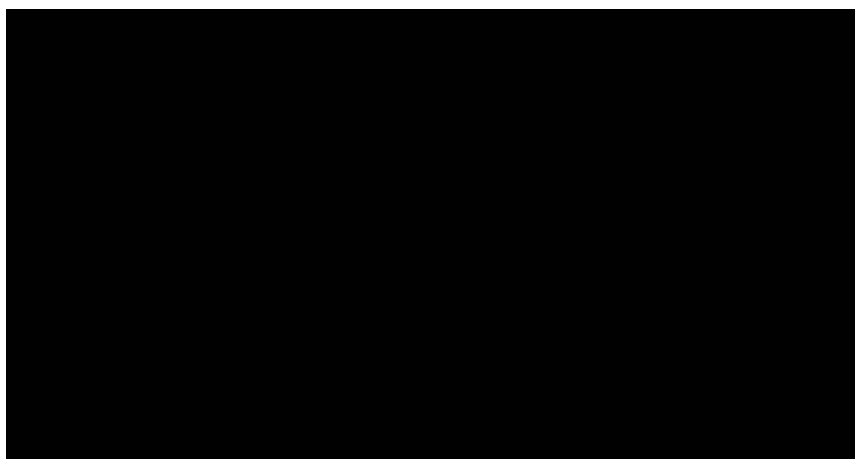


Figure 6 The sequences C/D and D/C
 x axis = terms of both sequences y axis = sequences C/D and D/C.





Okagbue et al.

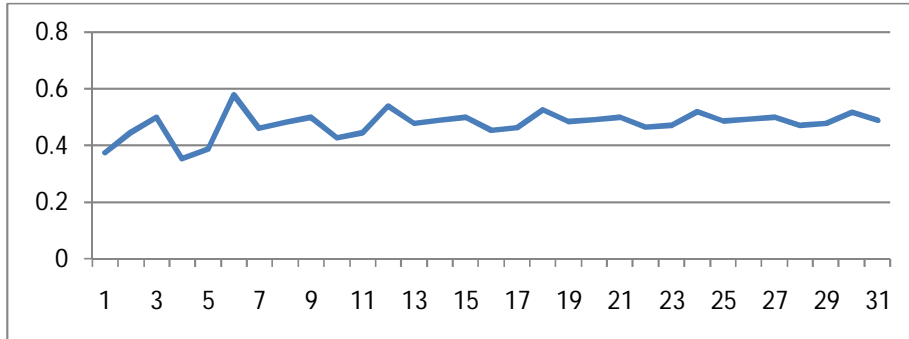


Figure 7 The sequence D/ C with the first term removed

x axis = terms of the sequence y axis = sequence D.C with first term removed.

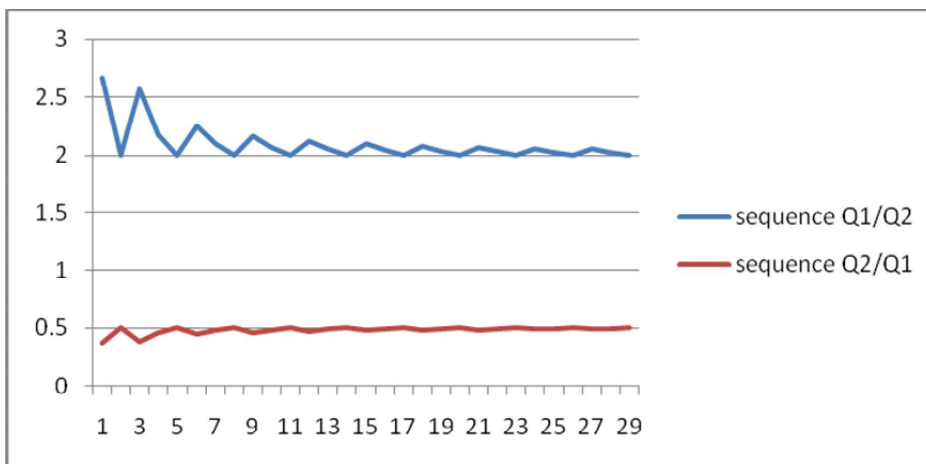


Figure 8 The sequences Q1/Q2 and Q2/Q1

x axis = terms of both sequences y axis = sequences Q1/Q2 and Q2/Q1.





Altered Reproductive Performance of High Calorie Diet Induced Obese Female Rats and their Male and Female Offspring

Harish Navya¹ and Hanumant Narasinhacharya Yajurvedi^{2*}

¹Research Scholar, Department of Zoology, University of Mysore, Manasagangotri, Mysore 570 006, India

²Professor, Department of Zoology, University of Mysore, Manasagangotri, Mysore 570 006, India

Received: 20 Jul 2015

Revised: 25 Aug 2015

Accepted: 28 Sep 2015

*Address for correspondence.

Hanumant Narasinhacharya Yajurvedi
Department of Zoology,
University of Mysore, Manasagangotri,
Mysore 570 006, India.
E-mail: hnyajurvedi@rediffmail.com



This is an Open Access Journal / article distributed under the terms of the **Creative Commons Attribution License (CC BY-NC-ND 3.0)** which permits unrestricted use, distribution, and reproduction in any medium, provided the original work is properly cited. All rights reserved.

ABSTRACT

Adult female rats were fed with high calorie diet (HCD) along with normal diet (ND) for 8 weeks. Significant increases in anthropometric and biochemical parameters in HCD group over controls confirmed induction of obesity and were allowed to mate with normal males. The HCD rats continued to receive HCD during pregnancy and lactation periods. A significant decrease in litter size and weight, a significant increase in weight/pup and mortality rate and no significant difference in gestation index, fertility index and parturition index were found in HCD rats compared to controls. The obese F1 females showed increase in number of estrous cycles/2months and a decrease in length of estrous cycle. These F1 rats were mated in different combinations viz., ND♂ x ND♀, ND♂ x HCD♀, HCD♂ x ND♀, HCD♂ x HCD♀. The females in ND♂ x HCD♀ and HCD♂ x HCD♀ groups showed significant increases in anthropometric measurements during pregnancy where as females in other two groups did not show these changes. The fertility index, gestation index and parturition index did not significantly differ among all groups. However, in ND♂ x HCD♀ and HCD♂ x HCD♀ groups litter size and litter weight were decreased whereas body weight/ pup and mortality rates were increased compared to ND♂ x ND♀, the HCD♂ x ND♀ also showed decrease in litter size and weight and an increase in mortality rate compared to ND♂ x ND♀. The results indicate that F1 born to obese females and fed with HCD show low reproductive performance and increased pup mortality.

Key words: body weight; offspring; fertility index; litter size; litter weight; mortality rate.



**Harish Navya and Hanumant Narasinhacharya Yajurvedi****INTRODUCTION**

Maternal obesity has well-recognized short-term complications for both mother and child (Garbaciak *et al.*, 1985) and it is commonly associated with fetal overgrowth rather than growth restriction (Catalano *et al.*, 2012). Children of obese parents have an increased risk of becoming obese compared to children of parents of normal weight (Lyra *et al.*, 2003). In obese women, pregnancy rate and live birth rate is consistently decreased especially due to an increased miscarriage rate (Wang *et al.*, 2002; Lintsen *et al.*, 2005; Maheshwari *et al.*, 2007). Pregnancy complications viz. hypertensive disorders, gestational diabetes, prolonged duration of labour, increased need of operative delivery, macrosomia increased blood loss occur due to obesity (Garbaciak *et al.*, 1985; Edwards *et al.*, 1996; Weiss *et al.*, 2004). Ovulatory and anovulatory subfertile women are overweight or obese (Koning *et al.*, 2010).

In animal models, offspring of mothers consuming a high-fat diet (HFD) throughout pregnancy and lactation, showed increased blood glucose level (Ainge *et al.*, 2011). Offspring of rats on a high-fat diet had increased pancreatic β -cell mass, replication and neogenesis leading to hyperglycemia and type 2 diabetes in the adult life (Gniuli *et al.*, 2008). Studies in rodents show that exposure to maternal obesity or over nutrition during both pregnancy and lactation is associated with the development of obesity in the offspring (Guo and Jen 1995, Levin & Govek 1998, Bayol *et al.* 2007, 2008, Samuelsson *et al.* 2008, Shankar *et al.* 2008, Liang *et al.* 2009, Nivoit *et al.* 2009, Tamashiro *et al.* 2009, Yan *et al.* 2010). Offspring are more prone to develop obesity due to increasing maternal obesity and maternal weight gain in rats in addition to increased risk of pregnancy-related complications in mother rats (Li *et al.*, 2011).

A maternal cafeteria or high-fat diet induces obesity and insulin and leptin resistance in rats (Bayol *et al.*, 2005; Taylor and Poston, 2007; Morris and Chen, 2009), hypertension in mice (Elahi *et al.*, 2009; Liang *et al.*, 2009) and in rats (Khan *et al.*, 2004; Samuelsson *et al.*, 2010) and fatty pancreas disease in mice (Oben *et al.*, 2010). Consuming a high fat diet reduces a rat's capacity to conceive and ability to maintain her litter during the perinatal period (Shaw *et al.*, 1997). Histological evaluation of ovaries showed similar morphology and number of antral follicles in both cafeteria and standard chow fed groups of rats (Sagae *et al.*, 2012). Obese rats experienced greater difficulty than controls in delivering their pups and more number of their pups died in the first few days of life (Rasmussen, 1998). Continued feeding on high fat diet, for longer duration reduced pups weight and increased mortality rate with early age of puberty in rats (Suker *et al.*, 2013).

Diet-induced (60% of fat in diet) obese male C57BL/6J mice showed a significant reduction in fertility after natural mating (Ghanayem *et al.*, 2010). High fat diet induced paternal obesity in mice induced oxidative stress, sperm DNA damage and reduction in fertilizing ability (Bakos *et al.*, 2010). Likewise paternal obesity caused intergenerational transmission of a decline in fertility, particularly in males, through both F1 parental lines to F2 generations (Fullston *et al.*, 2012).

In the present day human societies, prevalence of overweight and obese conditions in adults and children are increasing. Studies conducted in animal models thus far do not mimic this situation, because reproductive effect of induced obesity in adults (Akamine *et al.*, 2010; Balasubramanian *et al.*, 2012) or paternal or maternal obesity (Fullston *et al.*, 2012; Suker *et al.*, 2013) effect on offspring have been studied. In the present study, a model of childhood obesity extending to prepubertal and pubertal period in offspring born to obese mothers has been mimicked in rats to study effect on reproductive performance. Since gonads develop, differentiate and mature during these periods, studying reproductive performance of rats having obese condition in these periods gains importance.



**Harish Navya and Hanumant Narasinhacharya Yajurvedi****MATERIALS AND METHODS****Experimental Design**

Three months old adult healthy female rats were randomly divided into two groups viz. normal diet (ND) and high calorie diet (HCD). Rats in ND group were fed with normal diet and served as controls whereas those in second group were fed with high calorie diet (HCD) (10g/rat/day) in addition to normal diet for 8 weeks to induce obesity. The rats were provided with ad libitum of water. Anthropometric parameters viz., body weight (BW), body mass index (BMI), thoracic circumference (TC) and abdominal circumference (AC) were recorded at weekly intervals. The serum concentrations of glucose, cholesterol and triglyceride were determined after completion of 4th and 8th week of the experimental period.

The female rats (F0 generation) of both the groups were allowed to mate with normal healthy male rats. Vaginal smear was observed every day morning at 10. A. M. and presence of spermatozoa in the smear confirmed conception. The day on which spermatozoa were present in the smear was considered as day zero of pregnancy. Different fertility parameters viz. fertility index, parturition index, gestation index, litter size, litter weight, weight/pup and pups mortality were recorded. Normal diet (ND) and high calorie diet (HCD) were fed to respective groups of females during gestation and lactation periods. The offspring (F1) of controls were fed with ND and those of HCD mothers with HCD after weaning period up to post natal day (PND) 100. Anthropometric parameters as mentioned above were recorded on PND 0, 30, 60 and 100. The male and female offspring (F1) after attaining the age of PND 100 were allowed to mate in different combinations, viz., ND♂ x ND♀, ND♂ x HCD♀, HCD♂ x ND♀, HCD♂ x HCD♀. The conception was confirmed as described above and after gestation period fertility indices were recorded. The experimental protocols were approved by the institutional animal ethics committee and animal care and treatments were as per guide lines of the committee.

Fertility parameters

The percentage of number of females conceived, litter size, and litter weight of each rat were recorded. Other parameters were determined according to the procedure of Adilaxmamma *et al.* (1994) and Narayana *et al.* (2005) as follows:

- (i) fertility index of male = number of fertile males/number of males used in the test x100,
- (ii) fertility index of female = number of pregnant rats/number of females mated x100,
- (iii) parturition index=number of females delivered/ number of pregnant rats x100,
- (iv) gestation index= number of pups born alive/ total number of pups born x100.

The mortality of pups was expressed as percentage of dead pups at parturition.

Anthropometric measurements

Body weight (BW), body mass index (BMI), thoracic circumference (TC) and abdominal circumference (AC) were measured according to the procedure of Novelli *et al* (2007).

Estrous cyclicity

The vaginal smear of each F1 female rat was observed under light microscope every day (10 AM) as per the description of Cooper *et al.* (1993) to record the stage of estrous cycle and mean number of estrous cycles per 2 months period was computed based on this data.



**Harish Navya and Hanumant Narasinhacharya Yajurvedi****Statistical analyses**

The mean value of each parameter was computed using data on at least 5 rats in each group and the mean values of control and HCD groups were compared using Student's t-test wherein there were only two groups, whereas one way ANOVA followed by Duncan's multiple range test was used, if groups were more than 2 and judged significant if $P < 0.005$.

RESULTS**HCD induced alterations in adult female (F0) rats**

On day zero, BW, BMI, TC and AC of ND and HCD females did not significantly differ. However a consistent and significant increase in all these anthropometric parameters was observed from 1st week through 8th week in HCD females compared to ND (Table 1). In addition the serum concentrations of glucose, cholesterol and triglycerides were significantly higher in HCD females than ND females on 4th and 8th week (Table 2).

The fertility index, parturition index and gestation index of ND and HCD rats did not significantly differ. However a significant decrease in litter size and litter weight and a significant increase in body weight/ pup and mortality of pups were found in HCD rats compared to ND rats (Table 3).

HCD induced alterations in offspring (F1) of obese female rats

Male as well as female offspring of females (F0) fed with HCD, showed a significantly higher BW, BMI, TC and AC at birth, i.e. on PND zero. There was a consistent and significant increase in these anthropometric parameters at all time points studied i.e. PND zero, 30, 60, and 100, both in HCD male and female offspring (F1) compared to those of ND (Table 4).

A significant increase in number of estrous cycles/ 2 month period and a significant decrease in length of estrous cycle were observed in F1 HCD rats compared to ND rats (Table 5). Further, BW, BMI, TC and AC showed a consistent pattern throughout gestation (day zero, through 3rd week) i.e a significant increase in all anthropometric parameters of ND♂ x HCD♀ and HCD♂ x HCD♀ groups over ND♂ x ND♀ and HCD♂ x ND♀ (Fig. 1). Irrespective of groups all F1 females conceived (Table 6). There was no significant difference in fertility index and parturition index compared to ND rats. However there was a significant decrease in gestation index, litter size, litter weight and a significant increase in body weight/ pup and mortality of pups in ND♂ x HCD♀, HCD♂ x ND♀ and HCD♂ x HCD♀ groups compared to ND♂ x ND♀ group (Table 6).

DISCUSSION

Gonads differentiate during fetal life and develop to produce gametes during pre-pubertal and pubertal life in post-natal period. Studies thus far carried out have reported effects of paternal or maternal obesity on different aspects of reproduction and fertility of offspring (Fullston *et al.*, 2012; Balasubramanian *et al.*, 2013; Suker *et al.*, 2013). The present study aimed at finding out effects of exposure to high calorie diet *in utero* as well as during post-natal period up to attainment of sexual maturity, on reproductive performance of offspring born to obese female and normal male parents. This model of childhood obesity was developed because in humans obesogenic nutritional environment contributes to risk of developing obesity and early life nutritional adversity is associated with metabolic disorders (Li *et al.*, 2011).



**Harish Navya and Hanumant Narasinhacharya Yajurvedi**

In the present study the adult female rats fed with HCD developed obesity, which reduced their reproductive outcome. Likewise offspring, male as well as female born to these obese females, and exposed to HCD from fetal life through attainment of sexual maturity also developed obesity. Our study clearly demonstrates that, the severity of over nutrition effect on reproductive performance of obese offspring born to obese mothers was more compared to normal adult females developing obesity due to over nutrition as shown by 50% decrease in litter size and litter weight and 2 fold increase in pup mortality in offspring (F1) compared to obese mothers (F0).

The anthropometric parameters viz. BW, BMI, TC and AC and blood constituents viz. glucose, triglycerides and cholesterol are considered as markers of obesity (Novelli *et al.*, 2007). In agreement in the present study female rats fed with HCD for 8 weeks showed a consistent and significant increase in anthropometric parameters, measured over weekly intervals and concentrations of blood glucose, triglyceride and cholesterol level over controls thoroughly indicating development of obese condition. These females despite mating with normal diet fed males showed altered reproductive performance as shown by a decrease in litter size and weight and increase in mortality of pups compared to controls. Interestingly conception rate (fertility index) and parturition indices were 100%, and there was slight but not significant drop in gestation index in obese females, though other fertility parameters were adversely affected. These facts indicate adverse interference of HCD diet on post- conception growth and survival of fetus. Similarly, reduced fertility in overweight women (Bolumar *et al.*, 2000; Rich-Edwards *et al.*, 2002; Pasquali *et al.*, 2006; Gesink Law *et al.*, 2007) and anovulation and reduction in fertilization due to high fat diet feeding in mice (Gouveia *et al.*, 2004) have been reported. Likewise HFD consumption reduced rats capacity to conceive and ability to maintain her litter during post natal period (Shaw *et al.*, 1997) and obese rats experienced greater difficulty than controls in delivering pups and more pups died in the first few days of life (Rasmussen, 1998). Reduction in pup weight and increase in their mortality were observed due to high fat diet consumption in mothers (Suker *et al.*, 2013). Further HFD caused irregular estrous cycles (Balasubramanian *et al.*, 2012; Lie *et al.*, 2013) and anovulation and decrease in blood LH levels (Balasubramanian *et al.*, 2012) in rats. Anovulation is suggested to be due to high fat diet induced suppression of hypothalamo-gonadal- axis (Balasubramanian *et al.*, 2012), as it was accompanied by reduction in LH levels. Hence hormonal imbalance appears to be the cause of obesity induced alterations in female rats.

Maternal obesity is known to induce obese condition in their offspring. For instance, exposure to maternal obesity during pregnancy and lactation periods resulted in development of obesity in offspring (Guo and Jen 1995, Levin & Govek 1998, Bayol *et al.* 2007, 2008, Samuelsson *et al.* 2008, Shankar *et al.* 2008, Liang *et al.* 2009, Nivoit *et al.* 2009, Tamashiro *et al.* 2009, Yan *et al.* 2010; Li *et al.*, 2011).

Obese parents also affect reproductive parameters of offspring. However, in the study of Suker *et al* HFD caused reduction in pups weight and increase in mortality rate. Further, maternal HFD during pregnancy and lactation resulted in increase in offspring body weight and percentage of fat mass, whereas HFD during pregnancy alone increased offspring adiposity but not body weight in rats, indicating that weight gain in F1 offspring of obese rats was due to increased ingestion of milk that was high in calorie content (Desai *et al.*, 2014) . In the present study HCD feeding not only resulted in obesity in adult females but also in their male as well female offspring as shown by higher body weight/pup at the time of birth and significantly higher BW, BMI, TC and AC compared to controls on day zero. The pups were exposed to HCD until weaning period, as mother rats were fed with HCD, which resulted in maintaining obese condition until the offspring were fed with HCD. Since feeding with HCD or HFD increases the blood levels of glucose and lipids, exposure to these conditions *in utero* during pregnancy, might cause tendency for developing obesity.

The study of Desai *et al* (2014) reveals that HFD during pregnancy causes high adiposity in offspring. The continued exposure to high levels of nutrients during lactation might reinforce the tendency for obesity resulting in obese condition in offspring. This view is supported by the report that in rats HFD fed mothers produce milk with higher fat content than controls and also their offspring consume more milk (Purcell *et al.*, 2011). Hence, obesity in offspring of obese mothers is due to exposure to calorie rich nutrient content of blood during gestation and through milk



**Harish Navya and Hanumant Narasinhacharya Yajurvedi**

during pre-weaning period. In the present study, the pups were fed with HCD after weaning to maintain obesity during pre-pubertal and pubertal periods, to understand effects of obesity on reproductive performance.

Maternal obesity is known to impact on reproductive performance of their offspring. HFD for long periods in rats resulted in early onset of puberty in their offspring (Suker *et al.*, 2013). HFD during pregnancy and lactation caused alterations in structure and functions of the ovary of female offspring as shown by reduced AMH signaling and more number of atretic follicles due to reduced FSH signaling in adults of F1 generation (Tsoulis, 2014). Likewise pre-natal exposure to maternal HFD resulted in reduction in primordial, antral and graffian follicles number coupled with elevated expression of genes involved in apoptosis and follicular growth and development in the offspring ovary in C57Bl/6J mice. Interestingly paternal obesity also affects reproductive performance of F1 females as well as males. Fullston *et al* (2012) have demonstrated that paternal obesity causes intergenerational transmission of decline in fertility, particularly in males through both F1 and F2 generations in mice. The detrimental effects of male obesity on sperm are thought transmit to next generations through non- classical genetic mechanisms (e.g. epigenetic) (Fullston *et al.*, 2012). In view of these studies, present study investigated estrous cyclicity, mating, gestation, parturition performance of F1 offspring born to obese females as these reproductive outcome were not considered in earlier studies. The present study also differed from earlier studies in protocol, i.e. the obese pups born to obese mothers continued to receive HCD after weaning period, and also reproductive outcomes after mating alter between both obese F1 parents, and one F1 obese parent and one normal, have been studied. It is remarkable to note that impacts of obesity on some reproductive outcomes in F0 were also observed in F1, thereby indicating consistency in the results of our study. Fertility index was 100% in both generations, irrespective of whether a single parent was obese or both parents were obese, thereby indicating that the conception rate of female, was not affected by obesity though post-conceptual alterations were possible. Further gestation and parturition indices did not show significant variation in obese rats of either in F0 and F1 rats. However effects of obesity on other parameters were more severe in F1 obese rats than F0. There was a significant decrease in litter size, litter weight and increase in mortality rate in F0 as well as F1 obese rats compared to controls. However there was >50% reduction in litter size and weight and > 2 fold increase in pup mortality rate in F2 obese rats compared to F0 obese rats. These more intense reproductive impacts may be due to exposure of high nutrient content from pre-natal life through attainment of adulthood in F1 rats compared to exposure of HCD only during adult life for a short period of 8 weeks in F0. Thus our study reveals that duration of exposure to obesogenic factor determines severity of impact on reproductive outcome. Further our study also reveals another interesting fact that mating of HCD♂ of F1 with control female also decreased litter size, litter weight and increased pup mortality, without affecting body weight of F2 pups, thereby indicating involvement inheritance, classical or epigenetic in transmitting obesity across generations. Offspring (F1) born to obese females and fed with HCD during pre-pubertal and pubertal period showed low reproductive performance and increased pup mortality.

ACKNOWLEDGEMENTS

The work is supported by award of fellowship to first author by University Grant Commission, New Delhi under RFSMS Scheme.

Conflict of interest

The authors are declared that no conflicts of interest exist.

REFERENCES

1. Garbacia JAJr, Richter M, Miller S, Barton JJ. Maternal weight and pregnancy complications. Am J Obstet Gynecol 1985;152:238-245.



**Harish Navya and Hanumant Narasinhacharya Yajurvedi**

2. Catalano PM, McIntyre HD, Cruickshank JK. HAPO Study Cooperative Research Group The hyperglycemia and adverse pregnancy outcome study: associations of GDM and obesity with pregnancy outcomes. *Diabetes Care* 2012;35:780-786.
3. Lyra R, Neves G, Cavalcanti. Obesity In: Bandeira F (Editor), *Endocrinologia e diabetes*. Rio de Janeiro: Medisi 2003;1023-1032.
4. Wang JX, Davies MJ, Norman R.J. Obesity increases the risk of spontaneous abortion during infertility treatment. *Obes Res* 2002;10:551-554.
5. Lintsen AME, Pasker-De Jong PCM, De Boer EJ, Burger CW, Jansen CM, Braat DDM, van Leeuwen FE. Effects of subfertility cause, smoking and body weight on the success rate of IVF. *Hum Reprod* 2005;20:1867-1875.
6. Maheshwari A, Stofberg L, Bhattacharya S. Effect of overweight and obesity on assisted reproductive technology a systematic review. *Hum Reprod Update* 2007;13:433-444.
7. Edwards LE, Hellerstedt WL, Alton IR, Story M, Himes JH. Pregnancy complications and birth outcomes in obese and normal-weight women: effects of gestational weight change. *Obstet Gynecol* 1996;87:389-394.
8. Weiss JL, Malone FD, Emig D, Ball RH, Nyberg DA, Comstock CH, Saade G, Eddleman K, Carter SM, Craigo SD, Carr SR, D'Alton ME. Obesity, obstetric complications and Cesarean delivery rate—a population-based screening study. *Am J Obstet Gynecol* 2004;190:1091-1097.
9. Koning AMH, Kuchenbecker WKH, Groen H, Hoek A, Land JA, Khan KS, Mol BWJ. Economic consequences of overweight and obesity in infertility: a framework for evaluating the costs and outcomes of fertility care. *Human Reproduction Update* 2010;16: 246-254.
10. Ainge H, Thompson C, Ozanne SE, Rooney KB. Asystematic review on animal models of maternal high fat feeding and offspring glycaemic control. *Int J Obes (Lond)* 2011;35: 325-335.
11. Gniuli D, Calcagno A, Caristo ME, Mancuso A, Macchi V, Mingrone G, Vettor R. Effects of high-fat diet exposure during fetal life on type 2 diabetes development in the progeny. *J Lipid Res* 2008;49:1936-1945.
12. Guo F, Jen KL. High-fat feeding during pregnancy and lactation affects offspring metabolism in rats. *Physiology and Behavior* 1995;57:681-686.
13. Levin BE, Govek E. Gestational obesity accentuates obesity in obesity prone progeny. *American Journal of Physiology* 1998;275:1374-1379.
14. Bayol SA, Farrington SJ, Stickland NC. A maternal 'junk food' diet in pregnancy and lactation promotes an exacerbated taste for 'junk food' and a greater propensity for obesity in rat offspring. *British Journal of Nutrition* 2007;98: 843-851.
15. Bayol SA, Simbi BH, Bertrand JA, Stickland NC. Offspring from mothers fed a 'junk food' diet in pregnancy and lactation exhibit exacerbated adiposity that is more pronounced in females. *Journal of Physiology* 2008;586: 3219-3230.
16. Samuelsson AM, Matthews PA, Argenton M, Christie MR, McConnell JM, Jansen EH, Piersma AH, Ozanne SE, Twinn DF, Remacle C. Diet-induced obesity in female mice leads to offspring hyperphagia, adiposity, hypertension, and insulin resistance: a novel murine model of developmental programming. *Hypertension* 2008;51:383-392.
17. Shankar K, Harrell A, Liu X, Gilchrist JM, Ronis MJ, Badger TM. Maternal obesity at conception programs obesity in the offspring. *American Journal of Physiology. Regulatory, Integrative and Comparative Physiology* 2008;294:528-538.
18. Liang C, Oest ME, Prater MR. Intrauterine exposure to high saturated fat diet elevates risk of adult-onset chronic diseases in C57BL/6 mice. *Birth Defects Research. Part B, Developmental and Reproductive Toxicology* 2009;86:377-384
19. Nivoit P, Morens C, Van Assche FA, Jansen E, Poston L, Remacle C, Reusens B. Established diet-induced obesity in female rats leads to offspring hyperphagia, adiposity and insulin resistance. *Diabetologia* 2009;52:1133-1142.
20. Tamashiro KL, Terrillion CE, Hyun J, Koening JI, Moran TH. Prenatal stress or high-fat diet increases susceptibility to diet-induced obesity in rat offspring. *Diabetes* 2009;58: 1116-1125.



**Harish Navya and Hanumant Narasinhacharya Yajurvedi**

21. Yan X, Zhu MJ, Xu W, Tong JF, Ford SP, Nathanielsz PW, Du M. Up-regulation of Toll-like receptor 4/nuclear factor- κ B signaling is associated with enhanced adipogenesis and insulin resistance in fetal skeletal muscle of obese sheep at late gestation. *Endocrinology* 2010;151:380-387.
22. Li M, Sloboda DM, Vickers MH. Maternal Obesity and Developmental Programming of Metabolic Disorders in Offspring: Evidence from Animal Models. *Experimental Diabetes Research* 2011;2011:1- 9.
23. Bayol SA, Simbi BH, Stickland NC. A maternal cafeteria diet during gestation and lactation promotes adiposity and impairs skeletal muscle development and metabolism in rat offspring at weaning, *Journal of Physiology* 2005;567:951-961.
24. Taylor PD, Poston L. Developmental programming of obesity in mammals. *Experimental Physiology* 2007;92:287-298.
25. Morris MJ, Chen H. Established maternal obesity in the rat reprograms hypothalamic appetite regulators and leptin signaling at birth. *International Journal of Obesity* 2009; 33:115-122.
26. Elahi MM, Cagampang FR, Mukhtar D, Anthony FW, Ohri SK, Hanson MA. Long-term maternal highfat feeding from weaning through pregnancy and lactation predisposes offspring to hypertension, raised plasma lipids and fatty liver in mice. *The British Journal of Nutrition* 2009;102:514–519.
27. Khan I, Dekou V, Hanson M, Poston L, Taylor P. Predictive adaptive responses to maternal high fat diet prevent endothelial dysfunction but not hypertension in adult rat offspring. *Circulation* 2004;110:1097-1102.
28. Oben JA, Patel T, Mouralidarane A, Maj SA, Phillippa M, Joaquim P, Maelle M, Chad M, Junpei S, Marco N, Lucilla P, Paul T. Maternal obesity programmes offspring development of non-alcoholic fatty pancreas disease. *Biochemical and Biophysical Research Communications* 2010; 394: 24-28.
29. Shaw MA, Rasmussen KM, Myers TR. Consumption of a High Fat Diet Impairs Reproductive Performance in Sprague-Dawley Rats. *J. Nutr* 1997;127:64-69.
30. Sagae SC, Menezes EF, Bonfleur ML, Vanzela EC, Zacharias P, Lubaczeuski C, Franci CR, Sanvitto GL. Early onset of obesity induces reproductive deficits in female rats. *Physiology and behavior*. 2012;105:1104-1111.
31. Rasmussen KM. Effects of Under- and Overnutrition on Lactation in Laboratory Rats *J Nutr* 1998;128:390S-393S.
32. Suker DK, Thamer SJ, Taha TJA. The effect of maternal diet prior and during pregnancy in rats on obesity development in offspring. *European Journal of Experimental Biology* 2013; 3:191-198.
33. Ghanayem BI, Bai R, Kissling GE, Travlos G, Hoffler U. Diet-induced obesity in male mice is associated with reduced fertility and potentiation of acrylamide-induced reproductive toxicity. *Biol Reprod* 2010; 82: 94-104.
34. Bakos HW, Mitchell M, Setchell BP, Lane M. The effect of paternal diet induced obesity on sperm function and fertilization in a mouse model. *Int J Androl* 2011;34:402-410.
35. Fullston T, Palmer NO, Owens JA, Mitchell M, Bakos HW, Lane M. Diet-induced paternal obesity in the absence of diabetes diminishes the reproductive health of two subsequent generations of mice. *Human Reproduction* 2012;27:1391-1400.
36. Akamine EH, Marcal AC, Camporez JP, Hoshida MS, Caperuto LC, Bevilacqua E, Carvalho CRO. Obesity induced by highfat diet promotes insulin resistance in the ovary. *Journal of Endocrinology* 2010;206:65-74.
37. Balasubramanian P, Jagannathan LK, Subramanian M, Gilbreath ET, Kumar PSM, Kumar SMJM. High fat diet affects reproductive functions in female diet-induced obese and dietary resistant rats. *J Neuroendocrinol* 2012; 24:748-755.
38. Adilaxamma K, Janardhan K, Reddy KS. Monocrotophos: reproductive toxicity in rats. *Indian J. Pharmacol* 1994;26:26-129.
39. Narayana K, Prashanthi N, Nayanatara A, Harish HCK, Abhilash K, Bairy KL. Effects of methyl parathion (*o,o*-dimethyl *o*-4- nitrophenyl phosphorothioate) on rat sperm morphology and sperm count, but not fertility, are associated with decreased ascorbic acid level in the testis. *Mutat. Res* 2005;588:28-34.
40. Novelli ELB, Diniz YS, Galhardi CM, Ebaid GMX, Rodrigues HG, Mani F, Fernandes AAH, Cicogna AC, Filho JLVBN. Anthropometrical parameters and markers of obesity in rats. *Laboratory Animals*. 2007;41:111–119.
41. Cooper RL, Goldman JM, Vanderburgh JG. Monitoring of the estrous cycle in the laboratory rodent by vaginal lavage. In: Heindel J. J. and Chapin R. E., eds. *Methods in toxicology: Female reproductive toxicology* 1993;3b:45-56.





Harish Navya and Hanumant Narasinhacharya Yajurvedi

42. Bolumar F, Olsen J, Rebagliato M, Saez-Lloret I, Bisanti L. Body mass index and delayed conception: a European Multicenter Study on Infertility and Subfecundity. *Am J Epidemiol* 2000;151:1072-1079.
43. Rich-Edwards JW, Spiegelman D, Garland M, Hertzmark E, Hunter DJ, Colditz GA, Willett WC, Wand H, Manson JE. Physical activity, body mass index, and ovulatory disorder infertility. *Epidemiology* 2002;13:184-190.
44. Pasquali R, Gambineri A, Pagotto U. The impact of obesity on reproduction in women with polycystic ovary syndrome. *Br J Obstet Gynaecol* 2006;113:1148-1159.
45. Gesink Law DC, Maclehorse R.F, Longnecker MP. Obesity and time to pregnancy. *Hum Reprod* 2007;22:414-420.
46. Gouveia EM, Franci CR. Involvement of serotonin 5ht1 and 5ht2 receptors and nitric oxide synthase in the medial preoptic area on gonadotropin secretion. *Brain Res Bull.* 2004;63:243-251.
47. Desai M, Jellyman JK, Han G, Beall M, Lane RH, Ross MG. Maternal obesity and high-fat diet program offspring metabolic syndrome. *Am J Obstet Gynecol* 2014;211:1-13.
48. Purcella RH, Bo Suna, Lauren L, Pass, Michael L, Power, Timothy H., Moran, Tamashiro K.L.K. Maternal stress and high-fat diet effect on maternal behavior, milk composition, and pup ingestive behavior. *Physiol Behav* 2011;104:474- 479.
49. Tsoulis MW. Characterizing the impact of maternal obesity on offspring ovarian development in rats. Thesis for the degree of Master Science; 2014.

Table-1: Effect of high calorie diet on anthropometric parameters of adult female (F0) rats

Duration	Groups	Mean ± SE			
		Body Weight(gm)	Body Mass Index(BMI) (gm/cm ²)	Thoracic Circumference (TC) (cm)	Abdominal Circumference (AC)(cm)
Day zero	ND	155.4 ± 2.48	0.55 ± 0.01	11.06 ± 0.05	13.04 ± 0.05
	HCD	155.8 ± 1.98	0.55 ± 0.0	11.02 ± 0.03	13.06 ± 0.05
1 st week	ND	156 ± 1.70	0.55 ± 0.0	11.2 ± 0.03	13.06 ± 0.04
	HCD	163 ± 2.04*	0.59 ± 0.0*	11.4 ± 0.07*	13.24 ± 0.02*
2 nd week	ND	157.1 ± 1.87	0.57 ± 0.0	11.2 ± 0.02	13.1 ± 0.03
	HCD	173.6 ± 1.56*	0.61 ± 0.0*	11.6 ± 0.08*	13.4 ± 0.05*
3 rd week	ND	158.8 ± 1.77	0.58 ± 0.0	11.34 ± 0.08	13.16 ± 0.05
	HCD	182.6 ± 1.46*	0.64 ± 0.0*	11.94 ± 0.09*	13.68 ± 0.06*
4 th week	ND	161 ± 1.92	0.58 ± 0.01	11.5 ± 0.05	13.2 ± 0.03
	HCD	190.8 ± 1.31*	0.67 ± 0.01*	12.2 ± 0.11*	13.86 ± 0.05*
5 th week	ND	163.2 ± 1.74	0.59 ± 0.0	11.68 ± 0.02	13.3 ± 0.04
	HCD	196.8 ± 0.86*	0.71 ± 0.01*	12.5 ± 0.11*	13.92 ± 0.23*
6 th week	ND	164.6 ± 1.77	0.6 ± 0.01	11.96 ± 0.02	13.34 ± 0.04
	HCD	201.6 ± 1.28*	0.74 ± 0.0*	12.7 ± 0.06*	14.28 ± 0.06*
7 th week	ND	168 ± 1.51	0.61 ± 0.0	11.9 ± 0.15	13.36 ± 0.04
	HCD	207 ± 0.94 *	0.78 ± 0.0*	13.02 ± 0.04*	14.46 ± 0.05*
8 th week	ND	170.6 ± 1.43	0.62 ± 0.01	12.2 ± 0.06	13.48 ± 0.03
	HCD	212 ± 1.04 *	0.82 ± 0.0*	13.1 ± 0.03*	14.68 ± 0.05*

ND, normal diet, HCD , high calorie diet.

Mean values of ND and HCD groups were compared using student's t test and judged significant (*) if P< 0.05





Harish Navya and Hanumant Narasinhacharya Yajurvedi

Table-2: Effect of high calorie diet on blood biochemical constituents in adult female (F0) rats

Duration	Groups	Mean serum concentration (mg/100 ml) ± SE		
		Glucose	Cholesterol	Triglyceride
1 month	ND	69.12 ± 2.26	63.28 ± 2.05	62.14 ± 2.26
	HFD	101.1 ± 1.37*	100.2 ± 3.08*	99.9 ± 5.69*
2 month	ND	72.04 ± 1.93	67.66 ± 1.73	65.68 ± 1.73
	HFD	110.7 ± 0.8*	110.4 ± 2.96*	107.3 ± 4.34*

Note: ND, normal diet, HCD, high calorie diet.

Mean values of ND and HCD groups were compared using student's t test and judged significant (*) if P< 0.05.

Table-3: Effects of high calorie diet on reproductive performance of female (F0) rats

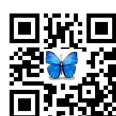
Parameter	Groups	
	ND	HCD
Fertility index (%)	100	100
Parturition index (%)	100	84.21
Gestation Index	100	93. ± 1.04*
Litter Size/rat	8.88 ± 0.61	6.38 ± 0.78*
Litter weight (gm)/rat	43.74 ± 2.74	35.79 ± 3.03*
Body weight/ pup (gm)	5.0 ± 0.05	5.18 ± 0.07*
Mortality of pups (%)	0	10

Note: ND, normal diet, HCD, high calorie diet; NS, Not significant.

Mean values of ND and HCD groups were compared using student's t test and judged significant (*) if P< 0.05.

Table-4: Effect of high calorie diet on anthropometric parameters of offspring (F1) born to obese mothers.

Age in post natal days	Groups	Mean ± SE			
		Body Weight (gm)	Body Mass Index(gm/cm ²)	Thoracic Circumference (cm)	Abdominal Circumference (cm)
Male rats					
PND zero	ND	5.06 ± 0.04	0.21 ± 0.0	3.9 ± 0.08	3.98 ± 0.07
	HCD	5.56 ± 0.13*	0.24 ± 0.0*	4.6 ± 0.17*	4.76 ± 0.16*
PND 30	ND	46.8 ± 2.10	0.31 ± 0.0	7.04 ± 0.53	8.12 ± 0.33
	HCD	68.2 ± 7.13*	0.45 ± 0.04*	8.9 ± 0.52*	9.9 ± 0.54*
PND 60	ND	138 ± 5.77	0.43 ± 0.02	9.9 ± 0.1	11 ± 0.15
	HCD	154.6 ± 3.5*	0.50 ± 0.0*	11.12 ± 0.09*	12.18 ± 0.09*
PND 100	ND	189 ± 2.68	0.48 ± 0.0	11.4 ± 0.16	12.26 ± 0.19
	HCD	239.2 ± 5.58*	0.61 ± 0.02*	12.9 ± 0.18*	14.26 ± 0.22*
Female rats					
PND zero	ND	4.9 ± 0.07	0.19 ± 0.0	3.4 ± 0.07	3.54 ± 0.05
	HCD	5.14 ± 0.05*	0.21 ± 0.01	3.76 ± 0.11*	3.84 ± 0.12*
PND 30	ND	40.2 ± 3.15	0.33 ± 0.01	7.16 ± 0.09	7.4 ± 0.17
	HCD	52.3 ± 4.0*	0.40 ± 0.02*	8.0 ± 0.17*	8.34 ± 0.20*





Harish Navya and Hanumant Narasinhacharya Yajurvedi

PND 60	ND	141.7 ± 1.78	0.44 ± 0.02	10 ± 0.0	11.0 ± 0.15
	HCD	155.6 ± 2.92*	0.50 ± 0.0*	11.12 ± 0.09*	12.18 ± 0.09*
PND 100	ND	163.2 ± 2.9	0.63 ± 0.01	13.26 ± 0.07	14.25 ± 0.02
	HCD	196.6 ± 2.82*	0.82 ± 0.0*	15.13 ± 0.05*	17.15 ± 0.04*

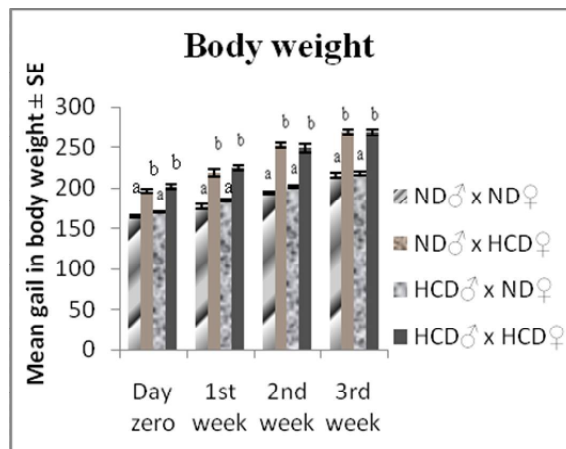
ND, normal diet, HCD, high calorie diet. Mean values of ND and HCD groups were compared using student's t test and judged significant (*) if P < 0.05.

Table-5: Effects of high calorie diet on estrous cyclicity of F1 rats

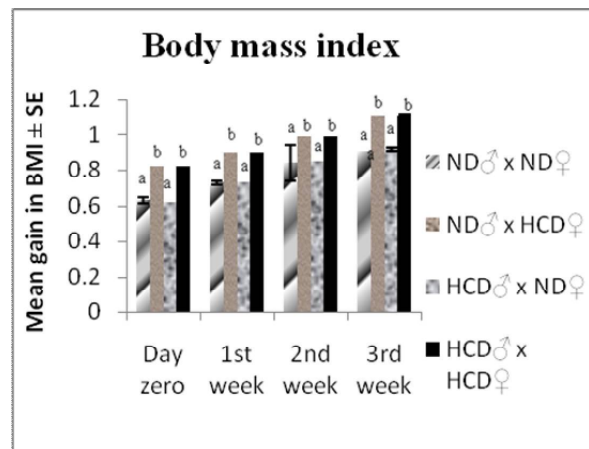
Estrous cycle	Groups	
	ND	HCD
Mean number of estrous cycles/ 2 month ± SE	19.3 ± 1.05	22.3 ± 0.9*
Mean length of estrous cycle ± SE	4.9 ± 0.14	4.4 ± 0.17*

Note: ND, normal diet, HCD, high calorie diet;

All values are mean ± SE; Mean values of ND and HCD groups were compared using student's t test and judged significant (*) if P < 0.05.



A.

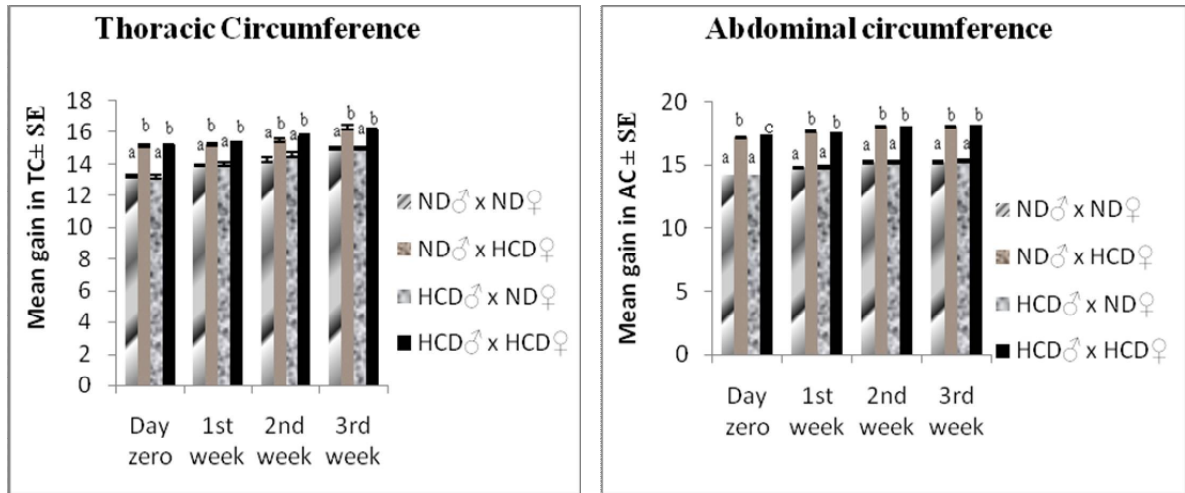


B.





Harish Navya and Hanumant Narasinhacharya Yajurvedi



C. D. **Fig.1: A-D: Anthropometric parameters of F1 female rats during gestation period.** ND, normal diet, HCD, high calorie diet.

Table-6: Effects of high calorie diet on F1 offspring born to obese (F0) rats

	ND♂ x ND♀	ND♂ x HCD♀	HCD♂ x ND♀	HCD♂ x HCD♀
Fertility index of male (%)	100	100	100	100
Fertility index of female (%)	100	100	100	100
Parturition index (%)	100	100	100	100
Gestation index	100 ^a	81.0 ± 9.27 ^a	91.0 ± 5.56 ^a	80.32 ± 8.3 ^a
Litter size/rat	9.8 ± 0.66 ^a	4.4 ± 0.5 ^b	4.6 ± 1.36 ^b	4.2 ± 0.37 ^b
Litter weight (gm)/rat	46.3 ± 2.5 ^a	20.5 ± 3.8 ^b	21.8 ± 6.3 ^b	24.04 ± 2.64 ^b
Body weight / pup (gm)	4.9 ± 0.18 ^a	5.36 ± 0.15 ^b	4.85 ± 0.08 ^a	5.5 ± 0.08 ^b
Mortality Rate of pups (%)	0	18.7	13.04	19.04

Note: ND, normal diet, HCD, high calorie diet.

All values are mean ± SE. Mean values in each column were compared by one way ANOVA followed by Duncan's multiple range test. Values with same superscript letters are not significantly different, whereas those with different superscript letters are significantly (P<0.05) different.





RESEARCH ARTICLE

cAMP regulate Morphology and Pathogenesis in the Fungal Pathogen *Tilletia indica*.

Shalini Purwar^{1*}, Shanthy Sundaram¹, Jitendra Jaiswal¹, V.K. Pati¹ and Anil Kumar²

¹Centre for Biotechnology, University of Allahabad, India.

²GB Pant University of Agriculture and Technology, Pantnagar, India.

Received: 24 Jul 2015

Revised: 29 Aug 2015

Accepted: 30 Sep 2015

*Address for correspondence.

Shalini Purwar
Centre for Biotechnology,
University of Allahabad,
Pantnagar, India.
E-mail: purwarshalini@gmail.com



This is an Open Access Journal / article distributed under the terms of the **Creative Commons Attribution License (CC BY-NC-ND 3.0)** which permits unrestricted use, distribution, and reproduction in any medium, provided the original work is properly cited. All rights reserved.

ABSTRACT

T. indica is fungal pathogen that infects the spike of wheat during development stages. The development of monosporial culture of *T. indica* on PDA media. The monosporial culture allows growing on different concentration of dbcAMP. The mycelial biomass decreased at 21 days of growth in dbcAMP treated culture at 5.0 mM. Pathogenic variations among 3 different isolates were studied by inoculating cAMP treated and without treated monoteliosporic cultures on host genotypes comprising of susceptible and resistant wheat, at physiological growth stage Z-49. After maturity, the inoculated ear heads were categorized into five grades of infection on the basis of area of endosperm converted into sooty mass of fungal teliospores and coefficient of infection [CI] was calculated based on the formula. Based on disease responses of pathogenic groups were identified, without cAMP treated KB9 isolate was highly virulent; KB3 isolate moderately and PJK least virulent, while the Ms Cultures when inoculated individually did not produce infection. Matting between, Ms Cultures of KB9 and PJK produced infection while in presence of dbcAMP, combination, Ms Cultures of KB9 and PJK did not produced infection. It is concluded that, *T. indica*, the basidiomycete bunt pathogen of wheat, exhibit dimorphism in which mating between haploid budding cells establishes a pathogenic filamentous cell type, and cAMP A signaling cascade controlling mating and virulence in *T. indica*.

Key words: c-AMP, *Tilletia indica*, wheat, Pathogenesis.



**Shalini Purwar et al.**

INTRODUCTION

Wheat is one of the important staple crops of India. Wheat occupies more than 25 million hectares area in India with a production of about 70 million tones. Although there is quantum jump in the productivity of wheat yet it's adversely affected by several fungal diseases like brown, yellow and black rusts, leaf blight, loose smut and bunt. Karnal bunt (KB) caused by *Tilletia indica* Mitra syn. *Neovossia indica* (Mitra) Mundukar is an economically important disease of wheat in the northwestern regions of India and other parts of the world. It is a floret-infecting disease that partially infects seed of wheat and hence also called partial bunt [1]. Many aspects concerning disease development are yet to be answered. The proper understanding of KB disease at cellular and molecular level would help to devise strategies for successful management of disease. Researchers interested in the study of bunt fungi recognized that KB can be made excellent model system because of the yeast like habit of bunt fungi in pure culture, and availability of both haploid (n) and diploid (2n) cells, it occurs in three morphologically distinct forms in the life cycle [2,3]. Mating is an essential step in the life cycle of most homobasidiomycetes. No special cells are required for mating; fusion between vegetative mycelial/sporidial cells is sufficient to trigger a well-characterized developmental sequence that converts monokaryon into dikaryon. However, evidence for mating interaction to establish the infectious cell type during morphological differentiation of KB is not clearly demonstrated [3]. The molecular signals required for establishing and maintaining the infectious dikaryons would have to be identified by investigating the role of c-AMP in fungal pathogenesis.

The pathogenic mechanism to cause KB disease can be traced out by understanding of cAMP-adenylate cyclase system in fungus, *T. indica*. The conversion of vegetative mycelial to sporidial phase in this pathogen may also be centered near this molecular signalling system. Distinct morphological and biochemical changes are invariably associated with morphological differentiation and/or transition of haploid mycelial to sporidial to diploid teliospore phase. During development, *T. indica* appears a phenotypic mixture of genetically identical (haploid) cells but morphologically differentiated cells like haploid mycelial and allantoid/filiform sporidial form or genetically different but mixture of haploid and diploid fungal populations. The process of sporidiation during developmental cycle of fungus accompanied the change in morphology and in turn to appearance and/or disappearance of developmentally related markers on fungal population. Number of these markers is small compared to common structural proteins of different fungal populations. Characterization of these changes in relation to growth and morphological differentiation has become difficult without suitable probe. Therefore, KB has become the bunt fungus of choice for studies the influence of dbc- AMP on induction of growth habit, morphological changes, sporidia formation, and to test the Pathogenic variability of *T.indica*.

MATERIALS AND METHODS

Collection of Fungus Stains

In present study two strain KB9 and PJ of *T.indica* and its monoteliosporic cultures were used. These cultures were collected from the Department of Molecular Biology and Genetic Engineering, GB Pant University of Agriculture and Technology Pantnagar (Table 1).

Collection of Wheat Genotype

In present study two genotypes (WH-542, HD-29) of bread wheat [*Triticum aestivum*] were used. The seeds of these genotypes- one highly susceptible and another resistance to Karnal bunt based on pathogenicity testing under field conditions were collected from the CRC, Pantnagar and from Department of Molecular Biology and Genetic Engineering, GB Pant University of Agriculture and Technology Pantnagar (Table 1).



**Shalini Purwar et al.****Morphological Studies**

T.indica grown in media containing dbcAMP and fungus growth was observed at 14 days and 21 day of inoculation using aniline blue. The fungal mycelia were teased to separate interwoven mycelial network with help of needle on side itself. After teasing, staining was done using mounted on lactophenol. To determine the effect of dbc-AMP on morphogenetic development, the stained mycelia or other structures from at least three different regions were examined by light microscopy and scored as morphologically differentiated if they possessed sporidia or chlamydospores

Inoculum Preparation and inoculation of host differentials

Monosporidial lines of the fungus were grown in shake culture in 250-ml flasks containing 50ml of potato extract solution to which mycelia and secondary sporidia were added from the PDA slants. Secondary sporidia developed in profuse numbers following 7 days of continuous shaking at 20° C. These were pelleted by centrifugation and the pellets were resuspended in 100 ml of dilute potato extract. Immediately thereafter, portions of the various sporidial suspensions were paired and used as inoculums. In all tests suspensions of unpaired monosporidial lines served as controls.

The seeds of resistance and susceptible genotypes were sown in field with a mixture of loamy soil and farm yard manure (3:1, v/v) supplemented with NPK fertilizer under polyhouse conditions. Sporidial suspension containing allantoids secondary sporidia @ 104/ml was prepared and five tillers of each differential host were inoculated during evening hours using hypodermic syringe [4]. High humidity was maintained by spraying the inoculated plants with water. Uninoculated checks for each genotype were also maintained. The experiment was conducted in a completely randomized design (CRD) with three replicate. After maturity, Disease Scoring was done on the basis of the percentages of infected kernels. Average percent-infected grains were calculated after harvesting. As most bunted grains, partially infected, numerical values, depending upon the extent of damage to the grains, were given for calculating coefficient of infection. Number of grains showing incipient infection, blackening extended up to half of the grain, three fourth of grain and infected grains were multiplied with the numerical values 0.25, 0.5, 0.75, and 1.0 respectively and then divided by 100 to obtain percent coefficient of infection.

Percentage coefficient of infection = $(\sum XY / \text{Total no of infected seed}) \times 100$

Dibutyryl cyclic-AMP treated fungal growth in liquid culture

The fungal mycelia in equal proportion will be inoculated in 50 ml PDB allowed to grow for 2 days. At the end of 48 h, concentration of 1× 25 mM dbc-AMP in was added in different wells and allowed to grow in BOD incubator at 22 ± 1°C. The fungal mycelia will grow either in the presence or absence of dbc-AMP[5].

Determination of Growth Kinetic and Microscopic Examination

All cultures treated and Without Treat with dbcAMP, were culture on Solid as well as liquid media. Radial diameters of mycelia were measured at 3 days intervals. To study the fungal morphology, mycelia were picked from the culture at desired 7 days and 21 days interval and placed on glass slides. A drop of cotton blue was added over the fungal mycelial and teased to get an even and thin mycelia spread over a slide. Then a drop of Lactophenol was added to fix the slide. The temporal mounted slides were examined through microscope.



**Shalini Purwar et al.**

Pathogenic variability of *T.indica* and Disease Scoring

Pathogenic variations among 2 different isolates was studied by inoculating monoteliosporic cultures on 2 differential host genotypes comprising of susceptible and resistant wheat lines (Table 1), at physiological growth stage Z-49 [6]. The genotypes were sown in 10 cm diameter pots filled with a mixture of loamy soil and farm yard manure (3:1, v/v) supplemented with NPK fertilizer under poly-house conditions. After germination, only five healthy seedlings were retained per pot. Sporidial suspension containing allantoids secondary sporidia @ 10^4 /ml was prepared and five tillers of each host were inoculated during evening hours using hypodermic syringe [4]. High humidity was maintained by spraying the inoculated plants with water. Uninoculated checks for each genotype were also maintained. After maturity, Disease Scoring was done on the basis on the basis of the percentages of infected kernels. Average percent-infected grains were calculated after harvesting by using the following formula.

Estimation of total protein by Lowry method

Total protein isolated from dbc AMP treated and non- treated *T.indica*. Protein concentration was measured by the method developed by [7] and modified by [8]. Take the optical density (measure the absorbance) at 660 nm. The amount of protein was estimated from a standard curve prepared by using BSA as a source protein.

Protein Profiling by SDS-PAGE

Protein Profiling of total protein isolated from dbc AMP treated and non- treated *T.indica* was done according to protocol of [23], by using 12.5% discontinuous polyacrylamide gel.

RESULTS AND DISCUSSION

In vitro culture of fungus is provides a useful system for generating good deal of information about molecular and cellular mechanisms underlying the transition of vegetative to sporidial phase. Analysis of sporidiation and biomolecules involved in their production offers the opportunity to explore mechanisms of intra cellular and extra cellular signalling, biochemical basis of recognition, fusion and development of sexual pathway and role of adenylate cyclase/c-AMP cascade [9]. This cascade is involved in sensing nutrient levels in Mutations in this pathway have pleiotropic effects on differentiation including cell division, mating and sporulation.

Morphological Studies

Two different strain of *T.indica* KB9 and PJ and its monoteliosporic culture grown under BOD at 21°C. Dikaryotic and monoteliosporic culture of KB9 and PJ stain of *T.indica* were treated with 5 mM concentration of dbcAMP, and grown in PDB under 120 rpm upto 14 day at 21°C. After 14 day exposure of fungal cells to dbc-AMP, mycelia collected and stained with lactophenol cotton blue, and under goes microscopic examination. Light microscopic observation of stained fungal cultures revealed morphogenetic alteration in the fungal population as indicated in Table 3. A significance variation was obserbed in both number, form of sporidium and morphology of mycelia in both Dikaryotic and monoteliosporic culture of KB9 and PJ. Light microscopic examination of lactophenol cotton blue stained fungal cultures revealed that following 14 days exposure of fungal cells to dbc-AMP, the fungal population appeared to undergo morphogenetic changes which showed condensation of mycelia and subsequently induced in the form of filiform sporidia (Figure1) cheek and count by Haemocytometer. Fungal cultures grown in the absence of dbc-AMP supported the mycelination in the form of network of fungal hyphae (Figure 1 a & b). The extent of sporidiation continuously increased following subsequent days of incubation in the presence of dbc-AMP. Although, morphological differentiation from mycelial to sporidial phase occurred spontaneously *in vitro* cultures, but the process was enhanced by addition of dbc-AMP (Table 3). The chemical agent like dbAMP could therefore, prove extremely useful in inducing sporidia formation and subsequent development as well as altering the



**Shalini Purwar et al.**

virulence of pathogen. Studies on mating in lower eukaryotes, including yeast and filamentous fungi, have revealed role of c-AMP in various aspects of fungal biology, including both growth and cell cyclic progression [10, 11]. In addition, in the phytopathogens, *Magnaporthe grisea* and *Colletotrichum trifolii*, c-AMP has been demonstrated to play an important role during appressorial differentiation [12,13]. [14] suggested that cAMP pathway is involved in early stages of saprophytic germination, in contrast to the pathogenic germination. However, whether c-AMP plays any such role in the regulation of morphological differentiation of *T. indica* during pathogenesis and host-parasite interaction or not, is yet to be investigated.

Pathogenic variability and Disease Scoring

To check the revelation about dbcAMP signaling in virulence, in present study two isolates and its Ms cultures of *T.indica* were inoculated with and without treatment of dbcAMP on a two differential hosts one resistant (HD 29) and susceptible genotype (WH542) at physiological growth stage Z-49 [6] **Figure 2**. Infection calculated on the basis of coefficient of infection and percentages of infection. dbcAMP treated KB 9 produced C.I. ranging between 0.025 on genotype HD29 and 0.065 on WH542. While without dbcAMP treated KB9 showed C.I. 0.07 on HD 29 and 0.225 on WH542. Isolate PJ (collected from Punjab and Jammu and Kashmir) treated with dbcAMP was least virulence showed immune reaction by this isolate on resistant genotype. This isolate induced moderately susceptible reaction on genotypes WH 542, highly susceptible genotypes, on which all KB9 isolates produced Susceptible 'S' response. Ms Cultures when inoculated individually produce infection after more suitable condition, while dbcAMP MS culture did not produce infection. In combination, Ms Cultures of KB9 and PJK produced infection. While dbcAMP treated KB9 PJ did not produce infection. The self paired Ms Cultures caused no infection but cross combination resulted in successful infection in both resistant and susceptible genotype against Kernal Bunt. (**Table 4**). Our results on pathogenic variability and previous results on the host pathogen interaction have indicated that there is no well-defined race concept in this pathogen based on the reaction on a set of hosts, as it exists in the wheat rusts [15] and rice variety against blast [16]. *T.indica* exhibits high level of genetic variability among the isolates [17] exhibiting varying degree of virulence like *Magnaporthe oryzae* exhibit distinctive pattern of genetic diversity [18].

Influence of dbAMP on Protein extractability from *T.indica*

The amount of protein extracted in Tris buffer saline (pH 6.8) and then precipitates in 70% acetone from dbcAMP treated and non-treated culture of *T.indica*. Measure the total protein from *T.indica* by Lowry (1951) method using BSA as control. Total protein was increase in dbcAMP treated KB9 and PJ isolate than in the non-treated culture (**Table 5**). In its monoteliosporic (ms) culture was showed decrease total protein when compared with the dbcAMP non-treated culture. Increase in the amount of proteins in dikaryotics strains (KB9 and PJ isolate) of *T.indica* indicates the induction of expression of proteins by dbcAMP treatment. This reveals both either synergistic or antagonistic expression of proteins **Figure 3**. [24] suggested that the role of c-AMP in signaling the nutritional status of the cell. Cellular cAMP levels activate the PKA catalytic subunits for induction of spore formation [19]. Cellular cAMP levels, influence by G α /Ras (G-proteins, Ras2p and Gpa2p) pathway via regulation adenylyl cyclase in *S. cerevisiae*. Both genes [*Ras2p* and *Gpa2p*] Mutants defective exhibits a very slow growth phenotype (forming less mycelination) on rich medium [20, 21]. Externally supply of c-AMP suppressed the effect by gene encoding c-AMP phosphodiesterase [20, 21, 22].

Influence of dbcAMP on protein profiles from *T.indica*

We tested the effect of external dbc-AMP on the differential expression of proteins. Total protein profiling carried out by SDS-PAGE 12.5% polyacrylamide gel. During gel electrophoresis loaded 50 ug of protein for comparative studies. Banding patterns of protein suggests marked changes that have been associated with the transition from vegetative mycelial phase to the sporidial phase. Such variations may be due to differential expressions of proteins at two stages of development or due to transition from vegetative mycelial to sporidial phase. There are certain bands, which are



**Shalini Purwar et al.**

present only in dbcAMP treated culture of the fungus. It has been supported by morphological examination at experimental phase of the growth of either mycelial or sporidial rich fungal population. The fungus is in vegetative phase; hence, these bands are vegetative phase-specific. The bands that are present in both treated and nontreated dbcAMP may be those of the structural proteins, which are required for the growth cycle of *T. indica*. Hence, they are continuously expressed (**figure 4**). Some bands were present in all the stages of growth cycle of the fungus but the intensity of the bands greatly varied. This variation may be due to some kind of transcriptional and post-translational changes, which may affect the mobility of the band slightly from their original position. There are certain bands, which are associated with only a specific stage. These represent a unique kind of protein whose presence marks specifically the actual stage of the culture, since they are expressed only in dbcAMP treated fungus. The characterization of this stage dbcAMP treated specific protein will enable to provide a useful marker for the study of morphological differentiation of *T. indica* **Table 6**.

Fungi employ dbc-AMP significantly in a variety of processes including the control of differentiation, sexual development and virulence in addition to the monitoring of nutritional status and stress. Furthermore, the c-AMP pathway influences transcription and cell cycle progression. Recent forays in to filamentous fungi including pathogens of plants and animals have provided revelations about c-AMP signalling in morphological development and virulence. Information accumulated on the role of c-AMP on morphogenesis and stress in these fungi indicates that similar components will be induced and play important role in phytopathogenic fungi like *T. indica*.

It is clear that general topic of nutritional status and signalling in phytopathogenic fungi requires considerable attention. Hence, these useful paradigms can also be applied in KB (*T. indica*) for understanding the transition, formation of specialized cell types and also in understanding the biology of pathogen. It provides an obvious entry point to learn more about aspects of cell-to-cell signalling, differentiation (e.g. mating structures, sporidia formation) and regulation of gene expression and alteration in surface properties in fungi. The mycelial biomass decreased with increasing concentrations of dbc-AMP. It was observed that dbc-AMP showed inhibitory growth response to *T. indica* and induced sporidia formation. Not only fungal mycelia grow at a slower pace in the presence of dbc-AMP but also the mycelial biomass was reduced by nearly 25%. It was dbcAMP Treated culture reduces virulence factor compare to the no treated culture. dbcAMP reduces mating between two different monosporidial culture of dbcAMP and hence reduce the pathogenicity between *T. indica*. Total protein concentration increases after treatment with dbcAMP. Some extra protein bands appear after treatment with dbcAMP. It is concluded that, *T. indica*, the basidiomycete bunt pathogen of wheat, exhibit dimorphism in which mating between haploid budding cells establishes a pathogenic filamentous cell type, and cAMP A signaling cascade controlling mating and virulence in *T. indica*.

ACKNOWLEDGEMENTS

Research here reported is supported by grants of Dr. D.S. Kothari Post Doc Fellow UGC, New Delhi. Author also acknowledge to Prof. Anil Kumar, GB Pant University of Agriculture and Technology, Pantnagar for provided me *Tilletia* culture for this work.

REFERENCES

1. Mitra M. 1931 A new bunt of wheat in India; *Ann. Appl. Biol.* 18 178–179
2. Dhaliwal H S. and Singh D V. 1988 Interrelationship of two types of secondary sporidia of *N. indica*; *Phytopathology* 41 276
3. Kumar A., Singh U S, Singh A., Malik V S. and Garg G K. 2000 Molecular signalling in pathogenicity and host recognition in smut fungi taking Karnal bunt as a model system; *Indian J. Exp. Biol.* **38**525
4. Aujla SS., Grewal AS., Gill KS, Sharma I. 1989 A screening technique for Karnal bunt disease of wheat. *Crop Improv* 7:145–146





Shalini Purwar et al.

5. Kumar A., Kaushlendra T., Rana M., Purwar S. and GARG G K. 2004 Dibutyryl c-AMP as an inducer of sporidia formation: Biochemical and antigenic changes during morphological differentiation of Karnal bunt (*Tilletia indica*) pathogen in axenic culture. *J. Biosci.* 29 (1) 23–31
6. Zadoks J.C., Chang T.T., Konzak CF.1974 A Decimal Code for the Growth Stages of Cereals", *Weed Research* 14:415-421.
7. Lowry OH, Rosebrough NJ, Farr AL, Randall RJ. 1951. Protein measurement with the Folin phenol reagent. *Journal Biological Chemistry.*193 [1]: 265–75.
8. Hartree, E.E. (1972). Determination of protein; a modification of the Lowry method that gives a linear photometric response. *Anal. Biochem.* 48, 422-427
9. Hall A A, Bindslev L, Rouster J, Rasmussen S W, Oliver R P and Gurr S J. 1999 The involvement of cAMP and protein kinase A in conidial differentiation by *Erysiphe graminis* flsp. *Plant microbe interact* 12: 960-968
10. Pasquale S M and Good Enough V W 1987 Cyclic-AMP func-tions as a primary sexual signal in gametes of *Chlamydomo-nas reinhardtii*; *J. Cell Biol.* 15279
11. Bencina M, Panneman H, Ruijter G J G, Legisa M and Visser J 1997 Characterization and overexpression of the *Aspergillusniger* gene encoding the cAMP dependent protein kinasescatalytic subunit; *Microbiology*143 1211–1220
12. Lee Y H and Dean R A 1994 Hydrophobicity of contact surfaces induces appressorium formation in *Magaporthe grisea*. *Plant cell* 5:693-670
13. Yang Z and Dickman M B 1997 Regulation of cAMP and cAMP dependent protein phosphorylation during conidial germination and appressorium formation in *Colletotrichumtrifolii*; *Physiol. Mol. Plant Pathol.*50117–127
14. Borhoom and Sharon Amir 2004. cAMP regulation of pathogenic and saprophytic fungal spore germination. *Fun. Genet. Biol.* 41: 317-326
15. Thirumalaisamy P.P., Singh D.V., Aggarwal R, Gogoi R, GUPTA and Singh P.K. 2006 Development of specific primers for detection of Karnal bunt pathogen of wheat Indian Phytopath. 64 (2): 164-172
16. Suh JP, Noh TH, Kim KY, Kim JJ, Kim YG, Jena KK 2009 Expression levels of three bacterial blight resistance genes against K3a race of Korea by molecular and phenotype analysis in japonica rice (*O. sativa* L.). *J Crop Sci Biotechnol* 12:103-108
17. Mishra A., Singh U.S., Goel R., and Kumar, A.2002 PCR based molecular technique for identification and discrimination of quarantined and non-quarantined *Tilletia* sps. *Indian J. Exp.Biol.* 40: 1137-1142.
18. Takan, J.P.; Chipili, J.; Muthumeenakshi, S.; Talbot, N.J.; Manyasa, E.O.; Bandyopadhyay, R.; Sere, Y.; Nutsugah, S.K.; Talhinhas, P.; Hossain, M.; Brown, A.E. & Sreenivasaprasad, S. 2011 *Magnaporthe oryzae* populations adapted to finger millet and rice exhibit distinctive patterns of genetic diversity, sexuality and host interaction. *Molecular Biotechnology* y, DOI 10.1007/s12033-011-9429-z [Online First], Available from http://cogeme.ex.ac.uk/talbot/pdf/2011_Takan_molbio_moryzae_population.pdf, ISSN 1559-0305.
19. Hatanaka & Shimoda C, 2001. The cAMP/ PKA signal pathway is required for initiation of spore germination in *Schizo sacchromyces pombe*. *Yeast* 18, 207-217
20. Kubler E, Mosch H U, Rupp S and Lisanti A 1997 G-protein, Gpa2p a subunit, regulates growth and pseudohyphal deve-lopment in *S. cerevisiae* via a cAMP-dependent mechanism; *J. Biol. Chem.*27220321–20323
21. Xue Y, Battle M and Hirsch J P 1998 GPRI encodes a putative G-protein-coupled receptor that associates with the Gpa2p Ga subunit and functions in a Ras-independent pathway; *EMBO J.*171996–2007
22. Lorenz M and Heitman J 1997 The MEP 2 ammonium permease regulates pseudohyphal differentiation in *S. cerevisiae*;

BOOKS

23. Sambrook J, Fritschi EF and Maniatis T [1989] *Molecular cloning: a laboratory manual*, Cold Spring Harbor Laboratory Press, New York.
24. Egel R., 1989 Mating type genes, meiosis and sporulation; in *Molecular biology of the fusion yeast* [eds] A Nasim, P Young and B F Johnson [San Diego: Academic Press] pp 31–73





Shalini Purwar et al.

Table 1. Collection of Fungal Strains

Serial No.	Isolates/ Monosporidial strains	Collected From
1	KB9	Pantnagar
2	KB9ms1	Pantnagar
3	KB9ms2	Pantnagar
4	KB9ms3	Pantnagar
5	PJ	Punjab and JK
6	PJmsa	Punjab and JK
7	PJmsb	Punjab and JK
8	PJmsc	Punjab and JK

Table 2: Various group and variety of wheat genotype used

Genotypes	Group	Susceptible /Resistant
HD 29	Aestivum	Resistant
WH542	Aestivum	Susceptible

Table 3: Morphological variation of fungal isolates and monosporidial strains under microscopic observation.

S. No.	Isolates/ Monosporidial strains	Sporidial count (Number×10 ⁶) Without cAMP	Sporidial count (Number×10 ⁶) With cAMP	Morphological Characteristics	
				14 days after inoculation Without cAMP	14 days after inoculation With cAMP
1.	KB9	37.0	672.0	thick mycelium few allantoidsporidium	Thin mycelium few allantoidsporidium
2.	KB9ms1	5.4	18.6	Thin mycelium few allantoidsporidium production	Thin and thick mycelium, all filiformsporidium.
3.	KB9ms2	3.3	37.5	thick mycelium	Thin and thick mycelium few allantoidsporidium





Shalini Purwar et al.

					production
4.	KB9ms3	2.3	259.0	thick mycelium	Thin mycelium and chlamyospore formation, moderate allantoid production
5.	PJ	87.0	1630.0	Thin and thick mycelium, Chlamyospores formation	Mycelium thinning and moderate allantoidsporidium production
6.	PJmsa	3.7	918.0	thick mycelium allantoidsporidium production	Thin mycelium heavy allantoidsporidium production
7.	PJmsb	130.0	1908.0	Thin and thick mycelium few allantoidsporidium production	Thin mycelium, Chlamyospores formation and few allantoidsporidium formation
8.	PJmsc	17.5	217.9	thick mycelium allantoid formation	Mycelium less and few allantoidsporidium formation
9.	PNKB1	328.0	2258.6	thick mycelium no sporidium formation	Thin mycelium moderate allantoid formation
10.	PNKB2	341.	1432.0	Thin mycelium	Mycelium clustering and few allantoid
11.	PNKB	289.0	1344.0	Mycelium thickening, Chlamyospores formation and few allantoidsporidium formation	Mycelial clustering moderate allantoid





Shalini Purwar et al.

Table 4: Coefficient of Infection and Disease response of *T.indica* isolates on differential host genotype

Host		Fungal Strain										
		Control	KB9 (with out treatment of cAMP)	KB9 (with treatment of cAMP)	KB9ms1 (with out treatment of cAMP)	KB9ms1 (with treatment of cAMP)	PJ (with out treatment of cAMP)	PJ (with treatment of cAMP)	PJmsa (with out treatment of cAMP)	PJmsa (with treatment of cAMP)	KB9ms X PJmsa (with out treatment of cAMP)	KB9ms X PJmsa (with treatment of cAMP)
Resistant Genotype	Total No of Seeds per plot	164	127	152	134	146	120	149	133	151	133	156
	Weight of 10 seeds	10gram	7.77	9.21	7.98	9.89	6.69	8.76	9.23	10	7.67	9.99
	No. of Seeds with susceptible reaction	0	16	2	14	0	18	5	3	0	12	0
	Percentage Infection	0	16	12	14	2	37	10	8	0	15.96	0
	Coefficient infection											
Susceptible Genotype	Total No of Seeds per plot	177	100	143	140	160	105	150	142	166	100	159
	Weight of 10 seeds	7	4.5	5.2	5.23	6.43	4.56	6.78	6.12	7.88		
	No. of Seeds with susceptible reaction	0	45	13	24	6	37	12	12	3	21	0
	Percentage Infection		45	18.59	33.6	9.6	38.85	18	17.04	4.9	21	0
	Coefficient infection	0										

Table 5: Influence of cAMP on Protein extractability from *T.indica*

S.No	Treatment	Weight of mycelium or spore	Protein Concentration Ug/ul	Volume of Extract (ml)	Protein /gram of mycelium	Percent increase and decrease in the protein extractability
1.	KB9 (with out treatment of cAMP)	2	1.5	2	1.5	
2.	KB9 (with treatment of cAMP)	2	4.2	2	4.2	+64%
3.	KB9ms1 (with out	2	3.3	2	3.3	





Shalini Purwar et al.

	treatment of cAMP)					
4.	KB9ms1(with treatment of cAMP)	2	3.0	2	3.0	-9.09%
5.	PJ (without treatment of cAMP)	2	0.5	2	0.5	
6.	PJ (with treatment of cAMP)	2	1.2	2	1.2	+58%
7.	PJmsa (with out treatment of cAMP)	2	3.9	2	3.9	
8.	PJmsa (with treatment of cAMP)	2	2.55	2	2.55	-34%

Table 6. Treatments and bands

S.no.	Treatments	In Presence of dbcAMP		
		Similar Band	Dissimilar Band	Total Number of band
1.	KB9	3	3	15
2.	KB9ms	3	1	7
3.	PJ	3	4	10
4.	PJmsa	3	3	12



Figure: 1a





Shalini Purwar et al.

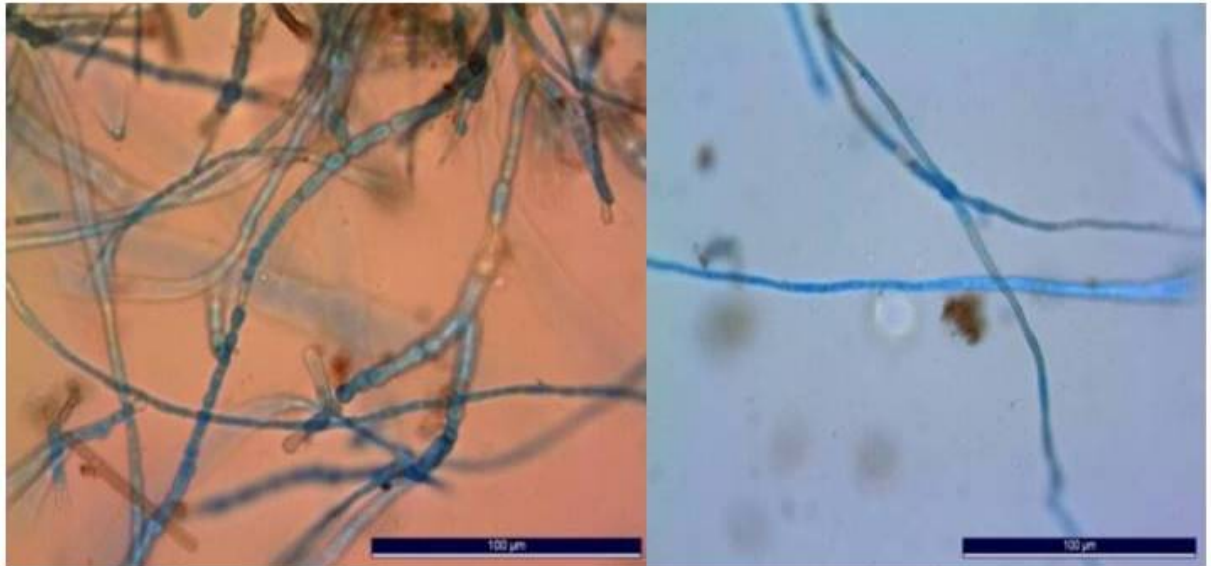


Figure: 1b



Figure 2





Shalini Purwar et al.

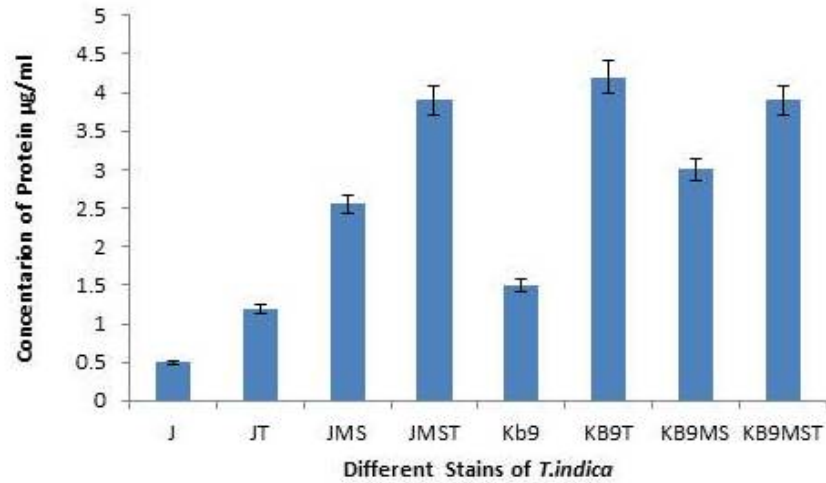
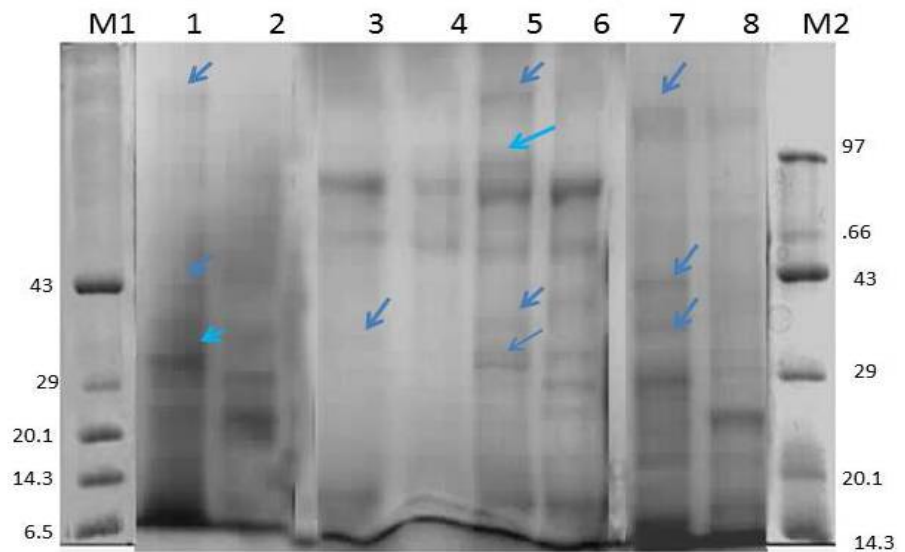


Figure: 3



- M1.Low molecular weight Marker)
- M2. Medium Molecular weight Marker
- 1. KB9 (with treatment of cAMP)
- 2. KB9 (without treatment of cAMP)
- 3. KB9ms1(with treatment of cAMP)
- 4.KB9ms1(without treatment of cAMP)
- 5.PJ (with treatment of cAMP)
- 6.PJ (without treatment of cAMP)
- 7.PJmsa (with treatment of cAMP)
- 8.PJmsa (without treatment of cAMP)

Figure 4





RESEARCH ARTICLE

Shelf Life Assessment of Rohu (*Labeo rohita*) in Ice and Ambient Temperature

K.Sravani, K.Dhanapal, A.Balasubramanian¹, N.Madhavan and GVS Reddy²

College of Fishery Science, SVVU, Muthukur-524 344, Andhra Pradesh, India.

¹Fisheries Research Station, Undi, West Godavari, Andhra Pradesh, India.

²Fisheries Research Station, Palair, Khammam, Telangana, India.

Received: 24 Mar 2015

Revised: 29 April 2015

Accepted: 15 May 2015

*Address for correspondence

K.Sravani

College of Fishery Science,

SVVU, Muthukur-524 344,

Andhra Pradesh, India.

E-mail: shine7sravani@gmail.com



This is an Open Access Journal / article distributed under the terms of the **Creative Commons Attribution License** (CC BY-NC-ND 3.0) which permits unrestricted use, distribution, and reproduction in any medium, provided the original work is properly cited. All rights reserved.

ABSTRACT

A study on the shelf life assessment of rohu (*Labeo rohita*) in ice and ambient temperature was carried out. The storage life of the fish was 18 days in ice and 12 hrs at ambient temperature. TVB-N and Peroxide Values continuously increased with the increase of storage period. TVB-N value did not support those of sensory evaluation and microbial analysis at ambient temperature. Where as peroxide value increased from 2.82 ± 0.28 meq O₂ /kg of fat to 10.42 ± 0.32 meq O₂ /kg of fat. Organoleptic acceptability was 18 days in ice and about 12 hours at room temperature. Results of bacterial load showed that the samples were in acceptable condition, not exceeding 10⁶ cfu/g for 18 days in ice and 12 hrs at ambient temperature. The initial bacterial load for ice stored samples was predominated by mesophiles. However, as storage period progressed total psychrophilic count, *Pseudomonas* sps, H₂S producing bacteria and *Aeromonas* sps increased in number showing that these microbes were the spoilage organisms in Ice. At ambient temperature, major spoilage organisms were *Aeromonas hydrophila*, *E.coli*, *Shigella* sps and *Bacillus* sps. Torrymeter and sensory assessment readings were also taken for both ice and ambient stored fishes where the values decreased with increase in storage period.

Key words: shelf life assessment, *Labeo rohita*, *Pseudomonas* sps, Peroxide Values.



**K. Sravani et al.**

INTRODUCTION

Very few studies have been conducted on the quality and shelf life of fresh water fish in storage condition in contrast to the lots of information that is available for marine species. Chandrashekar *et al.* (2004) established the relationship between the changes in muscle biochemical composition of *Labeo rohita* in relation to season. Adoga *et al.* (2010) carried out a study on storage life of tilapia in ice and ambient temperature. Azam *et al.* (2005) studied about the quality changes in pangus (*Pangassius hypothalamus*) in relation to size and season during storage in ice and their results showed that size, season and holding temperature seemed to have influence on the storage life of the fish.

Major carps are the most important species that supports fresh water fisheries in India, which ranks second in global fresh water fish production. Among the Indian Major Carps, *Labeo rohita* (rohu) is most preferred cultured fish (contributing more than 80%), since the species fetches higher price compared to the other cultured fish. The quality of fish decreases after death due to chemical reactions which produce changes in protein and lipid fractions (Ozogul *et al.*, 2006). The initial loss of freshness is caused by endogenous autolytic enzymes in muscle and subsequent spoilage is due to microbial activities, especially due to the rapid proliferation of specific spoilage organisms (Huss, 1995). Chilling of fish in ice or in the refrigerator slows down the destructive processes of enzymes and bacteria, because of which the shelf life of fish can therefore be extended by many days. The present study was carried out to investigate the shelf life of a fresh water rohu (*Labeo rohita*) fish, and also the spoilage mechanism of the fish in ice and ambient temperature.

MATERIALS AND METHODS

Fish sampling and storage

Labeo rohita (Rohu) fish harvested in the early morning from near by farmers ponds located at Muthukur were brought to the Fish Processing laboratory and used for ice storage and ambient temperature study. Immediately after sorting the samples according to sizes, they were washed with ice cold potable water and divided in to two lots. The first lot was stored in an insulated ice box (fish: ice ratio 1:1) with drainage holes, the ice being replenished twice a day. The second lot was kept in a plastic tray at ambient temperature (29-30°C). Samples were obtained from the ice box and ambient condition at 2 days and 3 hrs intervals respectively and used for organoleptic, biochemical and microbiological assessment.

Determination of pH

5g sample was ground with distilled water using pestle and mortar for 30 seconds and pH value of homogenate was recorded using a digital pH meter (Oakton, Eutech Instruments, Malaysia). Three readings were made for each sample and the mean value was recorded.

Determination of Total Volatile Base Nitrogen (TVB-N)

TVB-N was determined according to the Conway method (1962) and expressed as mg/100 g of meat.

Determination of Peroxide Value

Measurement of peroxide value was carried out by using Jacobs (1958) method and expressed as meq O₂ /kg of fat.



**K. Sravani et al.****Microbial Analysis**

Enumeration of different microbes in this study was carried out by following APHA (1992) methods.

Organoleptic Quality assessment

Organoleptic methods were used to assess the degree of freshness based on organoleptic characteristics. Raw samples were washed using potable water and presented whole to the taste panel. Samples were examined physically for general appearance of skin, consistency of flesh, odour, colour of the gills, colour and form of eyes and slime formation. Cooked attributes such as flavor, odour, taste, texture and raw attributes were evaluated by eight panelists and changes in quality of chilled and cooked fish were assessed at 2 days & 3 hrs intervals respectively. The scores are given as excellent (10), Like extremely (9), Like very much (8), Like moderately (7), Like slightly (6), Neither like nor dislike (5), Dislike slightly (4), Dislike moderately (3), dislike very much (2) and dislike extremely (1). A score of '5' (neither like nor dislike) was taken as acceptable limit.

RESULTS AND DISCUSSION**Changes in pH**

pH of rohu increased from an initial value of 6.51 ± 0.00 to 6.77 ± 0.01 on 8th day and later showed a decreasing trend up to 20th day (Table 1). The present results are in line with earlier findings of those of Ryder *et al.* (1993), Simeonidou *et al.* (1998), Rodriguez *et al.* (1999), Manzano *et al.* (2000) and Tejada *et al.* (2007). Where as at ambient study the value decreased initially and then increased during subsequent periods (Table 2). The initial decrease may be because of glycogen degradation in to lactic acid, then increased as a result of accumulation of volatile compounds. The relatively low pH values encountered till 9 hours of storage reflects the good nutritional state of fish. These results are in similar with observations made by Ababouch *et al.* (1996) and Sevim kose (2004).

Changes in TVB-N and Peroxide Value

TVB-N contents of *Labeo rohita* showed slow increase during the storage period under both ice and ambient storages, furnished in Table 3 and 4. TVB-N value for ice stored samples increased from 4.84 ± 0.06 to 32.75 ± 0.08 mg/100g of sample at the end of 18 day and the value increased to 39.46 ± 0.16 mg/100g of sample at the end of 20 day. The value of 30-35mg TVB-N/100g is recommended for fresh fish acceptability (Huss (1998), Connell (1995)). These results are corroborate those of sensory and microbial assessment in which *Labeo rohita*, were in acceptable condition for 18 days in ice. Acceptability was about 12 hrs at ambient temperature, the value increased from 4.84 ± 0.06 to 26.89 ± 0.07 mg/100g of sample at the end of 12 hours. The results of present study were similar to those of other earlier studies conducted by Joseph *et al.* (1988) in rohu. Low values of TVB-N have been related to the composition of the feed for cultured fish, which may modify the role of TMAO in osmotic regulation (Kyrana *et al.*, 1997). TVB-N might be considered as a good indicator of freshness in Ice and not at ambient temperature in the present study.

Results of Peroxide Values are presented in Figure 1 and 2. Peroxide value in *Labeo rohita* in ice was 2.82 ± 0.28 meq O₂ /kg of fat at 0 day and at the end of 18 days the value increased to 10.42 ± 0.21 meq O₂ /kg of fat on 18 day. Results suggests that the fish are in good condition throughout the storage period based on values of 10-20 meq O₂ /kg of fat as recommended by Connell (1995). At ambient storage results similarly indicated acceptability through out 12 hrs storage period. In the present study it was observed that changes in peroxide value of the sample were initially very low indicating a low level of oxidation in this fish. PV might not be considered as a good indicator of freshness in this study as values were with in the range of acceptability throughout the storage period. This may be attributed to the low levels of oil in this fish



**K. Sravani et al.**

Changes in Organoleptic Quality

The results of organoleptic changes and torry meter readings were furnished in Table 5 and 6 in ice and ambient storage study respectively. The quality of fish in organoleptic method was graded using the score from 1-10. The score points more than 5 were considered acceptable and less than 5 were considered as bad or disliked. The range of torry scale varied from 1-16 and the scores more than 8 are considered as good and less than 8 as bad quality. On the basis of the scores, the samples were found in acceptable conditions for 18 days in ice storage and 12 hrs at ambient temperature.

Changes in Bacterial load

The results of changes in bacterial load were shown in Figure 3 and 4 at ice and ambient temperatures respectively. The initial total viable count in ice-stored samples was 8.10×10^2 cfu/g which increased to 8.08×10^5 cfu/g on 18 day. At this day the fish were in acceptable condition according to International Commission for Microbiological Safety of Foods (ICMSF, 1988) i.e., not exceeds 10^6 cfu/g. But on the 20th day of ice storage the bacterial load increased to 6.87×10^7 . Results of samples stored at ambient temperature showed that the sample retained most of their freshness only for 12 hrs. The initial total bacterial load was 8.10×10^2 cfu/g and by the 12th hour the value is 6.28×10^5 cfu/g, by the end of 15th hour the value increased to 7.29×10^7 cfu/g.

CONCLUSION

The results of the above studies showed that *Labeo rohita* was found in edible condition for 18 days in ice storage and 12 hrs at ambient temperatures. Storage of fishes at very low temperature is effective method of preservation technique to reduce rate of spoilage. From this study the consumers are advised to buy or consume the ice stored fish than the fishes stored at room temperature.

REFERENCES

1. Ababouch, L.H., Souibri, L., Rhaliby, K., Ouahdi, O., Battal, M and Busta, F.F. (1996) Quality changes in sardines (*Sardinella pilchardus*) stored in ice and at ambient temperature. *Food Microbiology*, **13**: 123-132.
2. Adoga, I.J., Joseph, E and Samuel, O.F. (2010) Storage life of Tilapia (*Oreochromis niloticus*) in ice and ambient temperature. *Researcher*, **2(5)**: 39-44.
3. APHA. (1992) Compendium of methods for the microbiological examination of foods. (Ed. M.L. Speck) APHA publications, Washington, USA.
4. Azam, K., Pervin, S., Naher, S.S., Ali, Y., Alam, M.I., Haque, K.M.B and Ahmed, B. (2005) Quality changes in pangus (*Pangassius hypothalamus*) in relation to size and season during storage in ice. *Pakistan Journal of Biological Sciences*, **8(4)**: 636 -640.
5. Chandra shekar, Rao, A.P and Abidi, A.B. (2004) Changes in muscle biochemical composition of *Labeo rohita* (Ham.) in relation to season. *Indian Journal of Fisheries Technology*, **51(3)**: 319-323.
6. Connell, J.J. (1995) *Control of Fish quality*, 4th edition, *Fishing News Books*, London.
7. Conway, E.J. (1962) *Microdiffusion Analysis of Volumetric Error*, 5th eds., Crosby Lockwood and Sun limited., London.
8. Huss, H.H. (1995) Quality and quality changes in fresh fish. FAO Fisheries Technical Paper 348, Sub-committee on Fish Trade, *Food and Agriculture Organization of the United Nations*.
9. Huss, H.H. (1998) Fresh fish quality and quality changes. *FAO, Fishery Service*, No. 29.
10. ICMSF (International commission on Microbiological Specifications for Foods) (1986) *Micro organisms in Foods 2. Sampling for Microbiological Analysis, Principles and Specification Application*. 2nd Edition. Oxford: Blackwell Science.





K. Sravani et al.

11. Jacobs, M.B. (1958) The chemical analysis of food and food products, *Kre Publishing co.*, Newyork, USA.
12. Joseph, J., Surendran, P.K and Perigren, P.A. (1988) Studies on iced storage of cultured rohu (*Labeo rohita*). *Fishery Technology*, **25**: 105-109.
13. Kyrana,V.R., Lougovois, V.P and Valsamis, D.S. (1997) Assessment of shelf-life of maricultured gilthead sea bream (*Sparus aurata*) stored in ice. *International Journal of Food Science and Technology*, **32**: 339-347.
14. Manzano, M.A.M., Pacheco- Aguilar, R., Diaz- Rojas, E.I.D and Lugo- Sanchez, M.E.L. (2000) Postmortem changes in Black skip jack muscle during storage in ice. *Journal of Food Science*, **65(5)**: 774-779.
15. Ozogul, F., Kuley, E and Ozogul, Y. (2006) Sensory, chemical and microbiological quality parameters in sea bream (*Sparus aurata*) stored in ice. *International Journal of Food Science and Technology*, 1-6.
16. Rodriguez, C.J., Besteiro, I and Pascual, C. (1999) Biochemical changes in fresh water rainbow trout (*Oncorhynchus mykiss*) during chilled storage. *Journal of Food and Agriculture*, **79**, 1473 – 1480.
17. Ryder, J.M., Fletcher, G.C., Stec, M.G and Seelye, R.J. (1993) Sensory, microbiological and chemical changes in hoke stored in ice. *International Journal of Food Science and Technology*, **28**: 169-180.
18. Sevim kose. (2004) An investigation of quality changes in anchovy (*Engraulis encrasicolus*) stored at different temperatures. *Turkey Journal of Veterinery and Animal Science*, **28**: 575-582.
19. Simeonidou, S., Govaris, A and Vereltzis, K. (1998) Quality assessment of seven Mediterreanean fish species during storage on ice. *Food Research International*, **30 (7)**: 479-484.
20. Tejada. M, Heras. C.D and Kent, M. (2007) Changes in the quality indices during ice storage of farmed Senegalese sole (*Solea senegalensis*). *European Food Research Technology*, **225**: 225- 232.

Table 1 Changes in pH value in rohu fish during Ice Storage

Storage period (In Days)	pH*
0	6.51±0.00 ^{ab}
2	6.59±0.02 ^c
4	6.63±0.02 ^{cd}
6	6.70±0.02 ^f
8	6.77±0.01 ^f
10	6.70±0.01 ^e
12	6.68±0.01 ^{de}
14	6.64±0.01 ^{cde}
16	6.53±0.02 ^b
18	6.47±0.03 ^a
20	6.32±0.02 ^{cde}

*Each value is represented as arithmetic mean ± SD of n=3

^{abcdef} Means followed by the same superscript with in a column are not significantly different (p>0.01)





K. Sravani et al.

Table 2 Changes in pH value in rohu fish during ambient study

Storage period (In Hours)	pH*
0	6.17±0.00 ^f
3	6.05±0.01 ^e
6	5.86±0.01 ^c
9	5.87±0.02 ^b
12	5.98±0.01 ^d
15	6.03±0.00 ^a

Each value is represented as arithmetic mean ± SD of n=3

^{abcdef} Means followed by the same superscript with in a column are not significantly different (p>0.01)

Table 3 Changes in TVB-N values in rohu fish during Ice Storage

Storage period (In Days)	TVB-N (mg/100g of sample)
0	4.84±0.06 ^a
2	5.81±0.36 ^b
4	7.99±0.09 ^c
6	11.80±0.06 ^d
8	13.42±0.41 ^e
10	17.64±0.74 ^f
12	21.23±0.22 ^g
14	26.40±0.28 ^g
16	29.32±0.56 ^h
18	32.75±0.08 ⁱ
20	39.46±0.16 ^h

*Each value is represented as arithmetic mean ± SD of n=3

^{abcdefghi} Means followed by the same superscript with in a column are not significantly different (p>0.01)

Table 4 Changes in TVB-N values in rohu fish during ambient study

Storage period (In Hours)	TVB-N (mg/100g of sample)
0	4.84±0.06 ^a
3	6.60±0.11 ^b
6	12.2±0.48 ^c
9	19.42±0.56 ^d
12	26.89±0.07 ^e
15	29.46±0.24 ^f

Each value is represented as arithmetic mean ± SD of n=3

^{abcdef} Means followed by the same superscript with in a column are not significantly different (p>0.01)





K. Sravani et al.

Table 5 Changes in Organoleptic and Torry meter readings of rohu fish during ice storage

Storage period (In Days)	Organoleptic scores (1-10)	Torry meter readings (1-16)
0	9.82±0.12 ^j	15.10±0.08 ⁱ
2	9.22±0.02 ⁱ	13.96±0.12 ^h
4	8.45±0.10 ^h	13.13±0.20 ^f
6	8.02±0.12 ^g	11.86±0.04 ^e
8	7.41±0.12 ^f	11.00±0.08 ^d
10	6.57±0.13 ^e	10.26±0.04 ^b
12	6.53±0.23 ^d	9.93±0.12 ^b
14	6.05±0.17 ^c	9.60±0.21 ^c
16	5.89±0.12 ^b	9.12±0.16 ^b
18	4.99±0.05 ^a	8.10±0.21 ^a
20	3.82±0.07 ^a	7.01±0.12 ^d

* Each value is represented as arithmetic mean ± SD of n=8 for organoleptic scores and n=3 for torry meter readings
^{abcdehghij} Means followed by the same superscript with in a column are not significantly different (p>0.01)

Table 6 Changes in Organoleptic and Torry meter readings of rohu fish during ambient study

Storage period (In Hours)	Organoleptic scores (1-10)	Torry meter readings (1-16)
0	9.82±0.12 ^f	15.10±0.08 ^f
3	8.36±0.08 ^e	13.36±0.12 ^e
6	7.44±0.42 ^d	11.26±0.38 ^d
9	6.52±0.36 ^c	9.56±0.12 ^c
12	4.99±0.33 ^b	8.13±0.12 ^b
15	3.78±0.56 ^a	7.13±0.16 ^a

*Each value is represented as arithmetic mean ± SD of n=8 for organoleptic scores and n=3 for torry meter readings
^{abcdef} Means followed by the same superscript with in a column are not significantly different (p>0.01)

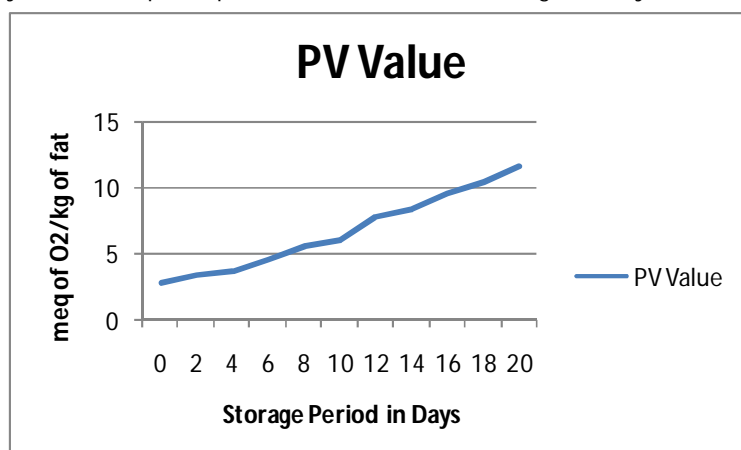


Figure 1. Changes in PV values of rohu fish during Ice storage





K. Sravani et al.

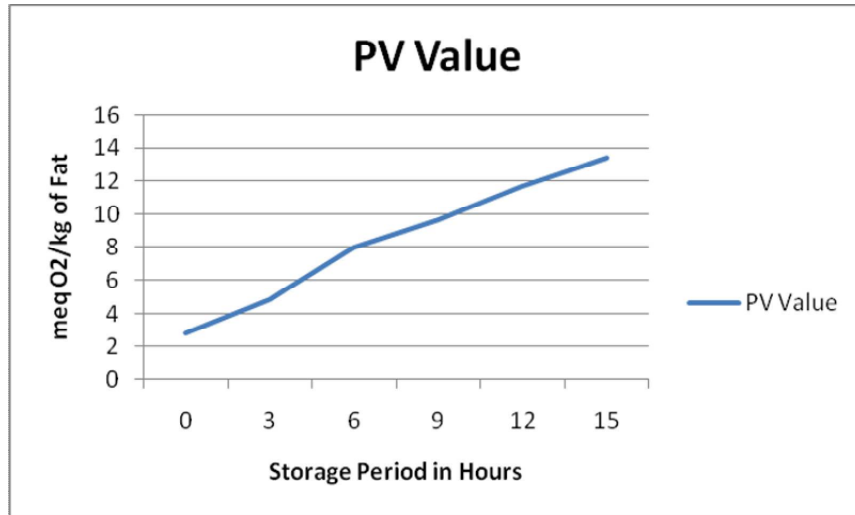


Figure 2. Changes in PV values of rohu fish during ambient study

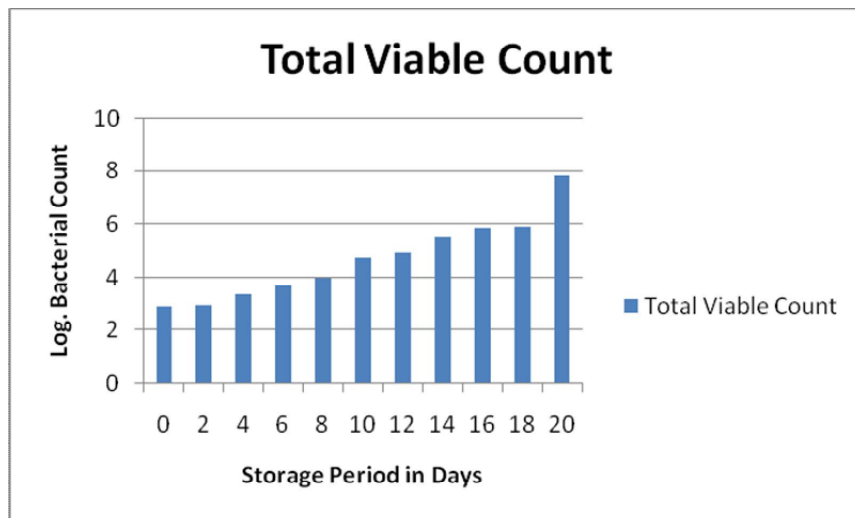


Figure 3. Changes in Total Viable Count of rohu fish during Ice storage





K. Sravani et al.

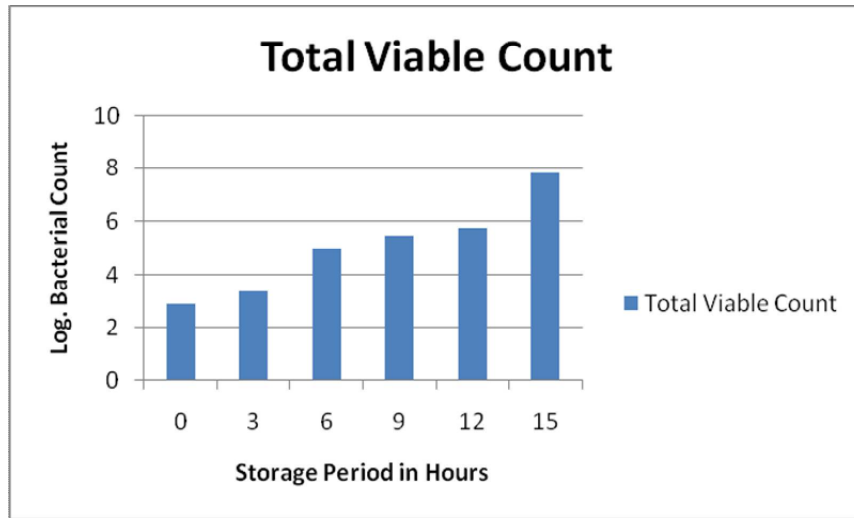


Figure 4. Changes in Total Viable Count of rohu fish during ambient study





RESEARCH ARTICLE

Cadmium Induced Toxicity in Wistar Rats: Ameliorative Effect by Methanolic Extract of *Asteracantha longifolia* Seeds

Ranjith D

Assistant Professor, Department of Veterinary Pharmacology and Toxicology, College of Veterinary and Animal Sciences, Lakkidi (P.O), Pookode, Wayanad- 673 576, Kerala.

Received: 22 Jul 2015

Revised: 20 Aug 2015

Accepted: 30 Sep 2015

*Address for correspondence

Ranjith D

Assistant Professor

Department of Veterinary Pharmacology and Toxicology,

College of Veterinary and Animal Sciences,

Pookode,Wayanad – 673 576.

Kerala, India.

E-mail: ranjith946@gmail.com



This is an Open Access Journal / article distributed under the terms of the **Creative Commons Attribution License (CC BY-NC-ND 3.0)** which permits unrestricted use, distribution, and reproduction in any medium, provided the original work is properly cited. All rights reserved.

ABSTRACT

Methanolic extract of *Asteracantha longifolia* seed powder was tested on cadmium induced toxicity in Wistar albino rats. Rats were administered with cadmium chloride (CdCl_2) @ 200 ppm, orally daily for 60 days simultaneously with plant extracts @ 500 ppm showed significant improvement in levels of haemoglobin, Total serum protein, Aspartate amino transferase (AST), Alanine amino transferase (ALT). Thus, findings may be concluded that administration of plant extract reduced the severity of cadmium toxicity in rats.

Keywords: Methanolic extract, *Asteracantha longifolia*, cadmium chloride, Toxicity.

INTRODUCTION

Cadmium, a heavy metal toxic to both human and animals, the major sources of cadmium to the environment is mainly from battery industry, nickel-cadmium manufacturing industries (Adams RG., 1992). International and government agencies have made efforts to control and lower the cadmium exposure to the general public in recent years. Nevertheless, Cadmium has a long biological half-life approximately 20-40 years in humans and can accumulate in the body over a considerable period of time, particularly in the kidneys and liver (WHO., 2000). Liver is the principal target organ for the accumulation of cadmium and mercury (S. Yannai and K. M. Sachs., 1993). Several previous studies showed that cadmium and mercury causes hepatotoxicity (D. F. Hwang and L. C. Wang., 2001 and I. Bando *et al.*, 2005). *Asteracantha longifolia* (L.) Nees, Acanthaceae is an important source of many ayurvedic

10236





Ranjith

drugs(Nadkarni, K.M., 1978) and can be used in various blood related disorders (Kirtikar K.R and Basu B.D., 1987).Shailajan *et al.* (2005) reported the whole plant slurry of *A. longifolia* is hepatoprotective against Carbon tetrachloride (CCl₄) induced liver dysfunction in rats and also revealed the slurry, aqueous extract and ethanolic extract of whole plant powder showed hepatoprotective effect against galactosamine induced hepatotoxicity(Shailajan S *et al.*, 2007).The aqueous extract of whole plant and root of *A.longifolia* showed hepatoprotective and antioxidative properties against CCl₄ and paracetamol induced hepatotoxicity [Hewawasam RP *et al.*, 2003 and Usha K *et al.*, 2007].Methanolic extracts of the seeds show hepatoprotective activity against paracetamol and thioacetamide intoxicification in rats [Singh A, Handa SS., 1999].Shanmugasundaram & Venkataraman (2006) studied the aqueous extract of the plant roots for hepatoprotective activity against CCl₄induced liver toxicity in rats and *in-vitro* antioxidant activity using Ferric thiocyanate (FTC) and Thiobarbituric acid (TBA) methods.The present investigation is carried out to assess the effect of simultaneous administration of cadmium chloride and methanolic extract of *Asteracantha longifolia* seeds on hepatoprotective activity in male Wistar rats.

MATERIALS AND METHODS

Animals

Healthy male Wistar albino rats weighing 150±30g procured from Raj Biotech India Ltd, Wing, Satara (Maharashtra). Animals were housed in polypropylene cages and provided with standard rodent pellet feed and water *ad libitum*. Male wistar rats maintained under identical feeding and managerial practices in the laboratory. They were housed at ambient temperature (21±1°C), relative humidity (55±5%) in a well ventilated room with a 12:12 h (Light: Dark) cycle. An acclimatization period of seven days was allowed before the start of experiment. All the experiments were carried out according to the guidelines recommended by the Committee for the Purpose of Control and Supervision of Experiments on Animals (CPCSEA), Government of India.

Chemicals

Cadmium chloride (CdCl₂) purchased from Qualigens, Mumbai, India. All other chemicals used were of analytical grade and purchased locally.

Collection of plant materials and Preparation of extract

Fresh plant part (seeds) were collected from the marshy areas of Gangakheda, Jintur, Manwath, Palam and Pathri areas of Parbhani District, Maharashtra, India. The botanical identity and authentication of plant done by Department of Botany, Marathwada Agricultural University, Parbhani, Maharashtra. A voucher specimen has been deposited at the herbarium unit of Department of Veterinary Pharmacology and Toxicology, College of Veterinary and Animal Sciences, Parbhani, Maharashtra Animal Fisheries Sciences University (MAFSU), Nagpur, Maharashtra. The seeds of the *Asteracantha longifolia* were shade-dried at room temperature and coarsely powdered using electrical pulverizer. The powder was extracted with methanol (95%) using soxhlet apparatus continuously for 72 hrs. The extract was dried under reduced pressure and temperature (55°C) using rotary flash evaporator. The percentage yield of extract was 7% w/w. It was stored at 4°C in airtight bottle for further use.

Phytochemical Analysis

The methanolic extracts of *Asteracantha longifolia* seeds were tested for the presence of various phytoconstituents by using standard chemical reagents(Harborne J B., 1991).





Ranjith

Acute toxicity study of plant extracts

Acute toxicity study of the methanolic extract of plant was carried out using acute toxic class method as per Organization of Economic Co-operation and Development (OECD) – 420 guidelines. (OECD, 2001).

Experimental Design

The experiment was approved by Institutional Animal Ethical Committee (IAEC)(04/Pharmacology/2007/MAFSU-COVAS/PBN/PG) dated 05/02/2007. Thirty male wistar rats were randomly divided in to three groups each consisting of ten rats. The experiment was conducted for a period of Sixty days.

- Group-I: Normal control (Tween 80), by using Intra Gastric Catheter Tube (IGC), po for 60days.
- Group - II: Cadmium Chloride solution in drinking water @ 200 ppm for 60days (daily) by IGC, po.
- Group -III: Methanolic extract of *Asteracantha longifolia* seeds @ 500 ppm (daily) by IGC, po simultaneously the rats were given Cadmium Chloride in drinking water at a dose of 200 ppm for 60 days.

Measurement of Body weight gain and Food intake

Body weight gain and Food intake were monitored during the entire experimental period.

Blood Samples

The blood samples were collected from the retro-orbital plexus from the rats in a clean, dry and sterilized test tubes with heparin as anticoagulant and analyzed for Haemoglobin (Hb) and the serum samples were collected for estimation of Total serum protein (TSP), Aspartate aminotransferase (AST) and Alanine amino transferase (ALT) using Ambika diagnostic reagent kits on Autoanalyser slim (SEAC).

Statistical Analysis

The data generated by using Equal Completely Randomized Block Design (Panse, U.G and P.V. Sukhatme., 1967). The treatment means compared by critical differences by statistical method and analysis of variance.

RESULTS AND DISCUSSION

Phytochemical evaluation

The phytochemical analysis of methanolic extracts of *Asteracantha longifolia* revealed the presence of alkaloids, flavanoids, glycosides, phytosterols, saponins, tannins, phenolic compounds, anthraquinone, carbohydrates, proteins and amino acids, gums and mucilages and oils and fats (Table 01).

Acute toxicity study

There were no observable signs of toxicity upon oral administration of the extract at high doses in all the animals (Table 02). No significant changes were observed in wellness parameters used for the evaluation of toxicity. Skin, fur, eyes, mucous membrane, behavioural pattern, salivation and sleep of the treated and control animals were found to be normal. There were no deaths resulted from the administration of test samples in all the animals used in this study up to the highest dose of 5000 mg/kg of body weight. This suggests that the extract, at the dose given caused no adverse effect on feed intake or metabolism. Therefore, the approximate LD₅₀ should be above 5 g/kg.



**Ranjith****Effects of methanolic extract of *A.Longifolia* and CdCl₂ treatments on Total serum protein(TSP), Aspartate amino transferase (AST) and Alanine amino transferase (ALT)**

The effects of methanolic extracts of seeds of *Asteracantha longifolia* on biochemical parameters were depicted in table 3. The mean total serum protein were significantly reduced ($P < 0.05$) in cadmium chloride treated rats (Group-II) as compared to control (group-I). Similar observation of inhibition of protein synthesis by cadmium had been reported both *in-vivo* and in isolated profused hepatocytes [Hidalga H A., 1976; Din S W *et al.*, 1985; Wakchaure S C., 2004; and Ayse C *et al.*, 2004]. However, concurrent administration with methanolic extract of *A.longifolia* seeds might be responsible for plant ability to accelerate repair mechanism after CdCl₂ induced damage. Aspartate amino transferase concentration has been increased by 29.99% in CdCl₂ treated rats, while 17.93% rise observed in CdCl₂ with methanolic extracts of *Asteracantha longifolia* seed treated group as compared to control. The mean Alanine amino transferase level has been raised to 72.28% in CdCl₂ treated group, while 24.44% rise observed in CdCl₂ with methanolic extract of *Asteracantha longifolia* seed treated rats (Group-III) as compared to control group (Group-I). Increased activity of enzyme like Alanine amino transferase (ALT) in blood is one of the common biochemical markers of liver damage (Ayse C *et al.*, 2004). Cadmium chloride significantly ($P < 0.05$) elevated the concentration of liver function marker enzymes like AST, ALT and ALP levels indicating the liver damage (Devy and Khan.A.B., 2006). The administration of aqueous extract of *A.longifolia* against galactosamine induced liver dysfunction in rats showed normalization of tissue parameters and plasma concentration of various enzymes indicating hepatoprotective action against galactosamine induced hepatotoxicity (Shailajan S *et al.*, 2007). Similar observations of *A.longifolia* as hepatoprotectant by several workers [Thakur C B *et al.*, 1991; Shanmugasundaram P and S. Venkataraman., 2006]. The administration of methanolic extract of *A.longifolia* seed in cadmium induced toxicity showed reduction in the activity of these enzymes supporting hepatic cell regeneration.

Effects of methanolic extract of *A.Longifolia* and CdCl₂ treatments on mean Haemoglobin levels (Hb)

Table.4 summarizes the mean haemoglobin levels, there was significant fall ($P < 0.01$) in mean value of haemoglobin in CdCl₂ treated rats compared to control rats. However, the mean value in CdCl₂ with methanolic extract of *Asteracantha longifolia* seeds were at par with control [Kirtikar KR *et al.*, 1987 and Pawar RS *et al.*, 2006].

CONCLUSION

It is concluded from the present study that simultaneous oral administration of methanolic extract of *Asteracantha longifolia* seeds in CdCl₂ treated rats showed significant improvement indicating its traditional use for the treatment of hepatic disorder.

ACKNOWLEDGEMENTS

The author likes to express special thanks of gratitude to Dr. M.I.Qureshi for his inspiring and untiring guidance during entire course of experiment.

REFERENCES

1. Adams, R.G (1992): Manufacturing process, resultant risk profiles and their control in the production of nickel-cadmium (alkaline) batteries. *Occup Med*: 42:101-106.
2. WHO. (2000): Air Quality Guidelines, World Health Organization. Regional Office for Europe: Copenhagen, Denmark: Cadmium.
3. S. Yannai and K. M. Sachs. (1993): Absorption and Accumulation of Cadmium, Lead and Mercury from Foods by Rats. *Food and Cheml Toxicol*, 31(5), 351-355.



**Ranjith**

4. D. F. Hwang and L. C. Wang. (2001). Effect of Taurine on Toxicity of Cadmium in Rats: *Toxicol*, 167(3):173-180.
5. I. Bando, M. I. Reus, D. Andrés and M. Cascales (2005). Endogenous Antioxidant Defense System in Rat Liver Following Mercury Chloride Oral Intoxication. *Journl. Of Biochem and Mol. Toxicol.*19 (3).154-161.
6. Nadkarni, K.M. (1978). Indian Materia Medica, Popular Prakshan, Bombay.
7. Kirtikar, K.R, Basu, B.D (1987). Indian Medicinal Plants, Periodical Export. New Delhi.
8. Shailajan. S, Naresh Chandran, R.T Sane and Sasikumar Menon. (2005). Effect of *Asteracantha longifolia* Nees. against CCl₄ induced liver dysfunction in rat. *Ind.J. of Exptl. Biol.*43,68-75.
9. Shailajan S, Chandra N, Sane RT, Menon S (2007). Effect of *Asteracantha longifolia* Nees. against galactosamine induced liver dysfunction in-rat. *Toxicol Int.*14: 7-13
10. Hewawasam RP, Jayatilaka KA, Pathirana C, Mudduwa LK (2003). Protective effect of *Asteracantha longifolia* extract in mouse liver injury induced by carbon tetrachloride and paracetamol. *J Pharm Pharmacol.*55: 1413-1418.
11. Usha K, Mary Kasturi G, Hemalatha P (2007). Hepatoprotective effect of *Hygrophila spinosa* and *Cassia occidentalis* on carbon tetrachloride induced liver damage in experimental rats. *Indian J Clinical Biochem* 22: 132-135.
12. Singh A, Handa SS (1999). Hepatoprotective activity of *Apium graveolens* and *Hygrophila auriculata* against paracetamol and thioacetamide intoxication in rats. *J Ethnopharmacol* 49: 119-126.
13. Shanmugasundaram Pand S. Venkataraman (2006). Hepatoprotective and antioxidant effects of *Hygrophila auriculata* (K. Schum) Heine Acanthaceae root extract. *J. of Ethnopharmacol.*104(1-2), 124-128.
14. The Organization for Economic Co-operation Development (OECD). The OECD guideline for Testing of Chemicals 420, adopted 17th December 2001.
15. Harborne J B (1991). Phytochemical methods - Guide to modern techniques of plant analysis, Second edition, (Chapman and Hall, India), 653.
16. Panse, U.G and P.V. Sukhatme (1967) Statistical Methods for Agril. Workers, ICAR Publications, New Delhi, 1801-1810.
17. Hidalgo H A, Koppa V and Bryan S E (1976). *FEBS.Lett.* 64,159-162.
18. Din S W and John M Frazer (1985). Protective effect of petallothionein on cadmium toxicity in isolated rat hepatocytes. *Biochem. J.* 230, 395-402.
19. Wakchaure S C (2004). Evaluation of toxicopathological effect of some heavy metals in slaughtered swine, M.V.Sc thesis, MAFSU, Nagpur (MS). India.
20. Ayse C; A Nuriye; O Nurten; B Sehnaz; P A Bahrye; Y Rafiye and O Alper (2004). Effect of Aloe vera leaf gel and pulp extracts on the liver in type II diabetic rat models. *Biol. Pharm. Bull.* 27(5): 694-698.
21. Devy and Khan.A.B. (2006). Cadmium chloride induced hepato-renal toxicity in the adult albino rats. *Toxicol.Int.*13 (1), pp 29-31.
22. Thakur C B, Dixit V P and Saraf S (1991): Hepatoprotective activity of *Asteracantha longifolia* Nees. *Indian drugs*, 28(9), 400-402.
23. Balachandran I and Sivarajan V V (1994). Ayurvedic drugs and their plant sources, in *Kokilakshya*: Oxford and IBH Publishing Company Pvt Ltd. (Eds: 1) New Delhi, 249-250.
24. Kirtikar KR, Basu BD. Indian Medicinal Plants, Periodical Export. New Delhi, 1987.
25. Pawar RS, Jain AP, Kashaw SK, Singhai AK (2006). Haematopoietic activity of *Asteracantha longifolia* on cyclophosphamide-induced bone marrow suppression, 68(3). 337-340.





Ranjith

Table 1. Phytochemical screening of *Asteracantha longifolia* methanolic seed extract

SI No.	Name of phytochemical	Methanolic extract (<i>A. longifolia</i> seed)
1	Alkaloids	+
2	Flavonoids	+
3	Glycosides	+
4	Phytosterols	+
5	Saponins	+
6	Tannins	+
7	Phenolic compounds	++
8	Terpenoids	-
9	Anthraquinone	-
10	Carbohydrates	+
11	Proteins and amino acids	+
12	Gum and mucilages	+
13	Oils and fats	+

+ Present - Absent

Table 2. Observations for Acute oral toxicity study test at the dose of 5000 mg/kg bodyweight of methanolic extract of *Asteracantha longifolia* seeds

Observations	30 mins		4 hrs		24 hrs		48 hrs		1 wks		2 wks	
	C	S	C	S	C	S	C	S	C	S	C	S
Skin and fur	N	N	N	N	N	N	N	N	N	N	N	N
Eyes	N	N	N	N	N	N	N	N	N	N	N	N
Mucous Membrane	N	N	N	N	N	N	N	N	N	N	N	
Salivation	N	N	N	N	N	N	N	N	N	N	N	N
Lethargy	Nil	Nil	Nil	Nil	Nil	Nil	Nil	Nil	Nil	Nil	Nil	Nil
Sleep	N	N	N	N	N	N	N	N	N	N	N	N
Coma	Nil	Nil	Nil	Nil	Nil	Nil	Nil	Nil	Nil	Nil	Nil	Nil
Convulsions	Nil	Nil	Nil	Nil	Nil	Nil	Nil	Nil	Nil	Nil	Nil	Nil
Tremors	Nil	Nil	Nil	Nil	Nil	Nil	Nil	Nil	Nil	Nil	Nil	Nil
Diarrhoea	Nil	Nil	Nil	Nil	Nil	Nil	Nil	Nil	Nil	Nil	Nil	Nil
Mortality	Nil	Nil	Nil	Nil	Nil	Nil	Nil	Nil	Nil	Nil	Nil	Nil

C – Control, S - Methanolic seed extract, N – Normal





Ranjith D

Table- 3: Effect of CdCl₂ alone and CdCl₂ with methanolic extract of *Asteracantha longifolia* seeds on mean Total Serum protein (TSP), Aspartate amino transferase (AST), Alanine aminotransferase (ALT) in male rats

Group No.	Treatment	TSP(g/dl) Mean±SE		AST (IU/L) (Mean±SE)		ALT (IU/L) (Mean±SE)	
		Pre-Treatment	Post-Treatment	Pre-Treatment	Post-Treatment	Pre-Treatment	Post-Treatment
I	Control (Normal feed)	6.68±0.12 (6.13-7.23)	6.80±0.11 (6.34-7.34)	95.14±1.11 (90.8-102.4)	99.13± 3.03 (80.3-115.8)	67.91±0.82 (63.5-71.4)	65.47±0.76 (62.5-69.8)
II	CdCl ₂ alone	6.79±0.11 (6.33-7.32)	6.06*±0.07 (5.84-6.64)	86.67±1.87 (79.5-99.4)	141.61*±2.71 (120.8-150.7)	69.49 ±0.92 (64.5-74.2)	235.81*±6.29 (200.7-280.6)
III	CdCl ₂ with <i>A.longifolia</i> a seed powder	6.97±0.06 (6.71-7.34)	6.55*±0.07 (6.14-6.86)	89.11±1.46 (82.4-100.5)	129.92*±4.38 (110.5-160.5)	70.33 ±0.67 (67.8-75.2)	86.84*±0.61 (84.5-90.4)

*P < 0.05 Control vs CdCl₂ treated group, *P < 0.05 CdCl₂ treated group vs Plant; Number of rats =10 in each group.

Table-4: Effect of CdCl₂ alone and CdCl₂ with methanolic extract of *Asteracantha longifolia* seedson mean Haemoglobin (Hb) in male rats:

Group No.	Treatment	Haemoglobin (g/100ml) Mean±SE	
		Pre- Treatment	Post-Treatment
I	Control (Normal feed)	14.63±0.07 (14.35-15.08)	14.9±0.07 (14.32-15.03)
II	CdCl ₂ alone	15.58±0.07 (15.21-15.94)	11.20*±0.06 (10.88-11.45)
III	CdCl ₂ with <i>A.longifolia</i> seed powder	14.10±0.07 (12.98-15.01)	12.10*±0.05 (11.84-12.34)

*P < 0.05 Control vs CdCl₂ treated group, *P < 0.05 CdCl₂ treated group vs Plant; Number of rats =10 in each group.





Maximum Power Point Tracking based on Novel Improved Variable Step Sized Incremental Resistance for Photovoltaic Systems

Amin Zeidabadi Nejad*, Mahmood Joorabian and Morteza Razaz

ShahidChamran University of Ahvaz, Department of Electrical Engineering, Ahvaz, Iran.

Received: 24 Jul 2015

Revised: 26 Aug 2015

Accepted: 29 Sep 2015

*Address for correspondence

Amin Zeidabadi Nejad
ShahidChamran University of Ahvaz,
Department of Electrical Engineering,
Ahvaz, Iran



This is an Open Access Journal / article distributed under the terms of the **Creative Commons Attribution License (CC BY-NC-ND 3.0)** which permits unrestricted use, distribution, and reproduction in any medium, provided the original work is properly cited. All rights reserved.

ABSTRACT

Maximum power point (MPP) tracking (MPPT) techniques are widely used in photovoltaic (PV) systems to make PV array generate maximum power which relies on solar irradiation. In this paper a novel MPPT algorithm based on variable step-size incremental resistance is introduced. Compared with other existing methods, the proposed method not only improves MPPT response speed, accuracy and dynamical performance but also can obtain wider operating range. Simulation results which are carried out by MATLAB confirm its feasibility.

Keywords: incremental resistance, MPPT, variable step-size, photovoltaic systems.

INTRODUCTION

The alarming rise in the demand and consumption of energy/power throughout the world has led to a global decline in natural fossil fuel resources [1-3]. At the same time, there has been a significant increase in global warming. Natural fossil fuels or the non-renewable energy resources such as coal, oil and natural gas have limited reserves which will be depleted. Subsequently, this has led to research and development in order to replace certain non-renewable energy resources with renewable ones [4-6]. Photovoltaic generation is becoming increasingly important as a renewable resource since it does not cause in fuel costs, pollution, maintenance, and emitting noise compared with other alternatives used in power applications. Recently, PV array systems have been used in several electric power applications [7-11]. These systems have made a successful transition from small standalone sites to large grid connected systems. The utility interconnection brings a new dimension to the renewable power economy by pooling the temporal excess or the shortfall in the renewable power with the connecting grid that generates base-load power using conventional fuel [1]. Several factors have led to the evolution of intensive use of photovoltaic systems. The most significant factors are the worldwide increase in energy demand and the fact that the fossil energy sources are





Amin Zeidabadi Nejad et al.

finite and that they are expensive. Another important issue is the impact of the energies technologies on the environment and the fact that photovoltaic has become a mature technology. The increase in number of PV systems installed worldwide has introduced the need of supervision and control algorithms [2–4] as well as design and simulation tools for researchers and engineers involved in these kinds of applications. Between the different approaches for PV system design and simulation existing nowadays [5,6], most popular tools are specific commercial software helping in design of PV systems like PVsol [7] and PVsyst [8]. These tools give a good approach of the PV system design and behavior in different conditions of work, but when a more detailed simulation is needed to a deep understand of the different components involved in the whole system these tools are not powerful enough. More powerful approaches have been developed using different commercial software for technical and engineering applications as Pspice [9–11] or Matlab [12–16].

Besides advantage of PVs, conversion energy efficiency is very low in solar systems especially under low irradiation and variable weather conditions. Every changing in these factors especially in irradiation can be affected on produced power depending on PV panel ambient condition. Also, the solar cell V-I characteristic is nonlinear and changes with irradiation and temperature. In general, there is a unique point on the V-I or V-P curve, called the Maximum Power Point (MPP), at which the entire PV system (array, inverter, etc...) operates with maximum efficiency and produces its maximum output power. The location of the MPP is not known, but can be located, either through calculation models or by search algorithms. Maximum Power Point Tracking (MPPT) techniques are used to maintain the PV array's operating point at the MPP. In recent years a lot of techniques for MPPT are proposed and implemented in PV systems. The approaches vary in complexity, sensors required, convergence speed, cost, range of effectiveness, implementation hardware, popularity, and in other respects. Among all different papers, much focus has been on hill climbing [17-18], and perturb and observe (P&O) [17-] methods. Hill climbing involves a perturbation in the duty ratio of the power converter, and P&O a perturbation in the operating voltage of the PV array. Although, these methods are not precise but they are used a lot in industry. On the other hand, other methods like fuzzy logic and neural network have improved accuracy and fast response but they increase complexity of system. Methods based on fuzzy logic and neural network depend on designing of basis law table and network training respectively [19-21]. Because of the fast and precision response, appropriate reliability and ability to work in variable weather condition, incremental conductance approach is used in PV systems as a best method for MPPT [19-20]. Common MPPT systems have been constituted of two separated control loop. The first loop and second one include MPPT algorithm and P or PI controller respectively. MPPT control loop produce an error signal which is zero at maximum power point. Second loop is used to reduce error signal to zero [21-22]. Because of simplicity in implementation, simple designing and costless maintains, PI controller is used a lot in PV systems [23-24].

In this paper a method based on variable step-size incremental resistance is studied. According proposed method, algorithm output is considered as reference current which must be produced on the output side of PV. This reference current at maximum power point has value equal with output current of solar array. Effects of fixed and variable step-size on dynamic and steady state oscillations are considered. Also, Results of both methods are compared and analyzed. Analysis of simulations show that proposed method can improve steady state and dynamic response of system.

Proposed MPPT Algorithm

Characteristic and Model of Solar Array

General PV panel comprises a number of PV cells connected in either series or parallel. PV cells can convert light photon energy into electricity [1-5]. Equivalent circuit of a PV cell is shown in Fig.1. In this figure R_s and R_p stand for series and parallel equivalent resistance respectively.

The P - V characteristic of the solar panels is modeled by the following:





Amin Zeidabadi Nejad et al.

$$I_0 = n_{ph} I_{ph} - n_p I_{rs} \left[\exp \left(k_0 \frac{V}{n_s} \right) - 1 \right] \tag{1}$$

Where I_0 is the PV array output current, V is the PV output voltage, I_{ph} is the cell photocurrent that is proportional to solar irradiation, I_{rs} is the cell reverse saturation current that mainly depends on temperature, k_0 is a constant, n_s represents the number of PV cells connected in series, and n_p represents the number of such strings connected in parallel. In (1), the cell photocurrent is calculated from following equations:

$$I_{ph} = [I_{scr} + k_i (T - T_r)] \frac{S}{100} \tag{2}$$

$$I_{rs} = I_{rr} \left[\frac{T}{T_r} \right]^3 \exp \left(\frac{q E_g}{k A} \left[\frac{1}{T_r} - \frac{1}{T} \right] \right) \tag{3}$$

Where I_{scr} , cell short-circuit current at reference temperature and radiation; k_i , short-circuit current temperature coefficient; T_r , cell reference temperature; S solar irradiation in mill watts per square centimeter; T_r , cell reference temperature; I_{rr} , reverse saturation at T_r ; E_g band-gap energy of the semiconductor used in the cell. For simulations and the experimental setup also, the KC85T module was chosen. The electrical parameters are tabulated in table(1).

Fig.2. and Fig.3. show effect of varying weather conditions on MPP location at $I-V$ and $P-V$ curves respectively. By attention to this figure, it can be concluded that PV cell has nonlinear performance. Also MPP position is influenced by weather condition.

MPP Algorithm based on Variable Step Sized Incremental Resistance

The proposed variable step-size INR method is also based on the fact that the slope of the PV array power curve is zero at the MPP, positive at the left of the MPP, and negative at the right, as given by:

$$\begin{aligned} \frac{dP}{dI} &= 0 \text{ in MPP} \\ \frac{dP}{dI} &< 0 \text{ in right side of MPP} \\ \frac{dP}{dI} &> 0 \text{ in left side of MPP} \end{aligned} \tag{4}$$

Since we have:

$$\frac{dP}{dI} = \frac{d(IV)}{dI} = V + I \frac{d(V)}{dI} \cong V + I \frac{\Delta(V)}{\Delta I} \tag{5}$$

Eq(5) can be written as:

$$\begin{aligned} \frac{\Delta V}{\Delta I} &= -\frac{V}{I} \text{ at MPP} \\ \frac{\Delta V}{\Delta I} &> -\frac{V}{I} \text{ at left side of MPP} \\ \frac{\Delta V}{\Delta I} &< -\frac{V}{I} \text{ at right side of MPP} \end{aligned} \tag{6}$$

According to above equations, MPP can be tracked by comparing instantaneous resistance and incremental resistance. In this paper, an improved variable step-size algorithm is proposed for the INR MPPT method. The basic idea for implementing this algorithm is based on following equation:





Amin Zeidabadi Nejad et al.

$$C = P^n \times \left| \frac{dP}{dI} \right| \tag{7}$$

Where, n is an index number. The product curve has two extreme values/points (M_1 and M_2) corresponding to two current values (I_1 and I_2) at the two sides of MPP as shown in Fig.4. The INR MPPT is in the decremented step-size mode when the PV array output current is between I_1 and I_2 . Otherwise, it is in the incremented step-size mode. The aforementioned idea can be formulated by:

$$\begin{aligned} \frac{\Delta C}{\Delta I} &\geq 0, \\ \text{incremented step - size mode (left of MPP)} \\ \frac{\Delta C}{\Delta I} &< 0, \\ \text{decremented step - size mode (left of MPP)} \\ \frac{\Delta C}{\Delta I} &> 0, \\ \text{decremented step size mode (right of MPP)} \\ \frac{\Delta C}{\Delta I} &< 0, \\ \text{incremented step - size mode (right of MPP)} \end{aligned} \tag{8}$$

Where, $\frac{\Delta C}{\Delta I}$ is the increment of the threshold function. The step-size modes are thus switched by above expression which will determine the response speed and the two extreme points of the threshold function are closing to the peak power point as the index n becomes larger, as shown in Fig.5. Thus, the larger the index n is, the faster the system response is, and vice versa. From Fig.5. And Fig.6. Show that this method can adapt itself with different weather condition. In Fig.8. Flowchart of the variable step-size INR MPPT algorithm has been shown. Obtaining MPP, array performance is kept here unless a voltage deviation caused by a change in weather condition is sensed.

$V(k), I(k), C(k)$ are supposed to be the PV array output voltage, current, and the proposed threshold function at time k. In addition, $I_{ref}(k)$ and $\Delta I_{ref}(k)$ are the output current reference and its change (step size) at time k, respectively. I_1 and I_2 is decremented and incremented step size respectively.

Selecting Power Electronic Converter

The major part of MPPT is power converter which completes switching activities. Among all the topologies available, both Cuk and buck-boost converters provide the opportunity to have either higher or lower output voltage compared with the input voltage. Although the buck-boost configuration is cheaper than the Cuk one, some disadvantages, such as discontinuous input current, high peak currents in power components, and poor transient response, make it less efficient. On the other hand, the Cuk converter has low switching losses and the highest efficiency among nonisolated dc-dc converters.

It can also provide a better output-current characteristic due to the inductor on the output stage. Thus, the Cuk configuration is a proper converter to be employed in designing the MPPT [8]. Fig.9. and Fig.10. Show CUK converter and its performance modes as interface between solar array and load. The first mode of operation is when the switch is closed (ON), and it is conducting as a short circuit. In this mode, the capacitor releases energy to the output. The equations for the switch conduction mode are as follows:





Amin Zeidabadi Nejad et al.

$$\begin{aligned}
 v_{L1} &= V_g \\
 v_{L2} &= -v_1 - v_2 \\
 i_{C1} &= i_2 \\
 i_{C2} &= i_2 - \frac{v_2}{R}
 \end{aligned} \tag{9}$$

On the second operating mode when the switch is open (OFF), the diode is forward-biased and conducting energy to the output. Capacitor C1 is charging from the input. The equations for this mode of operation are as follows:

$$\begin{aligned}
 v_{L1} &= V_g - v_1 \\
 v_{L2} &= -v_2 \\
 i_{C1} &= i_1 \\
 i_{C2} &= i_2 - \frac{v_2}{R}
 \end{aligned} \tag{10}$$

SIMULATION RESULTS

The diagram of the system under study in MATLAB is shown in Fig. 11, which includes the PV module electrical circuit based on kc200gt model, the DC-DC Cuk converter, and the MPPT algorithm. Parameters of this model are tabulated in Table.2. For performance evaluating of proposed method, fixed step size with low and high value and also variable step size are considered. Sampling time is 0.01s and irradiation will be changed from the first value $900 \frac{W}{m^2}$ to $1000 \frac{W}{m^2}$ at $t = 0.9s$. According to Fig.2. it is obvious that maximum output power in irradiation 900 and 1000 is 177.6w and 200w respectively. First, algorithm is considered as fixed step size with values 0.01A and 0.0005A. Then variable step size will be considered with low (0.005A) and high (0.0005A) step and n is regulated on 3. Simulation results are shown in Fig.12.

As observed in Fig.12. High step size can reduce settling time but can increase oscillations of steady state. On the other hand low step size can reduce oscillations of steady state but increase time of final response. These results are shown in table (3). By comparing results, it can be realized that using of variable step size can reduce oscillation and settling time.

CONCLUSION

In this paper a novel and improved MPPT method based on variable step size incremental resistance considered. This method was simulated in MATLAB software. Results of simulation show that proposed method can improve dynamical performance of system. Because of wide performance range, this method can implement for a lot of applications.

REFERENCES

1. S. Massoud, B. Wollenberg, Toward a smart grid: power delivery for the 21st Century, IEEE Power and Energy Magazine 3 (5) (2005) 34–41.
2. A. Chouder, S. Silvestre, Automatic supervision and fault detection of PV systems based on power losses analysis, Energy Conversion and Management 51 (2010) 1929–1937.
3. S.K. Firth, K.J. Lomas, S.J. Rees, A simple model of PV system performance and its use in fault detection, Solar Energy 84 (2010) 624–635.





Amin Zeidabadi Nejad et al.

4. Syafaruddin, Engin Karatepe, Takashi Hiyama, Polar coordinated fuzzy controller based real-time maximum-power point control of photovoltaic system, *Renewable Energy* 34 (2009).
5. S. Silvestre, Review of system design and sizing simulation tools, in: T. Markvart, L. Castañer (Eds.), *Practical Handbook of Photovoltaics, Fundamentals and Applications*, Elsevier, Oxford, 2003, pp. 544–561.
6. Esfandyar Mazhari, Jiayun Zhao, Nurcin Celik, Seungho Lee, Young-Jun Son, Larry Head, Hybrid simulation and optimization-based design and operation of integrated photovoltaic generation, storage units, and grid, *Simulation Modelling Practice and Theory* 19 (2011)
7. <http://valentin-software.com/xcartgold/Photovoltaics/>.
8. S. B. Kjaer and F. Blaabjerg, "Design optimization of a single phase inverter for photovoltaic applications," in *Proc. IEEE Power Electronics Specialists Conference*, 2003, vol. 3, pp. 1183–1190.
9. http://www.cadence.com/products/orcad/pspice_simulation/pages/default.aspx.
10. L. Castañer, S. Silvestre, *Modelling PV Systems Using Pspice*, Wiley, Chichester, 2002.
11. S. Silvestre, A. Boronat, A. Chouder, Study of bypass diodes configuration on PV modules, *Applied Energy* 86 (9) (2009) 1632–1640.
12. T. Brekken, N. Mohan, C. Henze, & L.R. Mounneh, "Utility-connected power converter for maximizing power transfer from a photovoltaic source while drawing ripple-free current," *IEEE PESC*, 2002.
13. Geoff Walker, Evaluating MPPT converter topologies using a MATLAB PV model, *Journal of Electrical & Electronics Engineering Australia* 21 (1) (2001)49–55.
14. Chao Shen, Ya-Ling He, Ying-Wen Liu, Wen-Quan Tao, Modelling and simulation of solar radiation data processing with Simulink, *Simulation Modelling Practice and Theory* 16 (7) (2008) 721–735.
15. E. Román, R. Alonso, P. Ibañez, S. Elorduzapatarietxe, D. Goitia, Intelligent PV module for grid-connected PV systems, *IEEE Transactions on Industrial Electronics* 53 (4) (2006) 1066–1073.
16. Xiao-Qiang Guo, Wei-Yang Wu, He-Rong Gu, Modeling and simulation of direct output current control for LCL-interfaced grid-connected inverters with parallel passive damping, *Simulation Modelling Practice and Theory* 18 (2010) 946–956.
17. G.Petrone, G.Spagnuolo, R.Teodorescu, M.Veerachary, M.Vitelli, "Reliability issues in photovoltaic power processing systems," *IEEE Trans. Ind. Electron.*, vol. 55, no. 7, pp. 2569–2580, Jul. 2008.
18. E.Koutroulis, K.Kalaitzakis, N.C.Voulgaris, "Development of a microcontroller-based, photovoltaic maximum power point tracking control system," *IEEE Trans. Power Electron.*, vol. 16, no. 1, pp. 46–54, Jan. 2001.
19. J.M.Kwon, B.H.Kwon, K.H.Nam, "Three-phase photovoltaic system with three-level boosting MPPT control," *IEEE Trans. Power Electron.*, vol. 23, no. 5, pp. 2319–2327, Sep. 2008.
20. J.L.Agorreta, L.Reinaldos, R.Gonzalez, M.Borrega, J.Balda, L.Marroyo, "Fuzzy switching technique applied to PWM boost converter operating in mixed conduction mode for PV systems," *IEEE Trans. Ind. Electron.*, vol. 56, no. 11, pp. 4363–4373, Nov. 2009.
21. A.Varnham, A.M.Varnham, G.S.Virk, D.Azzi, "Soft-computing model-based controllers for increased photovoltaic plant efficiencies," *IEEE Trans. Energy Convers.*, vol. 22, no. 4, pp. 873–880, Dec. 2007.
22. K.H.Hussein, I.Muta, T.Hshino, M.Osakada, "Maximum photovoltaic power tracking: An algorithm for rapidly changing atmospheric conditions," *Proc. Inst. Elect. Eng.*, vol. 142, no. 1, pp. 59–64, Jan 1995.
23. F.Salem, M.S.Adel Moteleb, H.T.Dorrah, "An enhanced fuzzyPI controller applied to the MPPT problem," *J. Sci. Eng.*, vol. 8, no. 2, pp. 147–153, 2005.
24. H. S. Bae, S. J. Lee, K. S. Choi, B. H. Cho, and S. S. Jang, "Current control design for a grid connected photovoltaic/fuel cell DC–AC inverter," in *Proc. 24th IEEE APEC*, Feb. 15–19, 2009, pp. 1945–1950.
25. M.G.Villalva, J.R.Gazoli, F.R.Filho, "comprehensive Approach to Modeling and Simulation of Photovoltaic Arrays", *IEEE Trans. Power Electron.*, vol. 24, no. 5, pp. 1198– 1208, MAY.2009.
26. KC200GT High Efficiency Multicrystal Photovoltaic Module Datasheet Kyocera. [Online]. Available: <http://www.kyocera.com.sg/products/solar/pdf/kc200gt.pdf>
27. D.Maksimovic, S.Cuk, "A unified analysis of PWMconverters in discontinuous modes," *IEEE Trans. Power Electron.*, vol. 6, no. 3, pp. 476– 490, Jul. 1991.





Amin Zeidabadi Nejad et al.

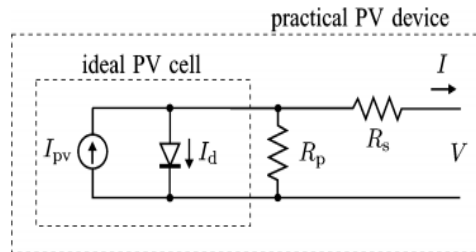


Fig. 1. Ideal PV Cell

Table 1 Electrical Parameters of KC85T Nodule

Parameters	Value
Maximum power (P_{max})	200w
Voltage at MPP (V_{mpp})	26.3v
Current at MPP (I_{mpp})	7.61A
Open circuit voltage (V_{oc})	32.9v
Short circuit current (I_{sc})	8.21A
Serried Cells	54

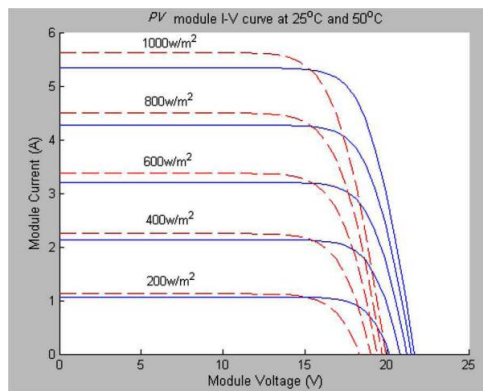


Fig. 2. I-V curve for different ambient temperature





Amin Zeidabadi Nejad et al.

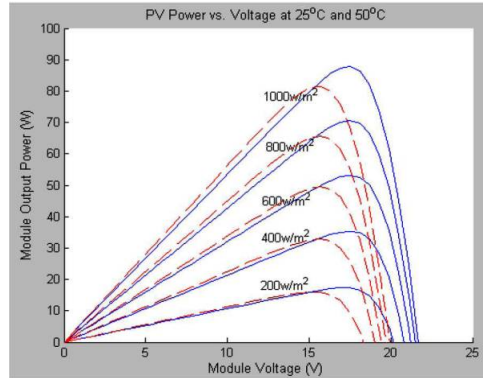


Fig. 3.P-V curve for different ambient temperature

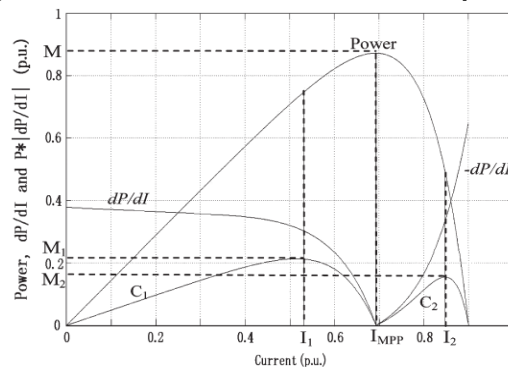


Fig. 4. Normalized power, slope of power versus current, and the product of power and its slope

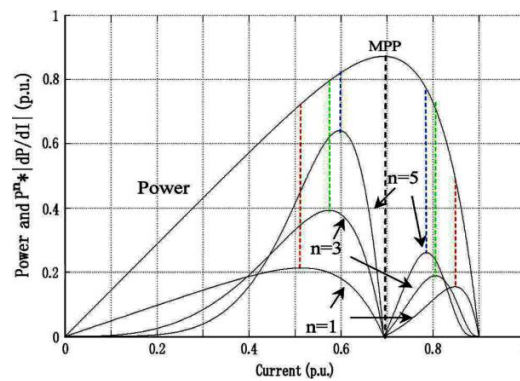


Fig. 5. Threshold function curve for different n





Amin Zeidabadi Nejad et al.

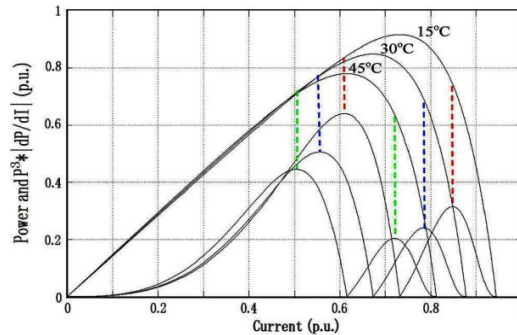


Fig. 6. Threshold function curve for different temperature

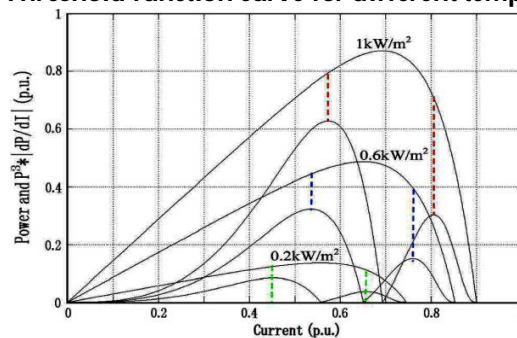


Fig. 7. Threshold function curve for different irradiation

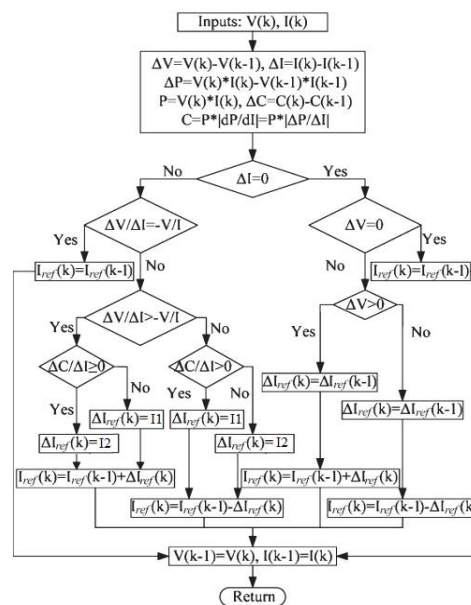


Fig. 8 Flowchart of the variable step-size INR MPPT algorithm





Amin Zeidabadi Nejad et al.

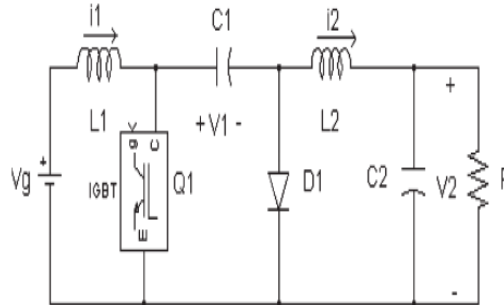


Fig. 9. Circuit of CUK Converter

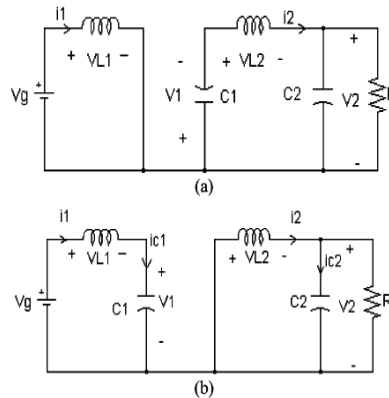


Fig. 10. Cuk converter with (a) switch ON and (b) switch OFF

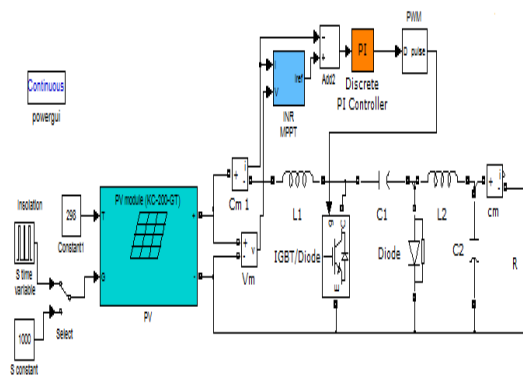


Fig. 11. System under Study





Amin Zeidabadi Nejad et al.

Table 2:Parameters of System

Parameters	Values
L_1	70mH
C_1	100mF
L_2	80mH
Switch	IGBT
C_2	100 μ F
Resistance of load	10 Ω
Switching Frequency	250Hz

Table 3Tracking Performance Comparison

ΔI_{ref}	Δt (s)	ΔP (w)	P_h (w)
0.005	0.08	1.8	199.5
0.01	0.01	5.4	199.5
variable	0.03	1.8	199.5

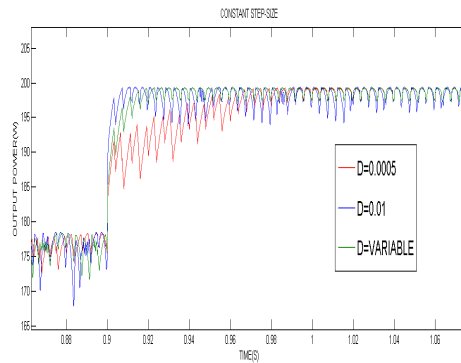


Fig. 12.Output Power Curve for Variable and Fixed Step Size

